Journal of the Physical Society of Japan
Vol. 75, No. 8, August, 2006, 082001

Stochastic Liouville, Langevin, Fokker–Planck, and Master Equation Approaches to Quantum Dissipative Systems

Yoshitaka TANIMURA*

Department of Chemistry, Graduate School of Science, Kyoto University, Kitashirakawa, Kyoto 606-8502

(Received December 22, 2005; accepted May 1, 2006; published August 10, 2006)

Half century has past since the pioneering works of Anderson and Kubo on the stochastic theory of spectral line shape were published in J. Phys. Soc. Jpn. **9** (1954) 316 and 935, respectively. In this review, we give an overview and extension of the stochastic Liouville equation focusing on its theoretical background and applications to help further the development of their works. With the aid of path integral formalism, we derive the stochastic Liouville equation for density matrices of a system. We then cast the equation into the hierarchy of equations which can be solved analytically or computationally in a nonperturbative manner including the effect of a colored noise. We elucidate the applications of the stochastic theory from the unified theoretical basis to analyze the dynamics of a system as probed by experiments. We illustrate this as a review of several experimental examples including NMR, dielectric relaxation, Mössbauer spectroscopy, neutron scattering, and linear and nonlinear laser spectroscopies. Following the summary of the advantage and limitation of the stochastic theory, we then derive a quantum Fokker–Planck equation and a quantum master equation from a system–bath Hamiltonian with a suitable spectral distribution producing a nearly Markovian random perturbation. By introducing auxiliary parameters that play a role as stochastic variables in an expression for reduced density matrix, we obtain the stochastic Liouville equation including temperature correction terms. The auxiliary parameters may also be interpreted as a random noise that allows us to derive a quantum Langevin equation for non-Markovian noise at any temperature. The results afford a basis for clarifying the relationship between the stochastic and dynamical approaches. Analytical as well as numerical calculations are given as examples and discussed.

KEYWORDS: Stochastic Liouville equation, quantum Fokker–Planck equation, 2D spectroscopy, NMR
DOI: 10.1143/JPSJ.75.082001

1. Introduction

Since Anderson[1] and Kubo[2] presented a random frequency modulation model for nuclear magnetic resonance (NMR), the stochastic theory has been proven to be a versatile tool for studying diverse topics in physics and chemistry. The well-known stochastic model describes perturbation in the Zeeman energy of a spin by a local random field that originates from dipolar interactions of many other spins in the environment. Such perturbation that causes random modulation can be regarded as a stochastic process. This model leads us to employ an effective Hamiltonian $\hat{H}(t)$ for the spin as a function of stochastic variables $\Omega(t)$ which represents the states of the environment (the bath), $\hat{H}(t) = \hat{H}_A + \hat{H}_I(\Omega(t))$, where $\hat{H}_A$ is the unperturbed Hamiltonian and $\hat{H}_I(\Omega(t))$ is the stochastic perturbation. Thus, the density matrix elements of a spin system become a function of the spin state and stochastic variable. The time evolution of the spin state follows the quantum Liouville equation, whereas the stochastic variables follow a certain law of stochastic time evolution. We call this type of approach a stochastic approach in contrast to a dynamical approach, in which one explicitly assumes a dynamical model for the bath and reduces the bath degrees of freedom using some perturbative calculations[3] or path integrals.[4] The stochastic approach has been used repeatedly to treat dynamical systems under the influence of their environment.[5–12] The model employed in the stochastic approach is a phenomenological one. The underlying stochastic process is merely a model appropriate for the problem rather than something to be derived from all-atom-in-one type microscopic considerations. This is regarded as an advantage since it can simplify the understanding of the problem and can cover a wide range of problems in physics and chemistry from a unified point of view.

The most important and sufficiently realistic stochastic process is a Gaussian one which is further assumed to be Markovian. The Gaussian nature arises if interactions between the system of interest (the main system) and environment (the bath) have a cumulative effect of a large number of weak interactions, and the regular central limit theorem comes into play. If the characteristic time of the main system is much longer than that of the bath, one can regard that the bath interaction is a Markovian process. The Markovian process is characterized by an exponential decay noise. When the correlation time is very short such that the noise is regarded as white, we may have a motionally narrowed limit, where perturbative calculations work well yielding a Lorentzian line shape of the NMR spectrum. On the other hand, if the noise varies very slowly, the line shape becomes Gaussian.[5–8]

To deal with the stochastic Gaussian–Markovian process, there are three possible approaches. (i) First approach utilizes the cumulant expansion technique to calculate a physical observable such as a magnetic response function which is essentially a multi-time correlation function of a magnetic dipole operator.[5] If $\hat{H}(t) = \hat{H}_A + \hat{H}_I(\Omega(t))$ is expressed simply as $\hat{H}(t) = \hbar[\omega_0 + \Omega(t)]\hat{S}_z$, where ω_0 is

*E-mail: tanimura@kuchem.kyoto-u.ac.jp

the resonant frequency of the system and $\hat{S}_z$ is the spin operator, the time evolution operator is expressed in terms of the noise correlation function as $\exp[-i\omega_0\hat{S}_z t - \int d\tau\langle\Omega(\tau)\Omega(0)\rangle\hat{S}_z]$. Then, by assuming the form of the noise correlation such as $\langle\Omega(\tau)\Omega(0)\rangle \propto \delta(\tau)$ (Gaussian-white noise) or $\propto \exp[-\gamma\tau]$ (Gaussian–Markovian noise), we can express the response function analytically. Although this approach is handy, its applicability is limited, since $\hat{H}_A$ and $\hat{H}_I(\Omega(t))$ are usually not commutable and the response function cannot be written down analytically. (ii) The second approach handles the noise explicitly.[13] We introduce a stochastic modulation by employing a sequence of random numbers in time, $\Omega(t) = \{\Omega_1, \Omega_2, \Omega_3, \ldots\}$, which satisfy a stochastic relation. Then, we integrate the quantum Liouville equation for this perturbation numerically to have a stochastic character on the system dynamics. At a glance, this approach looks similar to the classical (or semiclassical) Langevin approach as used in the simulations of Brownian particles.[14] In the Langevin approach, the equation contains a friction term in addition to a random modulation term, and the friction term is related to the random modulation term through the fluctuation–dissipation theorem. The present equation of motion, however, does not involve a friction term. As a result, the trajectory of the state for the given sample of $\Omega(t)$ is not stable for the quantum Liouville equation except for some simple cases. Thus the applicability of this approach is very limited. (iii) The third approach is based on the stochastic Liouville equation.[6–8] Here, instead of following the noise sequence, we deal with the distribution function $P(\Omega; t)$, which is the probability of finding the environment in the state Ω at time t. In this approach, the time evolution of the system state follows a quantum Liouville equation, whereas $P(\Omega; t)$ follows a Markov equation. The applicability of this approach is more extensive than those of the previous two approaches, since the stochastic Liouville equation formalism is based on a kinetic equation which is valid for any forms of $\hat{H}_A$. The calculations can be performed both analytically and computationally in a nonperturbative manner including the effect of a colored noise, which is not easy for dynamical system–bath Hamiltonian approaches without approximations.

From the above-mentioned three approaches, the stochastic theory has widened the scope of such diverse topics as NMR, ESR, muon spin rotation (μSR), Mössbauer spectroscopy, dielectric relaxation, and linear and nonlinear spectroscopies[8,12] as we will briefly review in §4. In this paper, we concentrate on the stochastic Liouville equation approach, since the results obtained using the other two approaches can always be derived by this approach, which allows one to describe the stochastic theory from a unified point of view.

Although there is overwhelming success in the treatment of dissipative phenomena, one drawback of the stochastic approach is that it ignores the reaction of the main system to the bath. The effect of the bath is considered merely as an external force disregarding its dynamic degrees of freedom that is equivalent to assuming an infinite temperature for the bath. This makes no harm in the case of NMR, but gives a serious limitation for a system represented by a coordinate, such as a harmonic or double well potential system, since one cannot define the equilibrium distribution at the infinite temperature.

To clarify the above-mentioned problem and to remedy the drawback, Tanimura and Kubo have explored the relation between the stochastic model and the dynamic model.[15–17] They have used an ensemble of harmonic oscillators as the dynamical bath system, which leads to a Gaussian modulation of the main system, and have employed the Feynman–Vernon formalism to reduce the density matrix for the main system. By assuming an appropriate spectrum for the frequencies of the bath oscillators, they were able to secure the Markovian character by high-temperature approximation yielding a set of equations of motion for the reduced density matrix. The set of equations has a similar hierarchy form to the stochastic Liouville equation. The result involves two terms representing the effect of the bath. One term corresponds to the stochastic interaction with a Gaussian noise and the other term corresponds to the friction term missing in the stochastic model. These two terms relate through the fluctuation–dissipation theorem and assure the equilibrium state at finite temperatures for time $t \to \infty$. This formalism can be applied to a system represented by a coordinate yielding a generalized quantum Fokker–Planck equation;[18,19] the equations of motion can cover the whole range of its correlation time and system–bath coupling strength.

These equations of motion are derived from a dynamic model and are fit for computational calculations; however, they do not have a random modulation (or a Langevin force) explicitly, since the bath degrees of freedom were completely reduced. To see the relation between the above-mentioned equations and stochastic equations, we introduce an auxiliary parameter that serves as a stochastic variable into the expression of a reduced density matrix derived from the dynamic model. We then obtain a stochastic Liouville-like equation, including temperature correction terms, using the framework of the dynamical theory. The auxiliary parameters may also be interpreted as a random noise that allows us to derive a quantum Langevin equation for a non-Markovian noise at any temperature. In this paper, we explain various extensions of the equations of motion.

In §2, we provide the unified and common theoretical basis of the present paper by demonstrating a derivation of a stochastic Liouville equation by means of path integrals. Then in §3, we present the necessary theoretical background for calculating experimental observables with the aid of nonequilibrium statistical mechanics. In §4, we elucidate the application of a stochastic approach to the analysis of the time evolution of a system. We shall illustrate this for several physical examples such as NMR, dielectric relaxation, Mössbauer spectroscopy, neutron scattering, nonadiabatic transition, and linear and nonlinear laser spectroscopies. In §5, we introduce the path-integral formalism to derive the quantum Fokker–Planck equation and the master equation from a system–bath Hamiltonian with a proper spectral distribution producing a nearly Markovian random perturbation. These equations are expressed as a set of simultaneous differential equations that have a similar form to the stochastic Liouville equation. Analytical and numerical methods are discussed to solve the equations for systems described in a discrete energy space and coordinate space as

subjects of nonlinear spectroscopy and chemical reactions. In §6, we introduce an auxiliary parameter that serves as stochastic variable in the path integral expression of a reduced density matrix. Then, we derive the stochastic Liouville equation including a temperature correction term. The auxiliary parameters can also be interpreted as a random noise and allows us to reduce a quantum Langevin equation for a non-Markovian noise at any temperature. We show how this result can be used to perform a Monte Carlo simulation. In §7, we derive the stochastic Liouville equation with a temperature correction from the Hamiltonian system. Section 8 is devoted to conclusions.

2. Stochastic Theory

2.1 Probability distribution function and Markov equation

In this section, we derive the stochastic Liouville equation by a path integral method. Consider a time-dependent real function $\Omega(t)$ whose stochastic property is specified as a Markovian process. Instead of explicitly following a time sequence of $\Omega(t)$, the stochastic Liouville equation approach utilizes a joint probability distribution function $P(\Omega_f; t_f|\Omega_i; t_i)$ which describes the probability of Ω_f appearing at time t_f for the initial Ω_i at time t_i.[10] The expectation value of the function $A(\Omega)$ at time t_f for the initial distribution $P_0(\Omega_i; t_i)$ is then defined by

$$\big\langle A(\Omega(t_f))\big\rangle \equiv \int_{-\infty}^{\infty} \mathrm{d}\Omega_f \int_{-\infty}^{\infty} \mathrm{d}\Omega_i\, A(\Omega_f) P(\Omega_f; t_f|\Omega_i; t_i) P_0(\Omega_i; t_i). \tag{2.1}$$

Similarly, a two-body correlation function is expressed as

$$\big\langle A(\Omega(t_f))B(\Omega(t_i))\big\rangle \equiv \int_{-\infty}^{\infty} \mathrm{d}\Omega_f \int_{-\infty}^{\infty} \mathrm{d}\Omega_i\, A(\Omega_f) P(\Omega_f; t_f|\Omega_i; t_i) B(\Omega_i) P_0(\Omega_i; t_i). \tag{2.2}$$

Here, the initial distribution function $P_0(\Omega_i; t_i)$ is often chosen to be an equilibrium one. We now consider the path integral representation of $P(\Omega_f; t_f|\Omega_i; t_i)$ denoted by $P[\Omega(\tau)]$ as a functional of $\Omega(\tau)$,[20–22]

$$P(\Omega_f; t_f|\Omega_i; t_i) \equiv \int_{\Omega(t_i)=\Omega_i}^{\Omega(t_f)=\Omega_f} D[\Omega(\tau)] P[\Omega(\tau)]. \tag{2.3}$$

For later convenience, we introduce the characteristic functional that is the Fourier transform of the probability density $P[\Omega(\tau)]$,

$$G[\xi(\tau)] \equiv \left\langle \exp\left[\mathrm{i}\gamma \int_{t_i}^{t_f} \mathrm{d}\tau\, \xi(\tau)\Omega(\tau) \right] \right\rangle. \tag{2.4}$$

The characteristic functional can be regarded as a generating functional of $P[\Omega(\tau)]$, which is conveniently used in calculating the various physical variables such as a two-body correlation function by $\gamma^2\langle\Omega(t')\Omega(t'')\rangle = -\delta^2 G[\xi(\tau)]/\delta\xi(t')\delta\xi(t'')|_{\xi(t)=0}$, where δ represents the functional derivative. We expand $G[\xi(\tau)]$ in terms of $\xi(\tau)$ as

$$G[\xi(\tau)] = 1 + \sum_{n=1}^{\infty} \frac{(\mathrm{i}\gamma)^n}{n!} \int_{t_i}^{t_f} \mathrm{d}\tau_1 \int_{t_i}^{t_f} \mathrm{d}\tau_2 \cdots \int_{t_i}^{t_f} \mathrm{d}\tau_n \xi(\tau_1)\xi(\tau_2)\cdots\xi(\tau_n)\langle\Omega(\tau_1)\Omega(\tau_2)\cdots\Omega(\tau_n)\rangle. \tag{2.5}$$

If $\Omega(\tau)$ is Gaussian, the correlation function $\langle\Omega(\tau_1)\Omega(\tau_2)\cdots\Omega(\tau_n)\rangle$ for $n = 2N+1$ is zero and that for $n = 2N$ can be subdivided into N uncorrelated pairs as

$$\langle\Omega(\tau_1)\Omega(\tau_2)\cdots\Omega(\tau_n)\rangle = \sum_{\{k_1,k_2,\cdots,k_n\}} \big\langle\Omega(\tau_{k_1})\Omega(\tau_{k_2})\big\rangle \cdots \big\langle\Omega(\tau_{k_{n-1}})\Omega(\tau_{k_n})\big\rangle. \tag{2.6}$$

Thus, we have[20,21]

$$G[\xi(\tau)] = \exp\left[-\frac{\gamma^2}{2} \int_{t_i}^{t_f} \mathrm{d}\tau \int_{t_i}^{t_f} \mathrm{d}\tau'\, \xi(\tau)\big\langle\Omega(\tau)\Omega(\tau')\big\rangle\xi(\tau') \right]. \tag{2.7}$$

By calculating the inverse Fourier transformation of $G[\xi(\tau)]$, we have the probability distribution function as

$$P[\Omega(\tau)] = C^{-1} \exp\left[-\frac{\gamma^2}{2} \int_{t_i}^{t_f} \mathrm{d}\tau \int_{t_i}^{t_f} \mathrm{d}\tau' \Omega(\tau)\big\langle\Omega(\tau)\Omega(\tau')\big\rangle^{-1}\Omega(\tau') \right], \tag{2.8}$$

where, for the correlation function $\langle\Omega(\tau)\Omega(\tau')\rangle$, the inverse function is defined by

$$\gamma \int_{t_i}^{t_f} \mathrm{d}t \langle\Omega(\tau)\Omega(t)\rangle^{-1}\big\langle\Omega(t)\Omega(\tau')\big\rangle = \frac{1}{\gamma}\delta(\tau-\tau'), \tag{2.9}$$

and C is the normalization constant that has to be set later.

We consider a process defined by the correlation function

$$\big\langle\Omega(\tau)\Omega(\tau')\big\rangle \equiv \mathrm{e}^{-\gamma|\tau-\tau'|}. \tag{2.10}$$

Since the above equation satisfies

$$\left(\frac{\partial^2}{\partial\tau^2} - \gamma^2\right)\big\langle\Omega(\tau)\Omega(\tau')\big\rangle = -2\gamma\delta(\tau-\tau'), \tag{2.11}$$

by multiplying $\langle\Omega(\tau')\Omega(\tau'')\rangle^{-1}$ to both sides and by integrating it over τ', we have the inverse function in the form

$$\big\langle\Omega(\tau)\Omega(\tau'')\big\rangle^{-1} = -\frac{1}{2\gamma^3}\left(\frac{\partial^2}{\partial\tau^2} - \gamma^2\right)\delta(\tau-\tau''). \tag{2.12}$$

The substitution of the above equation using integration by parts leads to the distribution function in the form,

$$P[\Omega(\tau)] = C^{-1} \exp\left[-\frac{1}{4\gamma} \int_{t_i}^{t_f} \mathrm{d}\tau \big(\dot\Omega(\tau) + \gamma\Omega(\tau)\big)^2 \right]. \tag{2.13}$$

Note that the boundary condition of the functional integral $[\dot\Omega(\tau)\Omega(\tau) + \gamma\Omega(\tau)\Omega(\tau)]|_{\tau=t_i}^{\tau=t}$ has been set to zero. The joint

probability distribution $P(\Omega_f;t_f|\Omega_i;t_i)$ is then expressed as eq. (2.3).

We now derive the time differential equation for $P(\Omega;t|\Omega_i;t_i)$. Consider $P(\Omega;t+\varepsilon|\Omega_i;t_i)$. If we set $\Omega(t+\varepsilon)=\Omega$, $\Omega(t)=\Omega_f$, and $\dot{\Omega}(t)=(\Omega-\Omega_f)/\varepsilon$, then we have

$$P(\Omega;t+\varepsilon|\Omega_i;t_i)=\frac{1}{C}\int_{-\infty}^{\infty}\mathrm{d}y\exp\left[-\frac{\gamma\varepsilon}{4}\left(\frac{y}{\gamma\varepsilon}+\Omega-y\right)^2\right]\times P(\Omega-y;t|\Omega_i;t_i), \tag{2.14}$$

where $y=\Omega-\Omega_f$. Since ε is very small, the integration of $\exp[-y^2/4\gamma\varepsilon]$ on y can contribute to the very small region of y. Therefore, we expand the above equation as

$$P(\Omega;t+\varepsilon|\Omega_i;t_i)=\frac{1}{C}\int_{-\infty}^{\infty}\mathrm{d}y\exp\left[-\frac{y^2}{4\gamma\varepsilon}\right]\times\left[1-\frac{\Omega^2}{4}\left(\varepsilon\gamma-\frac{y^2}{2}\right)+\frac{y^2}{2}\left(\frac{\partial^2}{\partial\Omega^2}+\Omega\frac{\partial}{\partial\Omega}+1\right)\right]\times P(\Omega;t|\Omega_i;t_i), \tag{2.15}$$

where we drop the terms proportional to y, since they will vanish after the Gaussian integrations. Then, by performing the integrals over y, we have

$$P(\Omega;t+\varepsilon|\Omega_i;t_i)-P(\Omega;t|\Omega_i;t_i)=\varepsilon\gamma\left(\frac{\partial^2}{\partial\Omega^2}+\Omega\frac{\partial}{\partial\Omega}+1\right)P(\Omega;t|\Omega_i;t_i), \tag{2.16}$$

where we set $C=2\sqrt{\gamma\varepsilon\pi}$ to have $P(\Omega;t+\varepsilon|\Omega_i;t_i)=P(\Omega;t|\Omega_i;t_i)$ at $\varepsilon=0$. If we take the limit $\varepsilon\to 0$, the above equation reduces to

$$\frac{\partial}{\partial t}P(\Omega;t|\Omega_i;t_i)=\hat{\Gamma}_\Omega P(\Omega;t|\Omega_i;t_i), \tag{2.17}$$

where

$$\hat{\Gamma}_\Omega\equiv\gamma\frac{\partial}{\partial\Omega}\left(\Omega+\frac{\partial}{\partial\Omega}\right). \tag{2.18}$$

The above result is known as the Markov equation for Gaussian distribution, which is usually derived from the Chapman–Kolmogorov equation.[3)]

2.2 *Eigenstate representation of Markov operator*

Consider the probability distribution function for the initial condition $P_0(\Omega_i;t_i)$ defined by

$$P(\Omega;t)\equiv\int_{-\infty}^{\infty}\mathrm{d}\Omega_i\,P(\Omega;t|\Omega_i;t_i)P_0(\Omega_i;t_i). \tag{2.19}$$

Since $P(\Omega;t)$ follows the same Markov equation as eq. (2.17), this can be solved formally as

$$P(\Omega;t)=\exp\left[\hat{\Gamma}_\Omega(t-t_i)\right]P_0(\Omega;t_i). \tag{2.20}$$

The equilibrium distribution $P_{\mathrm{eq}}(\Omega)=P(\Omega;t\to\infty)$ is given by

$$P_{\mathrm{eq}}(\Omega)=\frac{1}{\sqrt{2\pi}}\mathrm{e}^{-\Omega^2/2}, \tag{2.21}$$

which satisfies the condition $\hat{\Gamma}_\Omega P_{\mathrm{eq}}(\Omega)=0$.

We now introduce the stochastic operator $\hat{\Omega}$ and its eigenvectors $\hat{\Omega}|\Omega)=\Omega|\Omega)$ and $(\Omega'|\hat{\Omega}=(\Omega'|\Omega'$.[8)] Similarly to the bracket representation introduced by Dirac, these vectors satisfy the orthogonal relation $(\Omega'|\Omega)=\delta(\Omega'-\Omega)$ and the completeness relation $\int\mathrm{d}\Omega|\Omega)(\Omega|=1$. To describe the initial equilibrium distribution, we introduce $|i)$ defined by $P_{\mathrm{eq}}(\Omega)\equiv(\Omega|i)$. If we introduce $(f|\Omega)\equiv 1$ to represent the final trace operation, the equilibrium expectation value is expressed as

$$\langle A(\Omega)\rangle\equiv\int_{-\infty}^{\infty}\mathrm{d}\Omega\,A(\Omega)P_{\mathrm{eq}}(\Omega)=\big(f|A(\hat{\Omega})|i\big). \tag{2.22}$$

The two-body correlation function is also written as

$$\begin{aligned}\big\langle A(\Omega(t))B(\Omega(t'))\big\rangle&=\int_{-\infty}^{\infty}\mathrm{d}\Omega\,A(\Omega)\Big\{\mathrm{e}^{\hat{\Gamma}_\Omega(t-t')}\big[B(\Omega)P_{\mathrm{eq}}(\Omega)\big]\Big\}\\&=\big(f|A(\hat{\Omega})\mathrm{e}^{\hat{\Gamma}(t-t')}B(\hat{\Omega})|i\big),\end{aligned} \tag{2.23}$$

where we assume $t\geq t'$ and $\hat{\Gamma}$ is the operator whose matrix elements are defined by

$$(\Omega'|\hat{\Gamma}|\Omega)=\delta(\Omega'-\Omega)\hat{\Gamma}_\Omega. \tag{2.24}$$

Here, $\hat{\Gamma}_\Omega$ is given by eq. (2.18). We consider the transformation $\hat{O}'=\mathrm{e}^{\hat{\Omega}^2/4}\hat{O}\mathrm{e}^{-\hat{\Omega}^2/4}$ for any operator $\hat{O}$. This leads to

$$\mathrm{e}^{\hat{\Omega}^2/4}\hat{\Gamma}\mathrm{e}^{-\hat{\Omega}^2/4}\to\hat{\Gamma}'=-\gamma\hat{b}^+\hat{b}^-, \tag{2.25}$$

where

$$(\Omega'|\hat{b}^\pm|\Omega)\equiv\delta(\Omega'-\Omega)\left(\frac{\Omega}{2}\mp\frac{\partial}{\partial\Omega}\right), \tag{2.26}$$

so that $\hat{\Omega}=\hat{b}^-+\hat{b}^+$. The eigenstates of $\hat{b}^+\hat{b}^-$ are denoted by $|n)$. If we define

$$(\Omega|n)=\frac{2^{-n/2}}{n!\sqrt[4]{2\pi}}H_n\left(\Omega/\sqrt{2}\right)\mathrm{e}^{-\Omega^2/4}, \tag{2.27}$$

where $H_n(\Omega/\sqrt{2})$ is the Hermite polynomial functions, we have the relations

$$\hat{b}^+|n)=(n+1)|n+1),\quad \hat{b}^-|n)=|n-1), \tag{2.28}$$

and $\hat{b}^+\hat{b}^-|n)=n|n)$. The conjugate vector $(n|$ can be defined accordingly, and we have $(n|\Omega)=(\Omega|n)$, $(\Omega|i)=(2\pi)^{-1/4}\mathrm{e}^{-\Omega^2/4}(\Omega|0)$, and $(f|\Omega)=(2\pi)^{1/4}\mathrm{e}^{\Omega^2/4}(0|\Omega)$. The completeness relation is now given by $\Sigma|n)(n|=1$. By performing the transformation $\hat{O}\to\hat{O}'$, we have the equilibrium expectation value in the form $\langle A(\hat{\Omega})\rangle=(0|A(\hat{b}^-+\hat{b}^+)|0)$. The two-body correlation function eq. (2.23) is expressed as

$$\big\langle A(\Omega(t))B(\Omega(t'))\big\rangle=\big(0|A(\hat{b}^-+\hat{b}^+)\exp\big[-\gamma\hat{b}^+\hat{b}^-(t-t')\big]\times B(\hat{b}^-+\hat{b}^+)|0\big). \tag{2.29}$$

This leads to $\langle\Omega(t)\Omega(t')\rangle=\exp[-\gamma(t-t')]$.

Using $|n)$, we can express any probability distribution function $P(\Omega;t)=\sum_n P_n(t)(\Omega|n)$ as

$$\mathbf{P}(t)=\sum_n P_n(t)|n), \tag{2.30}$$

where $P_n(t)\equiv\int\mathrm{d}\Omega_i(n|\exp[\hat{\Gamma}(t-t_i)]|\Omega_i)P(\Omega_i;t_i)$.

If we employ only two eigenstates and construct the new states $P_+\equiv(P_0+P_1)/2$ and $P_-\equiv(P_0-P_1)/2$, then the Markov equation is written as

$$\frac{\partial}{\partial t}\begin{bmatrix}P_+(t)\\P_-(t)\end{bmatrix}=\frac{\gamma}{2}\begin{bmatrix}-1&1\\1&-1\end{bmatrix}\begin{bmatrix}P_+(t)\\P_-(t)\end{bmatrix}. \tag{2.31}$$

This equation describes a stochastic two-state jump Markovian process.[8] In this case, the equilibrium distribution is given by $P_+ = P_- = 1/2$. An extension to a multistate jump process is straightforward. Note that since we neglect the higher-order hierarchy, multistate jump processes are Markovian but no longer Gaussian.

2.3 Stochastic Liouville equation

Let us consider a system A coupled to a function $\Omega(\tau)$.

$$\hat{H}\big(\hat{a}^+, \hat{a}^-; \Omega(\tau)\big) \equiv \hat{H}_A(\hat{a}^+, \hat{a}^-) + \hat{V}(\hat{a}^+, \hat{a}^-)\Omega(\tau). \quad (2.32)$$

Here, $\hat{H}_A(\hat{a}^+, \hat{a}^-)$ is the Hamiltonian of A and $\hat{V}(\hat{a}^+, \hat{a}^-)$ is a coupling operator for A described by a set of creation and annihilation operators, $\hat{a}^+$ and $\hat{a}^-$, respectively. For a many-particle system, $\hat{a}^+$ and $\hat{a}^-$ can be regarded as a set of operators, $\{\hat{a}_j^+, \hat{a}_j^-\}$. The time evolution of the system for the function $\Omega(\tau)$ is determined by the quantal Liouville equation for the Hamiltonian eq. (2.32). We denote the density matrix of A for $\Omega(\tau)$ by $\hat{\rho}(\Omega; t)$. If the function $\Omega(\tau)$ is a Gaussian–Markovian process characterized by the probability distribution functional $P[\Omega(\tau)]$ given by eq. (2.13), the total density matrix at time t is expressed in the path integral form as

$$\begin{aligned}\rho(\phi^\dagger, \phi'; \Omega; t) = & \int D[\phi^\dagger(\tau)\phi(\tau)] \int D[\phi'^\dagger(\tau)\phi'(\tau)] \\ & \times \int_{-\infty}^{\infty} \mathrm{d}\Omega_i \int_{\Omega(t_i)=\Omega_i}^{\Omega(t)=\Omega} D[\Omega(\tau)] \\ & \times \exp\left\{\frac{\mathrm{i}}{\hbar} S[\phi^\dagger, \phi; \Omega; t]\right\} \rho'_A(\phi_i^\dagger, \phi'_i) \\ & \times \exp\left\{-\frac{\mathrm{i}}{\hbar} S^\dagger[\phi'^\dagger, \phi'; \Omega; t]\right\} P[\Omega(\tau)] P_{\mathrm{eq}}(\Omega_i), \end{aligned} \quad (2.33)$$

where ϕ and its conjugate $\phi^\dagger$ are the eigenvalue of the operators $\hat{a}^-$ and $\hat{a}^+$ for the eigenvector $|\phi\rangle$, respectively. They are complex variables for Bosons and Grassman variables for Fermions.[23] The functional integrals and actions are defined by

$$\int D[\phi^\dagger(\tau)\phi(\tau)] \equiv \lim_{M\to\infty} \mathrm{e}^{\phi_M^\dagger \phi_M} \prod_{k=1}^{M-1} \frac{1}{N} \iint \mathrm{d}\phi_k^\dagger \, \mathrm{d}\phi_k \quad (2.34)$$

in which $\phi_0 = \phi_i$ and $\phi_M = \phi$, and N is the normalization constant of the integrals. Then the functional integral runs from $\phi(t_i) = \phi_i$ to $\phi(t) = \phi$. The action is defined by

$$\begin{aligned} & S[\phi^\dagger, \phi; \Omega; t] \\ & = \lim_{M\to\infty} \sum_{k=1}^{M} \varepsilon \left[\mathrm{i}\hbar \phi_k^\dagger \frac{\phi_k - \phi_{k-1}}{\varepsilon} - H(\phi_k^\dagger, \phi_{k-1}; \Omega_k) \right] \\ & \equiv \int_{t_i}^{t} \mathrm{d}\tau \big[\mathrm{i}\hbar \phi^\dagger(\tau)\dot{\phi}(\tau) - H\big(\phi^\dagger(\tau), \phi(\tau); \Omega(\tau)\big) \big], \end{aligned} \quad (2.35)$$

where $H(\phi^\dagger, \phi; \Omega)$ is the coherent state representation of $\hat{H}(\hat{a}^+, \hat{a}^-; \Omega)$ and $\epsilon \equiv (t - t_i)/M$. The action for the right-hand-side wave function is the conjugate of the left one and is denoted by $S^\dagger[\phi'^\dagger, \phi'; \Omega; t]$. To achieve eq. (2.33), we assumed the initial state of the total system in factorized form as

$$\hat{\rho}(\Omega_i; t_i) = \hat{\rho}_A(t_i) P_{\mathrm{eq}}(\Omega_i), \quad (2.36)$$

where $P_{\mathrm{eq}}(\Omega_i)$ is the equilibrium distribution function for $\Omega_i \equiv \Omega(t_i)$ and $\hat{\rho}_A(t_i)$ is the initial density matrix of A; it is represented in the coherent state as $\hat{\rho}_A(t_i) \equiv N^{-2} \iint \mathrm{d}\phi_i^\dagger \, \mathrm{d}\phi_i \iint \mathrm{d}\phi_i'^\dagger \, \mathrm{d}\phi_i' |\phi_i\rangle \rho'_A(\phi_i^\dagger, \phi'_i) \langle\phi'_i|$ with $\rho'_A(\phi_i^\dagger, \phi'_i) \equiv \mathrm{e}^{\phi_i^\dagger \phi_i + \phi_i'^\dagger \phi'_i} \langle\phi_i|\hat{\rho}_A(t_i)|\phi'_i\rangle$. Note that the extension to the correlated initial condition will be discussed in §5.4 in the context of the quantum Fokker–Planck equation and master equation.

The time derivative of $\rho(\phi^\dagger, \phi'; \Omega; t)$ consists of the time derivative of the left- and right-hand side wave functions as expressed by the actions, and the time derivative of the stochastic distribution function $P(\Omega; t|\Omega_i; t_i)$ that is defined by eqs. (2.3) and (2.13). Since the density matrix is expressed as $\hat{\rho}(\Omega; t) = N^{-2} \iint \mathrm{d}\phi^\dagger \, \mathrm{d}\phi \iint \mathrm{d}\phi'^\dagger \, \mathrm{d}\phi' |\phi\rangle \rho(\phi^\dagger, \phi'; \Omega; t) \langle\phi'|$, the equation of motion for $\hat{\rho}(\Omega; t)$ is then given by

$$\begin{aligned} \frac{\partial}{\partial t}\hat{\rho}(\Omega; t) = & -\frac{\mathrm{i}}{\hbar}\hat{H}_A^\times \hat{\rho}(\Omega; t) - \frac{\mathrm{i}}{\hbar}\hat{V}^\times \Omega \hat{\rho}(\Omega; t) \\ & + \hat{\Gamma}_\Omega \hat{\rho}(\Omega; t), \end{aligned} \quad (2.37)$$

where

$$\hat{A}^\times \hat{\rho} \equiv \hat{A}\hat{\rho} - \hat{\rho}\hat{A}, \quad (2.38)$$

and $\hat{\Gamma}_\Omega$ is defined by eq. (2.18). This is Kubo's stochastic Liouville equation.[7,8] The density matrix for system A is expressed as $\hat{\rho}(t) = \int \mathrm{d}\Omega \, \hat{\rho}(\Omega; t)$.

2.4 Continued fractional expression of stochastic Liouville equation

In the operator representation eq. (2.28), the stochastic Liouville equation eq. (2.37) is written as

$$\begin{aligned} \frac{\partial}{\partial t}\hat{\boldsymbol{\rho}}(t) = & -\left(\frac{\mathrm{i}}{\hbar}\hat{H}_A^\times + \gamma \hat{b}^+ \hat{b}^-\right)\hat{\boldsymbol{\rho}}(t) - \frac{\mathrm{i}}{\hbar}\hat{V}^\times \hat{b}^+ \hat{\boldsymbol{\rho}}(t) \\ & - \frac{\mathrm{i}}{\hbar}\hat{V}^\times \hat{b}^- \hat{\boldsymbol{\rho}}(t), \end{aligned} \quad (2.39)$$

in which $\hat{\boldsymbol{\rho}}(t)$ is defined by

$$\hat{\rho}(\Omega; t) \Rightarrow \hat{\boldsymbol{\rho}}(t) = \sum_n \hat{\rho}_n(t)|n). \quad (2.40)$$

For each of the operator $|n)$, the equation of motion is expressed in hierarchy form as[8]

$$\frac{\partial}{\partial t}\hat{\rho}_0(t) = -\frac{\mathrm{i}}{\hbar}\hat{H}_A^\times \hat{\rho}_0(t) - \frac{\mathrm{i}}{\hbar}\hat{V}^\times \hat{\rho}_1(t), \quad (2.41)$$

$$\begin{aligned} \frac{\partial}{\partial t}\hat{\rho}_1(t) = & -\left(\frac{\mathrm{i}}{\hbar}\hat{H}_A^\times + \gamma\right)\hat{\rho}_1(t) - \frac{\mathrm{i}}{\hbar}\hat{V}^\times \hat{\rho}_2(t) \\ & - \frac{\mathrm{i}}{\hbar}\hat{V}^\times \hat{\rho}_0(t), \end{aligned} \quad (2.42)$$

and

$$\begin{aligned} \frac{\partial}{\partial t}\hat{\rho}_n(t) = & -\left(\frac{\mathrm{i}}{\hbar}\hat{H}_A^\times + n\gamma\right)\hat{\rho}_n(t) - \frac{\mathrm{i}}{\hbar}\hat{V}^\times \hat{\rho}_{n+1}(t) \\ & - \frac{\mathrm{i}n}{\hbar}\hat{V}^\times \hat{\rho}_{n-1}(t). \end{aligned} \quad (2.43)$$

Consider the Laplace transform of each operator element,

$$\hat{\rho}_n[s] = \int_{t_i}^{\infty} \mathrm{d}t \exp[-s(t - t_i)]\hat{\rho}_n(t). \quad (2.44)$$

Then the Laplace transformation of eqs. (2.41)–(2.43) is expressed as

$$\boldsymbol{\rho}[s] = (s\mathbf{I} + \mathbf{L})^{-1}\boldsymbol{\rho}(t_i), \tag{2.45}$$

where $\mathbf{I}$ is the unit matrix, $\boldsymbol{\rho}(t)$ and $\boldsymbol{\rho}[s]$ are column vectors with the elements $\hat{\rho}_n(t)$ and $\hat{\rho}_n[s]$, respectively, and $(s\mathbf{I} + \mathbf{L})$ is the matrix with operator elements expressed as

$$(s\mathbf{I} + \mathbf{L}) \equiv \left[\begin{array}{c|cccccc} s + \frac{\mathrm{i}}{\hbar}\hat{H}_A^\times & \frac{\mathrm{i}}{\hbar}\hat{V}^\times & 0 & 0 & 0 & 0 & \cdots \\ \hline \frac{\mathrm{i}}{\hbar}\hat{V}^\times & s + \gamma + \frac{\mathrm{i}}{\hbar}\hat{H}_A^\times & \frac{\mathrm{i}}{\hbar}\hat{V}^\times & 0 & 0 & 0 & \cdots \\ 0 & \frac{2\mathrm{i}}{\hbar}\hat{V}^\times & s + 2\gamma + \frac{\mathrm{i}}{\hbar}\hat{H}_A^\times & \frac{\mathrm{i}}{\hbar}\hat{V}^\times & 0 & 0 & \ddots \\ 0 & 0 & \frac{3\mathrm{i}}{\hbar}\hat{V}^\times & \ddots & \ddots & 0 & \ddots \\ 0 & 0 & 0 & \frac{\mathrm{i}n}{\hbar}\hat{V}^\times & s + n\gamma + \frac{\mathrm{i}}{\hbar}\hat{H}_A^\times & \frac{\mathrm{i}}{\hbar}\hat{V}^\times & \ddots \\ \vdots & \vdots & \vdots & \ddots & \ddots & \ddots & \ddots \end{array}\right]. \tag{2.46}$$

To evaluate the inverse of eq. (2.46), we shall divide the matrix into two square matrices $\mathbf{A}$ and $\mathbf{D}$ and the rectangular matrices $\mathbf{B}$ and $\mathbf{C}$. The $(1,1)$ element (the domain of $\mathbf{A}$) of the inverse matrix is expressed as[15]

$$\left[\begin{array}{c|c} \mathbf{A} & \mathbf{B} \\ \hline \mathbf{C} & \mathbf{D} \end{array}\right]^{-1}_{11} = \frac{\mathbf{1}}{\mathbf{A} - \mathbf{B}\frac{\mathbf{1}}{\mathbf{D}}\mathbf{C}}, \tag{2.47}$$

where the fractional expression means the inverse operator or matrix. By successive applications of the above equation to eq. (2.46), we have

$$\hat{\rho}_0[s] = \hat{G}_0[s]\hat{\rho}_0(t_i), \tag{2.48}$$

where we assumed that $\hat{\rho}_n(t_i) = 0$ for $n > 0$ as the initial condition and

$$\hat{G}_0[s] \equiv \cfrac{1}{s + \frac{\mathrm{i}}{\hbar}\hat{H}_A^\times + \frac{1}{\hbar^2}\hat{V}^\times \cfrac{1}{s + \gamma + \frac{\mathrm{i}}{\hbar}\hat{H}_A^\times + \frac{1}{\hbar^2}\hat{V}^\times \cfrac{2}{s + 2\gamma + \frac{\mathrm{i}}{\hbar}\hat{H}_A^\times + \frac{1}{\hbar^2}\hat{V}^\times \frac{3}{\ddots}\hat{V}^\times}\hat{V}^\times}\hat{V}^\times}. \tag{2.49}$$

This method developed for the Gaussian–Markovian process allows us to write the line shape of the spectrum in terms of a continued fraction expression.[5,8] The method covers the whole range of noise correlation times for any system–bath coupling, where perturbative approaches are not applicable.

To show how the above-mentioned method works, let us consider a two-level system defined by $|1\rangle$ and $|0\rangle$. The Hamiltonian of the system is given by

$$\hat{H}_A = \frac{1}{2}\hbar\omega_0\hat{\sigma}_z, \tag{2.50}$$

where $\hat{\sigma}_i$ for $i = x, y, z$ are Pauli matrices. The random modulation of the energy levels are taken into account by setting the stochastic interaction as

$$\hat{V} = \frac{1}{2}\hbar\Delta\hat{\sigma}_z. \tag{2.51}$$

We expand the density operator as $\hat{\rho}_n(t) \equiv \sum_{jk}\rho_{jk}^{(n)}(t)|jk\rangle\rangle$, where $|jk\rangle\rangle \equiv |j\rangle\langle k|$. Then the hyper-operators $\hat{H}_A^\times$ and $V^\times$ for each $\hat{\rho}_n(t)$ can be expressed in 4×4 matrices for the column vector expression $\rho_{jk}^{(n)}(t)$. Since all matrices are now diagonal, eq. (2.48) is calculated as

$$\begin{bmatrix} \rho_{11}^{(0)}[s] \\ \rho_{00}^{(0)}[s] \\ \rho_{10}^{(0)}[s] \\ \rho_{01}^{(0)}[s] \end{bmatrix} = \begin{bmatrix} s^{-1} & 0 & 0 & 0 \\ 0 & s^{-1} & 0 & 0 \\ 0 & 0 & G_+[s] & 0 \\ 0 & 0 & 0 & G_-[s] \end{bmatrix} \begin{bmatrix} \rho_{11}^{(0)}(t_i) \\ \rho_{00}^{(0)}(t_i) \\ \rho_{10}^{(0)}(t_i) \\ \rho_{01}^{(0)}(t_i) \end{bmatrix}, \tag{2.52}$$

where

$$G_\pm[s] \equiv \cfrac{1}{s \pm \mathrm{i}\omega_0 + \cfrac{\Delta^2}{s + \gamma \pm \mathrm{i}\omega_0 + \cfrac{2\Delta^2}{s + 2\gamma \pm \mathrm{i}\omega_0 + \ddots}}}. \tag{2.53}$$

If the correlation of noise γ is large compared with the amplitude of fluctuation Δ, i.e., $\gamma \gg \Delta$, ω_0 for a fixed $\gamma' = \Delta^2/\gamma$ (motional narrowing limit), $G_\pm[s]$ becomes

$$G_\pm[s] = \frac{1}{s \pm \mathrm{i}\omega_0 + \gamma'}. \tag{2.54}$$

In the slow modulation limit with the condition $\gamma \ll |s \pm \mathrm{i}\omega_0|$, we have[15]

$$G_{\pm}[s] = \frac{\sqrt{2}}{\Delta}\exp\left[\frac{(s \pm \mathrm{i}\omega_0)^2}{2\Delta^2}\right]\mathrm{erfc}\left(\frac{s \pm \mathrm{i}\omega_0}{\sqrt{2}\Delta}\right), \quad (2.55)$$

where we have used the Laplace–Jacobi formula. If we further assume $|s \pm \mathrm{i}\omega_0| \ll \sqrt{2}\Delta$, the error integral gives $\sqrt{\pi}/2$ and eq. (2.55) takes the Gaussian form

$$G_{\pm}[s] = \sqrt{\frac{\pi}{2\Delta^2}}\exp\left[\frac{(s \pm \mathrm{i}\omega_0)^2}{2\Delta^2}\right]. \quad (2.56)$$

The above results will be used in §4 to evaluate the Fourier spectrum of density matrix elements.

2.5 *Terminator of hierarchy equations*

The hierarchy of equations of motion introduced above continues to infinity, which is not easy to solve numerically. If the system–bath coupling Δ is small, the contribution of the higher members of hierarchy elements becomes smaller than that of the lower members, i.e., $\hat{\rho}_n(t) \gg \Delta\hat{\rho}_{n+1}(t)/\gamma$; thus, we can safely neglect the deeper hierarchy. This is not the case, however, if the system–bath interaction is strong. Fortunately, there is a simple relation between the higher members of hierarchy elements. Using this relation, we can terminate the hierarchy and obtain a set of simultaneous differential equations without loosing accuracy, which is convenient for numerical studies.[18] To determine the relation, we consider the Nth hierarchy that satisfies the condition $(N+1)\gamma \gg \omega_A$, where ω_A is a characteristic frequency of the system,

$$\frac{\partial}{\partial t}\hat{\rho}_N(t) = -\left(\frac{\mathrm{i}}{\hbar}\hat{H}_A^{\times} + N\gamma\right)\hat{\rho}_N(t) - \frac{\mathrm{i}}{\hbar}\hat{V}^{\times}\hat{\rho}_{N+1}(t) - \frac{\mathrm{i}N}{\hbar}\hat{V}^{\times}\hat{\rho}_{N-1}(t). \quad (2.57)$$

For $k \geq N+1$, we can formally solve the equation of motion as

$$\hat{\rho}_k(t) = -\frac{\mathrm{i}}{\hbar}\int_{t_i}^{t}\mathrm{d}\tau\exp\left[\left(-\frac{\mathrm{i}}{\hbar}\hat{H}_A^{\times} - k\gamma\right)(t-\tau)\right] \times \hat{V}^{\times}\left[\hat{\rho}_{k+1}(\tau) + k\hat{\rho}_{k-1}(\tau)\right], \quad (2.58)$$

in which we assumed $\hat{\rho}_k(t_i) = 0$. Since $k\gamma$ is sufficiently large compared with ω_A, the elements in the above equation can be approximated as $\hat{\rho}_{k+1}(\tau) \approx \hat{\rho}_{k+1}(t)$ and $\hat{\rho}_{k-1}(\tau) \approx \hat{\rho}_{k-1}(t)$. Integrating over time, we have

$$\hat{\rho}_k(t) \approx -\frac{\mathrm{i}}{k\hbar\gamma}\hat{V}^{\times}\hat{\rho}_{k+1}(t) - \frac{\mathrm{i}}{\hbar\gamma}\hat{V}^{\times}\hat{\rho}_{k-1}(t). \quad (2.59)$$

The hierarchy member for $k \geq N+1$ is then evaluated as

$$\hat{\rho}_{N+1}(t) = \cfrac{-\mathrm{i}}{\hbar\gamma + \hat{V}^{\times}\cfrac{1}{(N+1)\hbar\gamma + \hat{V}^{\times}\cfrac{N+1}{(N+2)\hbar\gamma + \ddots}\hat{V}^{\times}}\hat{V}^{\times}}\hat{\rho}_N(t). \quad (2.60)$$

Since the continued fractional part becomes constant for larger $(N+1)\gamma^2 \gg \Delta^2$, where Δ is the amplitude of the fluctuation, we have

$$\hat{\rho}_{N+1}(t) = -\frac{\mathrm{i}}{\hbar\gamma}\hat{V}^{\times}\hat{\rho}_N(t). \quad (2.61)$$

Inserting the above equation into eq. (2.57), we have the terminator for eqs. (2.41)–(2.43) in the form

$$\frac{\partial}{\partial t}\hat{\rho}_N(t) = -\left(\frac{\mathrm{i}}{\hbar}\hat{H}_A^{\times} + N\gamma\right)\hat{\rho}_N(t) - \frac{1}{\hbar^2\gamma}\hat{V}^{\times}\hat{V}^{\times}\hat{\rho}_N(t) - \frac{\mathrm{i}N}{\hbar}\hat{V}^{\times}\hat{\rho}_{N-1}(t). \quad (2.62)$$

Since we can always choose N to satisfy $(N+1)\gamma \gg \omega_A$, the hierarchy of equations of motion eqs. (2.41)–(2.43) can be safely truncated by eq. (2.62). Then, by numerically integrating this set of simultaneous differential equations, we can study the dynamics of a system under stochastic fluctuation. The application of this method will be discussed in §4.1.

For $\gamma \gg \omega_A$ with a fixed value of Δ^2/γ, we can set $N = 0$ leading to

$$\frac{\partial}{\partial t}\hat{\rho}_0(t) = -\frac{\mathrm{i}}{\hbar}\hat{H}_A^{\times}\hat{\rho}_0(t) - \frac{1}{\hbar^2\gamma}\hat{V}^{\times}\hat{V}^{\times}\hat{\rho}_0(t), \quad (2.63)$$

which is the quantum master equation.

For a two-level system with diagonal modulation, eqs. (2.50) and (2.51), we have

$$\frac{\partial}{\partial t}\hat{\rho}_0(t) = -\frac{\mathrm{i}}{2}\omega_0[\hat{\sigma}_z, \hat{\rho}_0(t)] - \frac{\gamma'}{4}\left[\hat{\sigma}_z, [\hat{\sigma}_z, \hat{\rho}_0(t)]\right], \quad (2.64)$$

where $\gamma' \equiv \Delta^2/\gamma$. The above equation describes phase relaxation ($T_2^{\dagger}$ relaxation in the Bloch equation) in NMR or laser spectroscopy.

2.6 *Two-state jump model*

Thus far, we have considered the Gaussian process whose equilibrium distribution is expressed by a Gaussian distribution. The stochastic Liouville equation approach, however, may also be applied to non-Gaussian processes. The simplest example is the stochastic two-state jump model, whose stochastic state consists only of $|+\rangle$ and $|-\rangle$. The equation of motion is given by[8]

$$\frac{\partial}{\partial t}\begin{bmatrix}\hat{\rho}_+(t)\\ \hat{\rho}_-(t)\end{bmatrix} = -\frac{\mathrm{i}}{\hbar}\begin{bmatrix}\hat{H}_A^{\times} & 0\\ 0 & \hat{H}_A^{\times}\end{bmatrix}\begin{bmatrix}\hat{\rho}_+(t)\\ \hat{\rho}_-(t)\end{bmatrix} - \frac{\mathrm{i}}{\hbar}\begin{bmatrix}\hat{V}^{\times} & 0\\ 0 & -\hat{V}^{\times}\end{bmatrix}\begin{bmatrix}\hat{\rho}_+(t)\\ \hat{\rho}_-(t)\end{bmatrix} + \frac{\gamma}{2}\begin{bmatrix}-1 & 1\\ 1 & -1\end{bmatrix}\begin{bmatrix}\hat{\rho}_+(t)\\ \hat{\rho}_-(t)\end{bmatrix}. \quad (2.65)$$

where $\hat{\rho}_+$ and $\hat{\rho}_-$ are the density matrices for the states $|+\rangle$ and $|-\rangle$, respectively. The above set of equations of motion can easily be solved analytically. This model has been applied to the study of the line shape of second-order optical processes and single molecular detections, as will be discussed in §4.

Note the apparent similarity of this equation to eqs. (2.41) and (2.62) for $N = 1$ with $\hat{\rho}_+ = (\hat{\rho}_0 + \hat{\rho}_1)/2$ and $\hat{\rho}_- = (\hat{\rho}_0 - \hat{\rho}_1)/2$. They are, however, generically distinct in that eq. (2.65) is an exact equation for the given stochastic processes, whereas the equations reduced from eqs. (2.41) and (2.62) are approximate description for which the higher-order correction terms are neglected via the terminator.

3. Physical Observables and Correlation Functions

We can study the dynamics of a system by measuring the change in physical quantity, such as a molecular dipole, after exciting the system in an equilibrium state by external forces such as laser pulses. In this section, we introduce the correlation functions of physical variables and argue how these functions are related to the experimentally observed quantities.

3.1 Response function approach

In quantum mechanics, any physical observable is expressed as an expectation value of a physical operator. We define an observable for the physical operator $\hat{A}$ at time t by

$$A(t) \equiv \mathrm{tr}\{\hat{A}\hat{\rho}(t)\}, \tag{3.1}$$

where $\hat{\rho}(t)$ is the density operator expressed as

$$\hat{\rho}(t) = \underset{\longleftarrow}{\exp}\left[-\frac{\mathrm{i}}{\hbar}\int_0^t \hat{H}_A(\tau)\,\mathrm{d}\tau\right]\hat{\rho}^{\mathrm{eq}}\underset{\longrightarrow}{\exp}\left[\frac{\mathrm{i}}{\hbar}\int_0^t \hat{H}_A(\tau)\,\mathrm{d}\tau\right], \tag{3.2}$$

for the Hamiltonian $\hat{H}_A(\tau)$. Here, the arrows indicate the time-ordered exponentials. We assumed that the system is in the equilibrium state at time $t = 0$ expressed by a time-independent Hamiltonian $\hat{H}_0$ as

$$\hat{\rho}^{\mathrm{eq}} = \mathrm{e}^{-\beta\hat{H}_0}/\,\mathrm{tr}\left\{\mathrm{e}^{-\beta\hat{H}_0}\right\}, \tag{3.3}$$

where $\beta \equiv 1/k_{\mathrm{B}}T$ is the inverse temperature. Note that if $\hat{H}_A(\tau)$ is identical to $\hat{H}_0$, we have $\hat{\rho}(t) = \hat{\rho}^{\mathrm{eq}}$, since $\hat{\rho}^{\mathrm{eq}}$ and $\mathrm{e}^{\mathrm{i}\hat{H}_0 t/\hbar}$ commute with each other; therefore, eq. (3.1) gives the equilibrium expectation value. We are interested in the response of a physical observable under external forces. The Hamiltonian with an external force is given by

$$\hat{H}_A(\tau) = \hat{H}_0 - f_1(\tau)\hat{B}_1, \tag{3.4}$$

where $f_1(\tau) = 0$ for $\tau \le 0$. If we expand the density matrix element by $f_1(\tau)\hat{B}_1$, then the expectation value is expressed as

$$A(t) = \langle\hat{A}\rangle + \frac{\mathrm{i}}{\hbar}\int_0^t \mathrm{d}\tau\, f_1(\tau)\langle[\hat{A}(t), \hat{B}_1(\tau)]\rangle + \cdots, \tag{3.5}$$

where $\hat{X}(t) \equiv \mathrm{e}^{\mathrm{i}\hat{H}_0 t/\hbar}\hat{X}\mathrm{e}^{-\mathrm{i}\hat{H}_0 t/\hbar}$ is the Heisenberg operator with the unperturbed Hamiltonian $\hat{H}_0$ for any operator $\hat{X}$ and $\langle\cdots\rangle$ represent the equilibrium ensemble average defined by

$$\langle\hat{Y}\rangle \equiv \mathrm{tr}\{\hat{Y}\hat{\rho}^{\mathrm{eq}}\} \tag{3.6}$$

for any operator $\hat{Y}$. From eq. (3.5), the deviation of expectation value from that in the equilibrium state, $\bar{A}(t) \equiv A(t) - \langle\hat{A}\rangle$, is written up to the lowest order in $f_1(t)$ as

$$\bar{A}^{(1)}(t) = \int_0^t \mathrm{d}t_1\, f_1(t - t_1)R^{(1)}(t_1), \tag{3.7}$$

where

$$R^{(1)}(t_1) \equiv \frac{\mathrm{i}}{\hbar}\langle[\hat{A}(t_1), \hat{B}_1]\rangle \tag{3.8}$$

is the response function that describes the response of the system for the function $f_1(\tau)$. Suppose that the external force consists of a train of nth excitation pulses denoted by

$$\hat{H}_A(\tau) = \hat{H}_0 - \sum_{n=1}^{N} f_n(\tau)\hat{B}_n. \tag{3.9}$$

The pulse with $n = 1$ operates first, then the pulses with $n = 2, 3, \ldots$ operate successively. We focus on the observables defined by the first-order expansion term of each excitation. For $N = 2$ and 3, the expectation values are, respectively, expressed as

$$\bar{A}^{(2)}(t) = \int_0^t \mathrm{d}t_2 \int_0^{t-t_2} \mathrm{d}t_1\, f_2(t - t_2)f_1(t - t_{12}) \times R^{(2)}(t_2, t_1), \tag{3.10}$$

and

$$\bar{A}^{(3)}(t) = \int_0^t \mathrm{d}t_3 \int_0^{t-t_3} \mathrm{d}t_2 \int_0^{t-t_{23}} \mathrm{d}t_1\, f_3(t - t_3) \times f_2(t - t_{23})f_1(t - t_{123})R^{(3)}(t_3, t_2, t_1), \tag{3.11}$$

where $t_{12} \equiv t_1 + t_2$, $t_{23} \equiv t_2 + t_3$, and $t_{123} \equiv t_1 + t_2 + t_3$ and the second- and third-order response functions are given by[24]

$$R^{(2)}(t_2, t_1) = -\frac{1}{\hbar^2}\langle[[\hat{A}(t_{12}), \hat{B}_2(t_1)], \hat{B}_1]\rangle \tag{3.12}$$

and

$$R^{(3)}(t_3, t_2, t_1) = -\frac{\mathrm{i}}{\hbar^3}\langle[[[\hat{A}(t_{123}), \hat{B}_3(t_{12})], \hat{B}_2(t_1)], \hat{B}_1]\rangle, \tag{3.13}$$

respectively. In conventional measurements, the response eq. (3.8) is a function of a single-time variable. In the nth excitation measurement, the signal is measured as a function of n-time variables. Since one can plot a profile of the signal as the n-dimension of the contour map, the measurements related to the multibody correlation functions of observables may be called multi-dimensional measurements. Once the equation of motion is presented, the calculations of the multibody correlation functions are straightforward.[25]

3.2 Linear and nonlinear response theories

If we set $f_1(t) = \cos\omega t$ in eq. (3.7), then

$$\bar{A}^{(1)}(t) = \chi'(\omega)\cos\omega t + \chi''(\omega)\sin\omega t, \tag{3.14}$$

in which

$$\chi(\omega) \equiv \int_0^{\infty} \mathrm{d}t_1\, \mathrm{e}^{-\mathrm{i}\omega t_1}R^{(1)}(t_1) \tag{3.15}$$

is the complex admittance and $\chi(\omega) \equiv \chi'(\omega) - \mathrm{i}\chi''(\omega)$. In eq. (3.15), we assumed that $R^{(1)}(t_1)$ decays to zero as $t \to \infty$. The real and imaginary parts of $\chi(\omega)$ satisfies the Kramers–Kronig relation.

By using Kubo's identity[26]

$$\frac{\mathrm{i}}{\hbar}\left[\mathrm{e}^{-\beta\hat{H}_0}, \hat{B}\right] = \mathrm{e}^{-\beta\hat{H}_0}\int_0^{\beta} \mathrm{d}\lambda\, \mathrm{e}^{\lambda\hat{H}_0}\frac{\mathrm{i}}{\hbar}[\hat{B}, \hat{H}_0]\mathrm{e}^{-\lambda\hat{H}_0}, \tag{3.16}$$

the response function eq. (3.8) can be rewritten as

$$R^{(1)}(t_1) = -\frac{\mathrm{d}}{\mathrm{d}t_1}\Psi(t_1). \tag{3.17}$$

Here, we introduced the relaxation function

$$\Psi(t_1) \equiv \beta\langle\hat{B}_1; \hat{A}(t_1)\rangle, \tag{3.18}$$

which is defined by the canonical correlation

$$\langle \hat{\boldsymbol{B}}_1; \hat{A}(t_1) \rangle \equiv \frac{1}{\beta} \int_0^\beta \mathrm{d}\lambda \, \mathrm{tr}\{ \hat{\rho}^{\mathrm{eq}} \hat{\boldsymbol{B}}_1(-\mathrm{i}\hbar\lambda) \hat{A}(t_1) \}. \tag{3.19}$$

Likewise, higher-order response functions can be expressed in canonical correlation form as

$$R^{(2)}(t_2, t_1) = -\beta \frac{\mathrm{i}}{\hbar} \left\langle \dot{\hat{\boldsymbol{B}}}_1(0); [\hat{\boldsymbol{B}}_2(t_1), \hat{A}(t_{12})] \right\rangle, \tag{3.20}$$

and

$$R^{(3)}(t_3, t_2, t_1) = \beta \left(\frac{\mathrm{i}}{\hbar} \right)^2 \left\langle \dot{\hat{\boldsymbol{B}}}_1(0); [\hat{\boldsymbol{B}}_2(t_1), [\hat{\boldsymbol{B}}_3(t_{12}), \hat{A}(t_{123})]] \right\rangle. \tag{3.21}$$

In the classical limit, the commutator $\mathrm{i}[\cdots]/\hbar$ is replaced by the Poisson bracket $\{\cdots\}$ and canonical correlation functions are reduced to classical correlation functions. The above expressions are used to carry out classical molecular dynamics simulations to calculate the higher-order optical response of molecular vibrational motions.[27–32)]

3.3 *Spontaneous emission and scattering: physical spectrum and neutron diffraction*

A signal emitted by an object entered in the instrument is generally expressed in the time convolution form $\hat{A}_{\mathrm{inst}}(t) = \int_0^t \mathrm{d}t' \, f(t-t') \hat{A}'(t')$, where $f(t)$ is a function that characterizes the instrument and $\hat{A}'(t)$ is the Heisenberg operator for the observable $\hat{A}$ with a Hamiltonian including the external force $\hat{\boldsymbol{H}}_A$. The signal measured by such instrument as a Fabry–Perot interferometer may be expressed by a simple form as $f(t) = \exp[-(\Gamma_f + \mathrm{i}\omega)t]$, where Γ_f is the bandwidth and ω is the detection frequency of the instrument. The intensity measured by the instrument is expressed as $S_{\mathrm{inst}}(\omega; t) = \langle \hat{A}^\dagger_{\mathrm{inst}}(t) \hat{A}_{\mathrm{inst}}(t) \rangle$. For a large t with $\Gamma_f t \ll 1$, we have[33)]

$$S_{\mathrm{inst}}(\omega; t) \approx \frac{1 - \mathrm{e}^{-2\Gamma_f t}}{\Gamma_f} \mathrm{Re} \left\{ \int_0^\infty \mathrm{d}\xi \, \mathrm{e}^{(\Gamma_f + \mathrm{i}\omega)\xi} \langle \hat{A}'^\dagger(0) \hat{A}'(\xi) \rangle \right\}. \tag{3.22}$$

We can rewrite the correlation function as[34–37)]

$$\begin{aligned} \langle \hat{A}'^\dagger(0) \hat{A}'(t) \rangle &= \mathrm{tr} \left\{ \hat{A} \, \exp\left[-\frac{\mathrm{i}}{\hbar} \int_0^t \mathrm{d}\tau \, \hat{\boldsymbol{H}}_A \right] (\hat{\rho}^{\mathrm{eq}} \hat{A}^\dagger) \right. \\ &\quad \left. \times \exp\left[\frac{\mathrm{i}}{\hbar} \int_0^t \mathrm{d}\tau \, \hat{\boldsymbol{H}}_A \right] \right\} \\ &\equiv \mathrm{tr} \left\{ \hat{A} \, \exp\left[-\frac{\mathrm{i}}{\hbar} \int_0^t \mathrm{d}\tau \, \hat{\boldsymbol{H}}_A^\times \right] (\hat{\rho}^{\mathrm{eq}} \hat{A}^\dagger) \right\}. \end{aligned} \tag{3.23}$$

Consequently, the above equation can be rewritten as

$$S_{\mathrm{inst}}(\omega; t) \approx \frac{1 - \mathrm{e}^{-2\Gamma_f t}}{2\Gamma_f} I(\omega), \tag{3.24}$$

where $I(\omega)$ is the Fourier–Laplace transformation of the correlation function given by

$$I(\omega) = 2 \, \mathrm{Re} \left\{ \mathrm{tr} \left[\hat{A} \left(s + \frac{\mathrm{i}}{\hbar} \hat{\boldsymbol{H}}_A^\times \right)^{-1} (\hat{\rho}^{\mathrm{eq}} \hat{A}^\dagger) \right] \Big|_{s=-\mathrm{i}\omega} \right\}. \tag{3.25}$$

Here, the equilibrium distribution functions are evaluated from any initial state $\hat{\rho}(t_i)$ using

$$\hat{\rho}^{\mathrm{eq}} = \lim_{s \to 0} s \left(s + \frac{\mathrm{i}}{\hbar} \hat{\boldsymbol{H}}_A^\times \right)^{-1} \hat{\rho}(t_i). \tag{3.26}$$

Note that $S_{\mathrm{inst}}(\omega; t)$ is proportional to t for a small $\Gamma_f t$; thus, $I(\omega)$ represents the emission ratio $I(\omega) \approx \mathrm{d}S_{\mathrm{inst}}(\omega; t)/\mathrm{d}t$.

Neutron, electron, and X-ray diffraction analyses probe the configuration of nuclei through the spatial and energy distributions of scattered particles or a photon beam. Using eq. (3.22), we can also define spectra for diffraction or scattering measurements. For a scattered particle or a photon with a wave vector $\mathbf{k}$, we consider the operator

$$\hat{A} \equiv \hat{A}_{\mathbf{k}} \exp[\mathrm{i}\mathbf{k} \cdot \hat{\mathbf{r}}], \tag{3.27}$$

with

$$\hat{A}_{\mathbf{k}} \equiv \sum_j c_k \hat{a}_k \exp\left[\mathrm{i}\mathbf{k} \cdot \left(\hat{\mathbf{R}}_j - \hat{\mathbf{r}} \right) \right], \tag{3.28}$$

where $\hat{\mathbf{R}}_j$ is the coordinate of the jth nucleon of the nucleus, $\hat{\mathbf{r}}$ is the coordinate of the center of mass of the nucleus, c_k is a constant, $\hat{a}_k$ is the annihilation operator of the particle or photon with a wave vector $\mathbf{k}$. The experiments measure the scattering (emission) intensity of a particle or a photon. We assume that the Hamiltonian of the nucleon and that of the particles or photons are well separated and can take the ensemble average separately. If the beams have a time envelop denoted by $f(t)$, the scattering intensity $S_{\mathbf{k}}(\omega; t) = \langle \hat{A}^\dagger_{\mathrm{inst}}(t) \hat{A}_{\mathrm{inst}}(t) \rangle$ is expressed as

$$\begin{aligned} S_{\mathbf{k}}(\omega; t) = \int_0^t \int_0^t \mathrm{d}t' \, \mathrm{d}t'' f(t-t') f(t-t'') \\ \times \left\langle \hat{A}'^\dagger_{\mathbf{k}}(t') \hat{A}'_{\mathbf{k}}(t'') \right\rangle G(\mathbf{k}; t''-t'), \end{aligned} \tag{3.29}$$

where $G(\mathbf{k}; t''-t')$ is the form factor defined by[38)]

$$G(\mathbf{k}; t''-t') \equiv \left\langle \mathrm{e}^{-\mathrm{i}\mathbf{k}\cdot\hat{\mathbf{r}}'(t')} \mathrm{e}^{\mathrm{i}\mathbf{k}\cdot\hat{\mathbf{r}}'(t'')} \right\rangle, \tag{3.30}$$

and $\hat{A}'_{\mathbf{k}}(t)$ and $\hat{\mathbf{r}}'(t)$ are the Heisenberg representations of $\hat{A}_{\mathbf{k}}$ and $\hat{\mathbf{r}}$ with the Hamiltonian $\hat{\boldsymbol{H}}_A$, respectively. The above expression is suitable for describing the time-dependent spectrum generated by a pulsed particle or photon source. If $f(t) = \mathrm{e}^{-(\Gamma_f + \mathrm{i}\omega)t}$ with $\Gamma_f \ll \omega$, we have the scattering ratio of the particles or photons with a wave vector $\mathbf{k}$, $I(\omega; \mathbf{k}) \approx \mathrm{d}S_{\mathbf{k}}(\omega; t)/\mathrm{d}t$. This function is often called the dynamical structure factor and expressed in conventional form as

$$I(\omega; \mathbf{k}) = 2 \, \mathrm{Re} \left\{ \int_0^\infty \mathrm{d}\tau \, \mathrm{e}^{\mathrm{i}\omega\tau} \left\langle \hat{A}'^\dagger_{\mathbf{k}}(0) \hat{A}'_{\mathbf{k}}(\tau) \right\rangle G(\mathbf{k}; \tau) \right\}. \tag{3.31}$$

This spectrum allows us to study a local movement of nuclei as a change in the momentum of a particle or a photon in terms of their correlation function.

4. Applications of Stochastic Approach

As explained in the introduction, there are three approaches to solving stochastic models. Although applications that we will review in this section have been studied from one of these approaches, we explain such results only from the stochastic Liouville equation approach. This is because we would like to discuss the applications from a unified point of view and the final results are the same aside from some technical differences, because these approaches assume the same stochastic process.

4.1 NMR, ESR, and μSR spectroscopies

An electron and a nucleus such as ^{1}H and ^{13}C, respectively, possess the magnetic dipole moment $\boldsymbol{\mu} = g\hbar\mathbf{S}$, where g is the gyromagnetic ratio and $\mathbf{S}$ is the nuclear spin such as $S = |\mathbf{S}| = 1/2$ or $3/2$. The energy of the nuclear spin in a magnetic field is then expressed as $U = -\boldsymbol{\mu}\cdot\mathbf{B}_0 = -g\hbar B_0\hat{S}_z$, where we set the magnetic field in the z-direction and $\hat{S}_z$ is the spin operator whose eigenvalues (Zeeman levels) are given, for example, by $S_z = \pm 1/2$ for $S = 1/2$ and $S_z = \pm 3/2, \pm 1/2$ for $S = 3/2$. Nuclear magnetic resonance (NMR) spectroscopy[39] or electron spin resonance (ESR) spectroscopy probes the transitions between these levels by applying a microwave perpendicular to the magnetic field. Note that the theoretical background of muon spin rotation (μSR), which measures the spin depolarization of implanted muons in substances, is also very similar to that of NMR or ESR.[12,40] The NMR and ESR measurements utilize the microwave in the xy-direction given by $\mathbf{B}_1(t) = (B_1(t)\cos(\omega t), B_1(t)\sin(\omega t), 0)$. The Hamiltonian for NMR and ESR measurements is then expressed as

$$\hat{H}_A(t) = \hbar\omega_0\hat{S}_z + \hbar\alpha_1(t)\big[\cos(\omega t)\hat{S}_x + \sin(\omega t)\hat{S}_y\big], \tag{4.1}$$

where we set $\omega_0 = gB_0$ and $\alpha_1(t) = gB_1(t)$. The operators $\hat{S}_x$ and $\hat{S}_y$ are respectively defined by the spin creation and annihilation operators $\hat{S}_+$ and $\hat{S}_-$ as $\hat{S}_x \equiv \hat{S}_+ + \hat{S}_-$ and $\hat{S}_y \equiv -\mathrm{i}(\hat{S}_+ - \hat{S}_-)$. For angular momentum S, there are $L = 2S + 1$ spin states denoted by $|S_z\rangle$. The density matrix of the nuclear system is then expressed as $\hat{\rho}(t) = \sum_{n,m=-S}^{S}\rho_{nm}(t)|nm\rangle\rangle$, where $|n\rangle\langle m| \equiv |nm\rangle\rangle$. Of special interest in this context is the occurrence of the local random field $\delta\mathbf{B}(t)$ caused by the thermal fluctuations of the surrounding atoms or molecules. For practical applications of the stochastic theory, one should specify a certain form of interaction. The widely known Kubo–Anderson process is defined by $\hat{H}(t) = \hat{H}_A(t) + \hat{H}_I(t)$, where the perturbation is given by[1,2]

$$\hat{H}_I(t) = \boldsymbol{\Omega}(t)\cdot\hat{\mathbf{V}}. \tag{4.2}$$

Here, we denote $g\delta\mathbf{B}(t)\cdot\hat{\mathbf{S}} \to \boldsymbol{\Omega}(t)\cdot\hat{\mathbf{V}}$ with $\hat{\mathbf{V}} = (\Delta_x\hat{S}_x, \Delta_y\hat{S}_y, \Delta_z\hat{S}_z)$, where Δ_j is the amplitude of the fluctuation in the j-direction. In the stochastic approach, $\boldsymbol{\Omega}(t)$ is regarded as the stochastic variable $\boldsymbol{\Omega} \equiv (\Omega_x, \Omega_y, \Omega_z)$. The equation of motion is then given by

$$\frac{\partial}{\partial t}\hat{\rho}(\boldsymbol{\Omega};\, t) = -\frac{\mathrm{i}}{\hbar}\hat{H}_A^{\times}(t)\hat{\rho}(\boldsymbol{\Omega};\, t) - \frac{\mathrm{i}}{\hbar}\big(\hat{\mathbf{V}}^{\times}\cdot\boldsymbol{\Omega}\big)\hat{\rho}(\boldsymbol{\Omega};\, t) + \hat{\Gamma}_{\boldsymbol{\Omega}}\hat{\rho}(\boldsymbol{\Omega};\, t), \tag{4.3}$$

where $\hat{\mathbf{V}}^{\times} = (\Delta_x\hat{S}_x^{\times}, \Delta_y\hat{S}_y^{\times}, \Delta_z\hat{S}_z^{\times})$ and $\hat{\Gamma}_{\boldsymbol{\Omega}}$ is the Markovian operator for $\boldsymbol{\Omega}$. Following Kubo and Toyabe,[41] we assume $\langle\Omega_i(\tau)\Omega_j(0)\rangle \equiv \delta_{ij}\exp[-\gamma_j|\tau|]$ for $i,\ j = x,\ y,\ z$. Therefore,

$$\hat{\Gamma}_{\boldsymbol{\Omega}} = \sum_{i=x,y,z}\gamma_i\frac{\partial}{\partial\Omega_i}\left(\Omega_i + \frac{\partial}{\partial\Omega_i}\right). \tag{4.4}$$

If we set $\alpha_1(\tau) = \alpha_1$, the equation describes the spin precession under a longitudinal magnetic field with a transverse microwave field. Since the stochastic modulation causes relaxation, the motion of spin eventually reaches the steady state after a sufficiently long time.

There are several means of NMR measurement. A simple one involves free induction decay, which measures the relaxation of the dipole in the z-direction after the microwave $\alpha_1(t)$ is switched off. The physical observable of this measurement is the emission spectrum of the microwave. From eqs. (3.22)–(3.25) for the spin operator $\hat{A} = \hat{S}_+$ and $\hat{S}_-$, this is expressed as

$$I(\omega) = 2\,\mathrm{Re}\left\{\int_0^{\infty}\mathrm{d}t\,\mathrm{e}^{\mathrm{i}\omega t}\big\langle\hat{S}_+\hat{S}_-(t)\big\rangle\right\}. \tag{4.5}$$

In stochastic Liouville formalism, the correlation function is written in the time ordered exponential form [see eq. (3.2)] as

$$\big\langle\hat{S}_+\hat{S}_-(t)\big\rangle = \mathrm{tr}\left\{(\mathbf{0}|\hat{S}_+\underleftarrow{\exp}\left[\int_0^t\mathrm{d}\tau\left(-\frac{\mathrm{i}}{\hbar}\hat{H}_A^{\times}(\tau) - \frac{\mathrm{i}}{\hbar}\hat{\mathbf{V}}^{\times}\cdot\boldsymbol{\Omega} + \hat{\Gamma}_{\boldsymbol{\Omega}}\right)\right]\big(\hat{\rho}^{\mathrm{eq}}\hat{S}_-\big)|\mathbf{0})\right\}. \tag{4.6}$$

where $|\mathbf{0})$ is the three-dimensional extension of $|0)$ presented in §2.2. For $|\alpha_1(t)| \ll \omega_0$, we have $H_A(t) \to H_0 = \hbar\omega_0\hat{S}_z$ and

$$I(\omega) = 2\,\mathrm{Re}\left\{\mathrm{tr}\left[(\mathbf{0}|\hat{S}_+\left(s + \frac{\mathrm{i}}{\hbar}\hat{H}_0^{\times} + \frac{\mathrm{i}}{\hbar}\hat{\mathbf{V}}^{\times}\cdot\boldsymbol{\Omega} - \hat{\Gamma}_{\boldsymbol{\Omega}}\right)^{-1}\big(\hat{\rho}^{\mathrm{eq}}\hat{S}_-\big)|\mathbf{0})\right]\Big|_{s=-\mathrm{i}\omega}\right\}, \tag{4.7}$$

where $\hat{\rho}^{\mathrm{eq}}$ is evaluated as

$$\hat{\rho}^{\mathrm{eq}} = \lim_{s\to 0}s\left(s + \frac{\mathrm{i}}{\hbar}\hat{H}_0^{\times} + \frac{\mathrm{i}}{\hbar}\hat{\mathbf{V}}^{\times}\cdot\boldsymbol{\Omega} - \hat{\Gamma}_{\boldsymbol{\Omega}}\right)^{-1}\hat{\boldsymbol{\rho}}(t_i). \tag{4.8}$$

Furthermore, if we have $B_0 \gg |\delta\mathbf{B}(t)|$, the effect of perturbation in the x- and y-directions is much smaller than the effect of $\delta B_z(t)$. Hence, the Hamiltonian $\hat{H}_0$ is now able to commute to the local field interaction $\hat{\mathbf{V}}^{\times}\cdot\boldsymbol{\Omega} = \Delta_z\Omega_z\hat{S}_z^{\times}$; we can diagonalize the density matrix that giving rise to the analytic result.[1,2,5] In this case, we have $(\hat{\rho}^{\mathrm{eq}}\hat{S}_-)|\mathbf{0}) = |\mathbf{0})|01\rangle\rangle$ and eq. (4.7) is evaluated as

$$I(\omega) = 2\,\mathrm{Re}\big\{G_-[s]|_{s=\mathrm{i}\omega}\big\}, \tag{4.9}$$

where $G_-[s]$ is defined by eq. (2.53) with $\Delta \equiv \Delta_z$ and $\gamma \equiv \gamma_z$. From eq. (2.54), if the correlation of noise γ is large compared with the amplitude of fluctuation Δ, i.e., $\gamma \gg \Delta$ for a fixed $\gamma' = \Delta^2/\gamma$ (motional narrowing limit), then the spectrum takes the Lorentzian form as

$$I(\omega) = \frac{2\gamma'}{\gamma'^2 + (\omega - \omega_0)^2}. \tag{4.10}$$

In the slow-modulation limit with the condition $\gamma \ll (\omega - \omega_0) \ll \sqrt{2}\Delta$, from eq. (2.56), we have the spectrum in the Gaussian form

$$I(\omega) = \frac{2\sqrt{2}}{\Delta}\exp\left[-\frac{(\omega - \omega_0)^2}{2\Delta^2}\right]. \tag{4.11}$$

This is identical to the case in which the spins with different resonant frequencies are distributed spatially with the Gaussian distribution function $S(\omega') = \exp[-\delta^2(\omega' - \omega_0)]$.

$$I_{\mathrm{inhomo}}(\omega) \propto 2\,\mathrm{Re}\left\{\int_0^{\infty}\mathrm{d}\omega'\,S(\omega')\mathrm{e}^{-\mathrm{i}\omega' t}\right\} \tag{4.12}$$

Here, we put $\Delta^2 = \delta^2/2$. Hence, the slow modulation limit of the stochastic model is often used to describe the

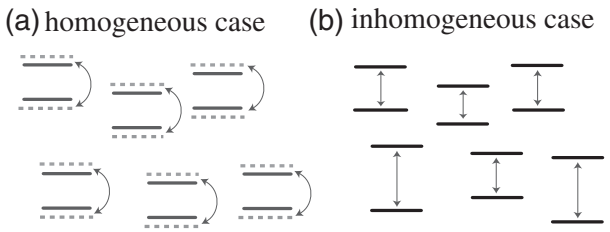

Fig. 1. Schematic view of homogeneous (fast modulation case) and inhomogeneous (slow modulation case) distributions of two-level spins system.

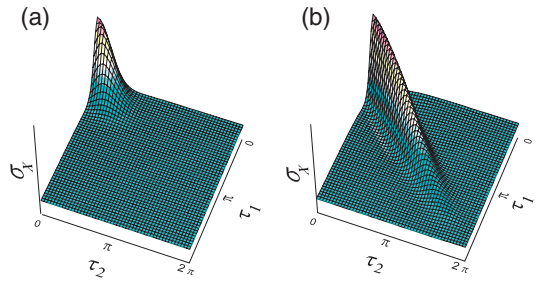

Fig. 2. Spin echo signals for (a) fast-modulation (homogeneous) case, $\gamma_z = 1$, and (b) slow-modulation (inhomogeneous) case, $\gamma_z = 0.01$, for fixed modulation amplitude $\Delta_z = 1$.

inhomogeneous distribution of the spins system (see Fig. 1). The significance of dephasing is that it depends on the local environment (the lattice) and thus is sensitive to local magnetic effects, like those of paramagnetic species, and the exchange of chemically similar protons between the environment and the irradiated sample. In the motional narrowing limit, the dephasing effect is characterized by the time decay constant $T_2^{\dagger} \equiv 1/\gamma'$.

Here, we consider inhomogeneous dephasing only. As shown by Bloch, one usually needs to take into account the longitudinal and transversal relaxations characterized by the time constants T_1 and T_2.[42] They can be incorporated in the equation of motion either phenomenologically or by introducing the fast stochastic modulation in the x- and y-directions in rotating wave approximation (RWA) form as will be shown in §6.3.

The above result represents the spectrum of spin precession under a strong z magnetic field. In the case of μSR or low-field NMR measurement, i.e., $B_0 \approx |\alpha_1(t)/g| \approx |\delta\mathbf{B}(t)|$, the perturbation in the $\hat{S}_x$ and $\hat{S}_y$ directions also becomes important. This situation was first studied by Kubo and Toyabe,[41,43] then experimentally explored by the μSR approach.[44] The stochastic Liouville equation was solved by variational and numerical approaches.[45] A similar model was also studied by various approaches.[46–48] The same model with external fields was also calculated by employing a sequence of time-dependent noises that satisfy eq. (2.10), instead of by solving stochastic Liouville equation.[13,49] Note that related results will be presented in Fig. 16 in §5.6. A nuclear spin system with $|\mathbf{S}| > 1/2$,[50] a coupled spin system,[51] two-dimensional NMR relaxation spectra of molecular solids,[52] and chemical exchange processes,[53] have also been studied by the stochastic Liouville equation approach.

These studies were, however, limited to the case of a free induction decay or a stationary response under a constant external field. Using a set of equations of motion given in eqs. (2.41)–(2.43) with the terminator eq. (2.62), we are now able to study the time evolution of a system under any time-dependent external field with a stochastic perturbation in the x-, y-, and z-directions.

As a demonstration, we present a spin echo signal for a spin system with a resonant frequency $\omega_0 = 1$. In spin echo measurement, the system is perturbed by $\pi/4$ and $\pi/2$ pulses separated by the period τ_1 then probed after another period τ_2. This measurement enables us to evaluate the inhomogeneous distribution of spin resonant frequencies as a profile of the echo peak. Since the slow modulation limit of the Gaussian–Markovian modulation model corresponds to the inhomogeneous distribution case of spins system, we can illustrate the difference in signals between the homogeneous and inhomogeneous cases by changing the inverse noise correlation time γ_z. In Fig. 2, we depicted the signal for (a) the homogeneous case $\gamma_z = 1$ and (b) the inhomogeneous case $\gamma_z = 0.01$ for the fixed modulation amplitude $\Delta_z = 1$. The other stochastic parameters were chosen to be $\Delta_x = \Delta_y = 0.1$ and $\gamma_x = \gamma_y = 1$. The frequency and amplitude of $\pi/4$ and $\pi/2$ pulses were given by $\omega = 1$ and $\alpha_1 = 10\pi$, respectively. The numbers of hierarchies n_x, n_y, and n_z for the x, y, and z elements, respectively, are chosen to be $n_x = n_y = 4$ and $n_z = 10$ for (a) and $n_z = 100$ for (b). After stabilizing the system by integrating the equations of motion in the time period of 2π from the initial conditions $\sigma_z = 0.5$ and $\sigma_x = \sigma_y = 0$, we apply $\pi/4$ and $\pi/2$ pulses and calculate the σ_x element as a function of τ_1 and τ_2. In the homogeneous case [Fig. 2(a)], the coherence is gradated by a fast stochastic modulation and the signal is localized at approximately $\tau_1 = \tau_2 = 0$. In the inhomogeneous case [Fig. 2(b)], however, the modulation is static and the spin can rephase after the $\pi/2$ pulse application at $\tau_1 = \tau_2$. Thus, there is a slow decay of the echo peak along $\tau_1 = \tau_2$.

Modern NMR and ESR spectroscopies probe the nature of interactions between spins using various configurations of pulsed microwaves; however, few theoretical studies of dephasing have been carried out.

4.2 Dielectric relaxation

The relaxation of polar molecules is known as dielectric relaxation. This relaxation is measured by applying external microwaves to a sample. Since Debye developed a theory of dielectric relaxation,[54] a rotational Brownian motion model has been used to analyze this phenomenon.[55] In this approach, a molecule is modeled as a rigid free rotator with a permanent electric dipole moment μ under an external field $E\cos\omega t$. For a two-dimensional system, the Hamiltonian for a single rotator is written as

$$\hat{H}_A(t) = -\frac{\hbar^2}{2I}\frac{\partial^2}{\partial\theta^2} - \mu E\cos\omega t\cos\theta, \qquad (4.13)$$

where I is the inertia momentum. The total Hamiltonian is denoted by $\hat{H}(t) = \hat{H}_A(t) + \hat{H}_I(\Omega)$, where the stochastic interaction is assumed to be $\hat{H}_I(\Omega) = \Omega\hat{V}$ with $\hat{V} = \theta$. This Hamiltonian is similar to that of a free Brownian particle. In the present case, however, the quantum state has to satisfy the periodic boundary condition $|\theta\rangle = |\theta + 2\pi\rangle$.

A physical observable commonly measured is dielectric susceptibility defined by

$$\varepsilon(\omega) = 1 + 4\pi\alpha(\omega), \tag{4.14}$$

or more commonly expressed as

$$\frac{\varepsilon(\omega) - \varepsilon(\infty)}{\varepsilon(0) - \varepsilon(\infty)} = \frac{\bar{\alpha}(\omega)}{\bar{\alpha}(0)}, \tag{4.15}$$

where $\bar{\alpha}(\omega) \equiv \alpha(\omega) - \alpha(\infty)$. The linear response theory for dielectric susceptibility leads

$$\bar{\alpha}(\omega) = \int_0^\infty \mathrm{d}t\, \mathrm{e}^{-\mathrm{i}\omega t} R^{(1)}(t), \tag{4.16}$$

where $R^{(1)}(t) \equiv \mathrm{i}\langle[\mu(t),\ \mu(0)]\rangle/\hbar$ is the response function of the dipole (see §3.1 and §3.2). If we further introduce the relaxation function $\Psi(t) = \beta\langle\mu(t);\ \mu(0)\rangle$, we have $R^{(1)}(t) = -\mathrm{d}\Psi(t)/\mathrm{d}t$.

Stochastic models have been used in the modeling of rotational relaxation assuming coupling to an environment. In the classical case, if the fluctuation from the environment can be represented by stochastic Gaussian Markovian modulation, the relaxation function

$$\Psi(t) = \beta\mu^2\langle\cos\theta(t)\cos\theta(0)\rangle, \tag{4.17}$$

can be evaluated from the Langevin-type equation expressed in a stochastic time convolution expression. Utilizing a continued fractional form, Uchiyama and Shibata studied the time evolution of dipoles and dielectric dispersion under stochastic modulation in Gaussian–Markovian and two-state jump cases.[56–58] Note that this is in principle a Brownian rotator problem; the second-, third- and fourth-order quantum response functions for general noise are now obtained by the Feynman–Vernon influence functional approach.[59,60]

These studies are limited to the two-dimensional rigid rotator case. Some studies have extended to the cases of three-dimensional rotators[61–63] and spins.[64,65] Some treatments include the effect of dissipation in addition to the fluctuation within classical approximation. As we will see in §5, such systems may be treated quantum-mechanically using the reduced equations of motion derived from the system–bath Hamiltonian.

4.3 Mössbauer spectroscopy and neutron scattering

Neutron scattering experiments probe the configuration of atoms through the spatial and energy distributions of scattered neutrons. Mössbauer spectroscopy detects resonant absorption of gamma-ray photons by nuclei in the ground state in crystals emitted from similar nuclei of the same element in the excited state. The observables of these measurements are characterized by the dynamical structure factor for a particle or a photon and given in §3.3. These measurements make it possible to explore a local movement of nuclei as a change in the momentum of a neutron or a photon. For such problem, the stochastic theory has been applied to study the effects of local perturbation on the emission or absorption spectrum of neutron or photon.[8,12] The relatively well-known example of a study of Mössbauer spectroscopy is the analysis of a hyperfine local field interaction which induces effects such as spin–spin and spin–lattice relaxations. Suppose that the system is under the magnetic fields; then, Zeeman energy splitting occurs. If the nucleus does not move, we can set the form factor $G(\mathbf{k};\tau)$ in eq. (3.31) to unity and the spectrum is determined by

$$I(\omega) = \frac{2}{\pi}\mathrm{Re}\int_0^\infty \mathrm{d}\tau\, \mathrm{e}^{-\mathrm{i}\omega\tau}\big\langle M_g\big|\hat{A}_{\mathbf{k}}^\dagger(0)|M_e\big\rangle\big\langle M_e|\hat{A}_{\mathbf{k}}(\tau)\big|M_g\big\rangle, \tag{4.18}$$

where $|M_e\rangle$ and $|M_g\rangle$ are the angular momentum indices in the excited and ground states of the nucleus. For the ^{57}Fe nucleus, there are four excited states and two ground states, because the spin in the excited and ground states are $S = 3/2$ and $1/2$, respectively. Thus, the result exhibits six Zeeman splitting peaks as long as the local perturbation is weak or slow. If Mössbauer nucleus is coupled to its ionic spin with $1/2$ along the z-axis, the eigenvalue of $\hat{S}_z$ jumps by $\pm 1/2$, getting energy from the thermal fluctuation of molecules or atoms. Since the noise source originates from spin flipping, one may assume that these two values will occur with equal probabilities; thus, the system is modeled by the stochastic two-state jump model. The results exhibit six Zeeman splitting peaks for a slow-modulation case, whereas they exhibit only a single peak for a fast modulation case.[8,66–69] Note that the same theoretical frame work can be used to analyze the electron paramagnetic resonance (EPR) measurement.[70]

Thus far, we have considered a fixed nucleus, but the real value of Mössbauer spectroscopy is the ability to detect a change in nucleus momentum through the form factor. As an application of the stochastic theory, we now turn to the problem of trapped interstitial impurities.[71,72] We consider an impurity atom in a host crystal lattice. Suppose there are several stable sites for the impurity as interstitial defects in the host lattice cage. A jump of the impurity causes a change in the form factor $G(k;\tau)$ defined by eq. (3.30), if it moves within the time scale of Mössbauer or the neutron scattering measurement. For a polycrystalline sample, this can be expressed as

$$G(k;\tau) = \sum_{n,m} p_n(n|\hat{P}(\tau)|m)\frac{\sin k|\mathbf{r}_n - \mathbf{r}_m|}{k|\mathbf{r}_n - \mathbf{r}_m|}, \tag{4.19}$$

where $\hat{P}(\tau)$ is the time evolution operator for $\exp[-\mathrm{i}\mathbf{k}\cdot\hat{\mathbf{r}}(0)]$, n and m refer to possible sites of impurity atoms, and p_n is the initial distribution of impurities at site n. The movement of impurity atoms is a low-frequency vibrational motion between the sites, but in a certain time range, we may regard this motion as hopping from one site to another, which follows a simple stochastic dynamics. Then one can evaluate $(n|\hat{P}(\tau)|m)$ by using the cumulant expansion method or by solving the stochastic Liouville equation as a multistate jump problem. Using this model, Dattagupta studied the thermal reorientation of Co impurity atoms in the octahedral cage of Al atoms in an fcc lattice as the diffusion broadening of the Mössbauer line shape.[71,72] The same theoretical framework can be applied to analyze the neutron scattering of molecular reorientation.[12]

4.4 Electronically resonant optical spectroscopy

Nonlinear optical interactions between the laser and electronic states of an atomic or molecular system provide powerful spectroscopic tools for the understanding of the dynamics of the system as well as its environment.[73] In an

early stage of the investigation on nonlinear optical phenomena, the stochastic theory has been widely used to include the effects of phase relaxation. Resonant optical experiments measure the optical transition between the ground and excited electronic states of atoms or molecules. The Hamiltonian is then expressed as

$$\hat{H}_A(t) = \hat{H}_0 + \hat{H}_E(t), \tag{4.20}$$

where

$$\hat{H}_0 = \sum_n \hbar\omega_n \hat{a}_n^+ \hat{a}_n^- \tag{4.21}$$

is the system Hamiltonian, and $\hat{a}_n^-$ and $\hat{a}_n^+$ are the creation and annihilation operators of atomic or molecular electronic states. The laser interaction is given by

$$\hat{H}_E(t) = -\left(\hat{\mu}^- + \hat{\mu}^+\right) \cdot E(t), \tag{4.22}$$

where $\hat{\mu}^+ \equiv \sum \mu_{nm} \hat{a}_n^+ \hat{a}_m$ with the transition amplitude μ_{nm} and $\hat{\mu}^-$ is its conjugate. One often uses the stochastic theory to account for the fluctuation in electronic resonant frequency, which is due to the random force on the system caused by the environment. If we may express the modulation of electronic energy gap as stochastic Gaussian–Markovian modulation, the total Hamiltonian is given by $\hat{H}(t) = \hat{H}_A(t) + \hat{H}_I(\Omega)$, where the interaction $\hat{H}_I(\Omega) = \Omega\hat{V}$ is expressed as

$$\hat{H}_I(\Omega) = \hbar\Omega\left[\sum_n \Delta_n \hat{a}_n^+ \hat{a}_n^- + \sum_{n\neq m} \Delta_{nm}\left(\hat{a}_n^+ \hat{a}_m^- + \hat{a}_n^- \hat{a}_m^+\right)\right]. \tag{4.23}$$

Here, Δ_n and Δ_{nm} are the amplitudes of the diagonal and off-diagonal modulations, respectively. If the optical observable is photon counting rate defined by eqs. (3.22) and (3.23), we have

$$\langle\hat{\mu}\hat{\mu}(t)\rangle = \mathrm{tr}\left\{\sum_n (0|\hat{\mu}\hat{G}_A(t)|n)(n|(\hat{\rho}^{\mathrm{eq}}\hat{\mu})|0)\right\}, \tag{4.24}$$

where $\hat{\mu} \equiv \hat{\mu}^- + \hat{\mu}^+$ and

$$\hat{G}_A(t) = \underleftarrow{\exp}\left\{\int_0^t \mathrm{d}\tau\left[-\frac{\mathrm{i}}{\hbar}\hat{H}^\times(\tau) + \hat{\Gamma}_\Omega\right]\right\}, \tag{4.25}$$

with $\hat{H}^\times(\tau) \equiv \hat{H}_A^\times(\tau) + \hat{H}_I^\times(\Omega)$, and we inserted the completeness relation of the stochastic state, $1 = \sum_n |n)(n|$. For $\hat{H}_I(\Omega) = \Omega\hat{V}$, the propagator for the stochastic state from $|n)$ to $(0|$ is evaluated as[16]

$$(0|\hat{G}_A[s]|n) = \hat{G}_0[s]\prod_{j=1}^{n}\left(\hat{V}^\times \hat{G}_j[s]\right), \tag{4.26}$$

where

$$\hat{G}_j[s] \equiv \cfrac{1}{s + j\gamma + \frac{\mathrm{i}}{\hbar}\hat{H}_A^\times[s] + \frac{1}{\hbar^2}\hat{V}^\times \cfrac{j}{s + (j+1)\gamma + \frac{\mathrm{i}}{\hbar}\hat{H}_A^\times[s] + \frac{1}{\hbar^2}\hat{V}^\times \cfrac{(j+1)}{s + (j+2)\gamma + \ddots}\hat{V}^\times}\hat{V}^\times}. \tag{4.27}$$

The conjugation of $(n|\hat{G}_A[s]|0)$ is also calculated accordingly. Then, using the expression $\hat{\rho}^{\mathrm{eq}}$ given by eq. (4.8), we can evaluate $(n|(\hat{\rho}^{\mathrm{eq}}\hat{\mu})|0)$. If $(n|(\hat{\rho}^{\mathrm{eq}}\hat{\mu})|0) = 0$ for $n > 0$, only the element with $n = 0$ remains in eq. (4.24), leading to a simple result as discussed in eq. (4.9) with eq. (2.53). In the general form of $\hat{H}_I(\Omega)$, however, $(n|(\hat{\rho}^{\mathrm{eq}}\hat{\mu})|0)$ is not zero and we have to evaluate all the products in eq. (4.26).

The emission and absorption spectra have been calculated using the expression eq. (4.27) for continuous-wave (cw) laser excitation for an arbitrary strength of a laser.[34,74–78] The interplay between stochastic modulation and the dynamical Stark effect has been studied in the case of a strong laser excitation. The time-dependent spectrum has also been evaluated for the two-state jump case.[36] By generalizing the hierarchy equations, one also has calculated time-dependent spectra for a non-Markovian noise including temperature effects.[37]

Laser pulses are characterized by their carrier frequency ω and wave vector $\mathbf{k}$. Modern laser experiments utilize more than two laser beams with different wave vectors and frequencies. The different orders of polarization as a power of laser fields can be detected separately by selecting a probe direction that satisfies a phase matching condition. Thus, optical polarization can be classified according to the power dependence of laser fields.[73] From eq. (3.1), the optical response to laser fields is expressed as

$$P(t) = \mathrm{tr}\{\hat{\mu}\hat{\rho}(t)\}, \tag{4.28}$$

in which $\hat{\rho}(t)$ involves the interaction between the driving fields and the system. As shown in §3.1, if we expand $\hat{\rho}(t)$ by a laser-system interaction, we can express $P(t)$ in powers of the electric fields. We consider that the system is initially in the ground equilibrium state $\hat{\rho}_{\mathrm{g}} \equiv |0\rangle\langle 0|P_{\mathrm{eq}}(\Omega)$. The expectation values with odd powers of dipole operators, i.e., $\mathrm{tr}\{\hat{\mu}\hat{\rho}_{\mathrm{g}}\}$, and $\mathrm{tr}\{\hat{\mu}\hat{\rho}_{\mathrm{g}}\hat{\mu}\hat{\mu}\}$ are zero. For short pulses $E_j(t)$, the signal is then written as[73]

$$P(t) = \sum_{N=1}^{\infty} P^{(2N-1)}(t), \tag{4.29}$$

where

$$P^{(1)}(t) = \int_0^\infty \mathrm{d}t_1\, E_1(t - t_1)R^{(1)}(t_1), \tag{4.30}$$

and

$$P^{(3)}(t) = \iiint_0^\infty \mathrm{d}t_3\, \mathrm{d}t_2\, \mathrm{d}t_1 E_3(t - t_3)E_2(t - t_{23}) \times E_1(t - t_{123})R^{(3)}(t_3,\ t_2,\ t_1), \tag{4.31}$$

and so forth. Here, $R^{(1)}(t_1)$ and $R^{(3)}(t_3,\ t_2,\ t_1)$ are the first- and third-order response functions defined by eqs. (3.8) and (3.13) with $\hat{A} = \hat{\mu}$ and $\hat{B}_n = \hat{\mu}$, respectively. By using the transformation given in eq. (3.23), they are expressed in explicit form as

$$R^{(1)}(t) = \frac{\mathrm{i}}{\hbar}\mathrm{tr}\left\{\hat{\mu}^-\hat{G}(t)\left(\hat{\mu}^+\hat{\rho}_{\mathrm{g}}\right)\right\} - \mathrm{c.c.}, \tag{4.32}$$

and

$$R^{(3)}(t_3,\ t_2,\ t_1) = \sum_{\alpha=1}^{4} R_\alpha^{(3)}(t_3,\ t_2,\ t_1) - \text{c.c.}, \quad (4.33)$$

respectively, where c.c. stands for the complex conjugate and

$$R_1^{(3)}(t_3,\ t_2,\ t_1) = -\frac{\mathrm{i}}{\hbar^3}\mathrm{tr}\{\hat{\mu}^-\hat{G}(t_3)[\{\hat{G}(t_2) \times [(\hat{G}(t_1)\hat{\mu}^+\hat{\rho}_\mathrm{g})\hat{\mu}^-]\}\hat{\mu}^+]\}, \quad (4.34)$$

$$R_2^{(3)}(t_3,\ t_2,\ t_1) = -\frac{\mathrm{i}}{\hbar^3}\mathrm{tr}\{\hat{\mu}^-\hat{G}(t_3)[\{\hat{G}(t_2) \times [\hat{\mu}^+\hat{G}(t_1)(\hat{\rho}_\mathrm{g}\hat{\mu}^-)]\}\hat{\mu}^+]\}, \quad (4.35)$$

$$R_3^{(3)}(t_3,\ t_2,\ t_1) = -\frac{\mathrm{i}}{\hbar^3}\mathrm{tr}\{\hat{\mu}^-\hat{G}(t_3)\hat{\mu}^+ \times [\hat{G}(t_2)\{[\hat{G}(t_1)(\hat{\rho}_\mathrm{g}\hat{\mu}^-)]\hat{\mu}^+\}]\}, \quad (4.36)$$

$$R_4^{(3)}(t_3,\ t_2,\ t_1) = -\frac{\mathrm{i}}{\hbar^3}\mathrm{tr}\{\hat{\mu}^-\hat{G}(t_3)\hat{\mu}^+ \times \hat{G}(t_2)\hat{\mu}^-\hat{G}(t_1)\hat{\mu}^+\hat{\rho}_\mathrm{g}\}. \quad (4.37)$$

In the above equations, $\hat{G}(t)$ is the propagator that does not involve the laser interactions defined by

$$\hat{G}(t) = \exp\left[-\frac{\mathrm{i}}{\hbar}(\hat{H}_0^\times + \hat{H}_I^\times(\Omega))t + \hat{\Gamma}_\Omega t\right]. \quad (4.38)$$

The first-order term eq. (4.32) is the observable for linear spectroscopy, whereas the third-order term eq. (4.33) with eqs. (4.34)–(4.37) is that for nonlinear spectroscopy. Pump-probe and photon echo signals can be expressed in terms of eqs. (4.34)–(4.37). Any order of polarizations is expressed by the elements of the response function with different configurations of operators corresponding to the different time evolutions of the density matrix element.[73,79] Each time evolution is characterized by the quantum Liouville paths illustrated in Fig. 3. Diagrams (1) and (2) in Fig. 3 contain the population state $|1\rangle\langle 1|$ related to excitation state dynamics, while (3) and (4) only contain $|1\rangle\langle 0|$ and $|0\rangle\langle 1|$ related to coherent states dynamics. Photon echo, impulsive pump–probe and hole-burning signals are calculated from diagrams (2) and (3), where the phase in the t_3 period is opposite to that in the t_1 period.[73]

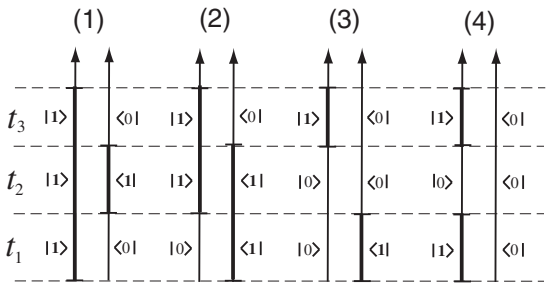

Fig. 3. Double-sided Feynman diagrams of third-order response functions. Diagrams (1)–(4) correspond to the processes for eqs. (4.34)–(4.37), respectively. In each figure, the time runs from the bottom to the top and t_1, t_2, and t_3 represent the time intervals between the successive laser-system interactions. The left line represents the time evolution of the ket, whereas the right line represents that of the bra. The excited states are represented by the fat lines. The complex conjugate paths of (1)–(4), which can be obtained by interchanging the ket and bra diagrams, are not shown here.

Numerous applications of frequency domain spectroscopy and time domain spectroscopy have been developed using eqs. (4.33)–(4.37) with the aid of the stochastic theory.[80–89] An early thorough investigation on nonlinear optical phenomena with the finite memory effect has been performed by Takagahara *et al.* using stochastic frequency modulation models; they have studied the memory effect of frequency modulation on the coherent optical transient, emission, and absorption spectra of multilevel systems.[80–84] For continuous wave excitation, the result can be obtained analytically by Laplace transformation. The emission power spectra of the three- and four-level systems with the Gaussian–Markovian and two-state Markovian modulations were investigated. The simplicity of the models allows us to study the nature of dynamical processes analytically under the influence of an environment.[35,90–92]

The expression of the signal in the second-order optical processes for a three-level system with its excited energy level randomly fluctuating as a Gaussian–Markovian modulation is analytically calculated using eqs. (4.34)–(4.36).[81] As illustrated in Fig. 4, this expression can be used to calculate spectra for (a) pump–dump (absorption–emission) and (b) doubly excited absorption processes. The explicit expression of physical spectrum is given in ref. 35. Here, we present the intensity of the spectra for the three-level system as a function of the absorption and emission frequencies ω_1 and ω_2, respectively, in Fig. 5. We chose the amplitude of fluctuation $\Delta = 5$, then plotted the spectra for the rates of fluctuation (a) $\gamma = 1.0$ and (b) $\gamma = 0.1$. The bandwidth of the instrument $\Gamma_f = 0.01$, and the longitudinal (T_1) and transversal (T_2) relaxations are phenomenologically taken

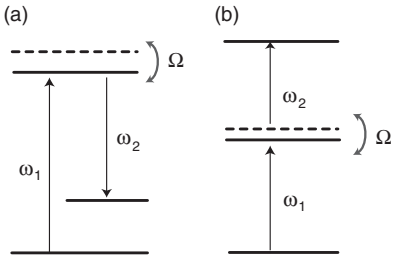

Fig. 4. Schematic view of second-order optical process of three-level system with an intermediate state modulation for (a) pump–dump transition and (b) doubly excited transition.

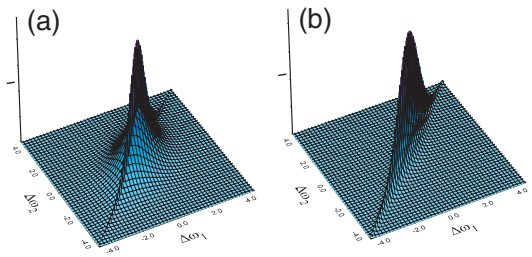

Fig. 5. Emission intensity for a three-level system with intermediate-state modulation plotted as function of absorption and emission frequencies $\Delta\omega_1$ and $\Delta\omega_2$, where we set $\Delta\omega_1 = 0$ and $\Delta\omega_2 = 0$ at resonant frequencies. (a) is for the fast-modulation case $\gamma = 1$, whereas (b) is for the slow-modulation case $\gamma = 0.1$. The intensities of spectra are plotted in arbitrary units.

into account and are set by adjusting the natural radiation damping rate γ_b ($\equiv 1/T_1 = 1/2T_2$) = 1. All parameters are dimensionless. The Raman component with the δ-function $\delta(\omega_1 - \omega_2)$ is not shown in the figure. For the fast modulation case Fig. 5(a), the coherence involved in the optical process is completely graded and a broadened peak centered at $\omega_1 = \omega_2 = 0$ appears. In Fig. 5(b), the incoherent element is seen at the Raman position $\omega_1 = \omega_2$. This is the broadened Raman peak that arises because the quantum coherence is partially graded by stochastic modulation.[90] To explain this peak, it is essential to treat the system-environment interactions nonperturbatively. Therefore this peak was not predicted from the theory based on perturbative equations such as the quantum master equation or Redfield equation. The importance of noise correlation was also pointed out experimentally.[93,94] The temperature effect of the modulation on the second-order optical process, which could not be included within the framework of the stochastic theory, was also discussed in ref. 35.

Contemporary laser instruments can handle a laser pulse shorter than subfemto second ($\leq 10^{-15}$ s) and can measure motions faster than most molecular and atomic movements. An analysis of the time-dependent signal in ultrafast spectroscopy gives us a deeper understanding of relaxation, but it requires more specific and detailed considerations. For molecular cases, a system is commonly modeled by several electronic excitation levels coupled with molecular vibrational modes that usually consists of one overdamped and several underdamped modes. The overdamped mode represents a nonoscillatory motion of molecules, which causes the inhomogeneous broadening of spectral lines. The underdamped modes represent inter- or intra-modes of molecular vibrations, which are usually modeled by Brownian oscillators. As mentioned in §4.1, the stochastic theory can be used to describe the inhomogeneous broadening expressed by a Gaussian distribution. In this framework, several researchers calculated the photon echo signal defined by the third-order response functions eqs. (4.35) and (4.37). It was shown that if the modulation is slow and the coherence of the electronic excitation is not degraded, a photon echo peak appears.[95–97] Although the overdamped motion can be treated by the stochastic approach, the underdamped modes are not so easy to handle except for harmonic modes where the quantum Brownian motion theory can be applied. The calculations of such signals are ongoing subjects. We shall briefly discuss one of such attempts in §5.8.

The problem of resonant spectroscopy is closely related to the nonadiabatic transition problem, which is known as the Landau–Zener problem.[98] Kayanuma has studied the effect of stochastic perturbation on nonadiabatic transition by assuming the Hamiltonian

$$\hat{H}(t) = \frac{1}{2}\big[vt + \hbar\bar{\Omega}(t)\big](|0\rangle\langle 0| - |1\rangle\langle 1|) + \big[J + \hbar\bar{\Omega}'(t)\big](|0\rangle\langle 1| + |1\rangle\langle 0|), \tag{4.39}$$

where $|0\rangle$ and $|1\rangle$ are adiabatic states, J is the nonadiabatic coupling, and v is the velocity of the particle. The change in energy between the adiabatic states is proportional to v. The effects of the diagonal and off-diagonal modulations were characterized by $\bar{\Omega}(t)$ and $\bar{\Omega}'(t)$, respectively, and were studied from the stochastic approach.[99–101]

4.5 Molecular vibrational spectroscopy

The stochastic theory has been applied to vibrational spectroscopy from the early stage of its development to explain vibrational dephasing.[102] The Hamiltonian for vibrational modes is expressed in the molecular coordinates $\hat{q}_s$ as

$$\hat{H}_{\rm sys} = \sum_s \left[\frac{\hat{p}_s^2}{2m} + U(\hat{q}_s)\right] + \sum_{s\neq s'} U'(\hat{q}_s, \hat{q}_{s'}), \tag{4.40}$$

where $U'(\hat{q}_s, \hat{q}_{s'})$ represents the interaction potential. We denote the set of coordinates by $\hat{\mathbf{q}} \equiv (\hat{q}_1, \hat{q}_2, \hat{q}_3, \ldots)$. The total Hamiltonian with external laser interactions is denoted by $\hat{H}(t) = \hat{H}_{\rm sys} + \hat{H}_E(t)$. Infrared (IR) spectroscopy probes the molecular dipole $\mu(\hat{\mathbf{q}})$, whereas off-resonant Raman spectroscopy probes the molecular polarizability $\alpha(\hat{\mathbf{q}})$. Laser interactions are then expressed as $\hat{H}_E(t) = -\mu(\hat{\mathbf{q}})E(t)$ for IR and $\hat{H}_E(t) = -\alpha(\hat{\mathbf{q}})E^2(t)/2$ for Raman. Notice that, to induce vibrational excitation, the Raman process requires two laser interactions, since $\hat{H}_E(t) \propto -\mu_{\rm ind}(\hat{\mathbf{q}})E(t)$ and the induced dipole is given by $\mu_{\rm ind}(\hat{\mathbf{q}}) = \alpha(\hat{\mathbf{q}})E(t)$. Hence, as illustrated in §3.1, both the first-order IR and third-order Raman response functions are expressed by two-time correlation functions as

$$R^{(1)}_{\rm IR}(t_1) \equiv \frac{\rm i}{\hbar}\big\langle\big[\mu\big(\hat{\mathbf{q}}(t_1)\big),\ \mu\big(\hat{\mathbf{q}}\big)\big]\big\rangle, \tag{4.41}$$

and

$$R^{(3)}_{\rm Raman}(t_1) \equiv \frac{\rm i}{\hbar}\big\langle\big[\alpha\big(\hat{\mathbf{q}}(t_1)\big),\ \alpha\big(\hat{\mathbf{q}}\big)\big]\big\rangle, \tag{4.42}$$

respectively, in which the Hamiltonian in $\langle\cdots\rangle$ does not involve laser interactions. We can always write the Hamiltonian eq. (4.40) in matrix form with the basis of the energy eigenstates of each mode $|n_s\rangle$ as

$$\hat{H} = \hbar\sum_s\sum_{n_s}\omega_{n_s}|n_s\rangle\langle n_s| + \hbar\sum_{s\,s'}\sum_{n_s\neq n'_{s'}}\omega_{n_s n'_{s'}}|n_s\rangle\langle n'_{s'}|, \tag{4.43}$$

where $\hbar\omega_{n_s}$ is the nth eigen energy for the mode s, and $\omega_{n_s n'_{s'}}$ represents the transition frequencies between the energy levels denoted by n_s and $n'_{s'}$. Suppose that only the i-th mode is optically active, i.e., $\mu(\hat{\mathbf{q}}) \to \mu(\hat{q}_i)$ or $\alpha(\hat{\mathbf{q}}) \to \alpha(\hat{q}_i)$, the other degrees of freedom can be regarded as the bath modes, which give rise to a fluctuation in the transition frequencies of the mode i. We then write $\hat{H}_{\rm sys} \to \hat{H}_{\rm sys}(t) = \hat{H}_0 + \hat{H}_I(t)$ as

$$\hat{H}_{\rm sys}(t) = \hbar\sum_{n_i}\big[\omega_{n_i} + \bar{\Omega}_{n_i}(t)\big]|n_i\rangle\langle n_i| + \hbar\sum_{n_i\neq n'_i}\bar{\Omega}_{n_i n'_i}(t)|n_i\rangle\langle n'_i|, \tag{4.44}$$

where the states n_i and n'_i belong to the same mode i. The dipolar interaction is expressed in terms of the elements $\mu_{n_i,n'_i} \equiv \langle n'_i|\mu(\hat{q}_i)|n_i\rangle$ as $\hat{H}_E(t) = -\sum_{n_i\neq n'_i}\mu_{n_i,n'_i}E(t)|n_i\rangle\langle n'_i|$. Polarizability can be defined in the same manner. The above Hamiltonian looks similar to that for electronically resonant spectroscopy [see eq. (4.21) with eq. (4.23)]. In the present case, however, the frequency fluctuations $\bar{\Omega}_{n_i}(t)$ for different n_i correlate, since they arise from the same interaction between the modes described by the coordinates q_i and the bath. Similarly, the off-diagonal fluctuations

$\bar{\Omega}_{n_i n_i'}(t)$ for different n_i and n_i' values also correlate. Suppose that the frequencies of the bath modes are much lower than that of the optically active mode i, the effects of the energy transition between the i mode and the bath modes may be neglected. The Hamiltonian is then expressed as[103,104]

$$\hat{H}_{\rm sys}(t) = \hbar \sum_{n_i} \left[\omega_{n_i} + \bar{\Omega}_{n_i}(t)\right] |n_i\rangle\langle n_i|. \qquad (4.45)$$

This Hamiltonian has the same form as that with the stochastic diagonal modulation. This model, however, has a critical drawback: Because we neglect the off-diagonal elements, the system never reaches the thermal equilibrium state. Furthermore, even if we include the terms $\bar{\Omega}_{n_i n_i'}(t)$, as long as we assume stochastic modulations for $\bar{\Omega}_{n_i}(t)$ and $\bar{\Omega}_{n_i n_i'}(t)$, the temperature of the system increases to infinity, since stochastic modulation is in principle an external adiabatic modulation. This may cause a serious problem particularly for low-frequency vibrational modes, where thermal excitations play an important role.[105] Nevertheless, due to its simplicity, this model has been used extensively to analyze high-frequency vibrational modes. An implicit assumption that is often made for this model is that the frequency fluctuations $\bar{\Omega}_{n_i}(t)$ can be described by a Gaussian–Markovian process. By utilizing molecular dynamics simulations, the Gaussian–Markovian character of frequency fluctuations is observed in some cases.[106–109]

4.6 *Single-molecular detection and two-dimensional vibrational spectroscopy*

Spectral line shapes in a condensed phase contain information from various dynamic processes, including important processes such as microscopic dynamics, intermolecular couplings, and solvent dynamics, all of which modulate the energy of a transition. Energy and phase relaxations take place whenever a system is affected by coupling to other degrees of freedom and the resultant line shape from molecules in condensed phase is broadened and overlapped. As a result, it is very hard to analyze the spectrum without assuming a model, but conventional laser experiments are not capable of detecting the validity of such a model. In the '90s, two new spectroscopic approaches, single molecular detection (SMD) and two-dimensional (2D) vibrational spectroscopy, were developed, which stimulated the development of the stochastic theory.

In SMD,[110] the resonant frequency of a dye molecule in a matrix environment is measured by high-resolution spectroscopy. Because such an environment changes due to the lattice vibration of the surrounding atoms or molecules, the frequency fluctuates with time.[111–116] SMD can probe this stochastic trajectory of frequency without taking an ensemble average, which is now called spectral diffusion[115] Reilly and Skinner explained spectral diffusion using a model of a chromophore coupled to a collection of stochastic two-state jump systems.[116]

In 2D spectroscopy, the multibody correlation functions of a molecular dipole or polarizability are measured using ultrashort pulses.[24,117] As outlined in §4.5, researchers have used the stochastic theory to investigate vibrational dephasing in linear IR and Raman spectroscopies. Unfortunately, the change of signals in linear spectroscopies does not easily reveal microscopic details of the underlying mechanism and process in the condensed phase. Thus, other extreme spectroscopic approaches, that is, multi-dimensional vibrational spectroscopies, were developed. The fifth-order two-dimensional (2D) Raman[24,118,119] and third-order 2D IR spectroscopies[117,120–127] are such examples. The pulse configurations of these measurements are shown in Fig. 6. For Raman and IR cases, the observables are polarizability and dipole moment, respectively. The fifth-order Raman and second-order IR processes are represented by their three-body correlation function eq. (3.12) whereas the seventh-order Raman and third-order IR ones by their four-body correlation function eq. (3.13). Then the response functions for the fifth-order Raman and third-order IR processes are given by[24]

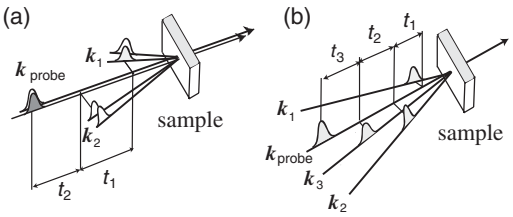

Fig. 6. Pulse configuration for (a) the fifth-order Raman and (b) the third-order IR experiments. To induce vibrational excitation, a Raman process requires a pair of laser pulses. Therefore, the $(2n+1)$th-order Raman process is equivalent to the nth order IR process.

$$R^{(5)}_{\rm Raman}(t_2,\ t_1) \equiv -\frac{1}{\hbar^2}\left\langle\left[\left[\alpha\left(\hat{\mathbf{q}}(t_{12})\right),\ \alpha\left(\hat{\mathbf{q}}(t_1)\right)\right],\ \alpha\left(\hat{\mathbf{q}}\right)\right]\right\rangle, \qquad (4.46)$$

and

$$R^{(3)}_{\rm IR}(t_3,\ t_2,\ t_1) \equiv -\frac{\mathrm{i}}{\hbar^3}\left\langle\left[\left[\left[\mu\left(\hat{\mathbf{q}}(t_{123})\right), \mu\left(\hat{\mathbf{q}}(t_{12})\right)\right],\ \mu\left(\hat{\mathbf{q}}(t_1)\right)\right],\ \mu\left(\hat{\mathbf{q}}\right)\right]\right\rangle, \qquad (4.47)$$

respectively, where we set $t_{12} \equiv t_1 + t_2$ and $t_{123} \equiv t_1 + t_2 + t_3$. Multi-dimensional vibrational spectra are obtained by recording the signals as a function of the time duration between the pulses. In practice, the fifth-order 2D Raman spectroscopy is designed to differentiate various motional modes whose origins are attributed to inhomogeneity,[24,27,28,128,129] anharmonicity,[25,130–133] and mode coupling mechanisms,[134–136] and to monitor inter- and intramolecular vibrational motions.[29,30,137–140] Third-order infrared or seventh-order Raman processes[141,142] are shown to be sensitive to the local fluctuation of the molecules surrounding the target molecules and the conformal change of molecules,[121,123,143] which are not so clear for the linear spectroscopy discussed in §4.5. Three-pulse vibrational echo techniques were applied to the molecular stretching mode[144] and hydrogen bonding interaction between the solute and the solvent.[125,126]

Some calculations in the fifth-order Raman and third-order IR measurements were carried out using the theory developed for the electronically resonant spectroscopy explained in §4.4. If the random force exerted on a molecule by solvents causes the stochastic modulation of vibrational energy levels, we can employ the Hamiltonian given by eq. (4.45). Thus, the model shown in Fig. 4 may be used to

explain the signals from multi-dimensional Raman[128,129] and IR spectroscopies.[145,146] The results in Fig. 5 may also be used for the analysis of third-order IR spectroscopy, which involves four laser excitations. The form of $\bar{\Omega}(t)$ is determined by molecular dynamics simulation.[145–150] The IR echo signal is then calculated from response functions similar to eqs. (4.35) and (4.37). The results reasonably explain the time scale of dephasing measured in the experiments, but the validity of the models must be carefully examined.[151]

5. Quantum Fokker–Planck Equation and Master Equation for Nearly Markovian Noise Bath

5.1 Reduced density matrix elements

Up to this point, we have treated phenomenological stochastic modulation for a spin or molecular system. The stochastic theory involves the fluctuation of energy states but does not treat damping or dissipation explicitly like a damping term in the Langevin equation. If the system interacts with a thermal bath, dissipation arises in addition to fluctuation.[3] Fluctuation supplies energy to the system, whereas dissipation takes energy out of the system: In the equilibrium state, fluctuation energy balances with dissipation energy. Since the stochastic theory assumes adiabatic modulation, it does not involve the energy transfer from the system to the environment. Therefore, the dissipation term does not appear in the stochastic Liouville equation. Thus, the stochastic theory is difficult to apply to a system described by momenta and coordinates as the case discussed in §4.5, since the temperature of the system increases to infinity and all vibrational energy levels are excited.

To overcome this problem, we consider a situation in which the system is subjected to a heat bath that gives rise to dissipation in addition to fluctuation in the system. To illustrate this, let us consider the model Hamiltonian,[152–155]

$$\hat{H} = H_A(\hat{p},\hat{q}) + \sum_j \left[\frac{\hat{p}_j^2}{2m_j} + \frac{1}{2} m_j \omega_j^2 \left(\hat{x}_j - \frac{c_j V(\hat{q})}{m_j \omega_j^2} \right)^2 \right], \tag{5.1}$$

where

$$H_A(\hat{p},\hat{q}) = \frac{\hat{p}^2}{2m} + U(\hat{q}) \tag{5.2}$$

is the Hamiltonian for the system with a mass m and a potential $U(\hat{q})$ described by the momentum $\hat{p}$ and the coordinate $\hat{q}$. The bath degrees of freedom are treated as an ensemble of harmonic oscillators, and the momentum, coordinate, mass, and frequency of the jth bath oscillator are given by $\hat{p}_j$, $\hat{x}_j$, m_j, and ω_j, respectively. The system–bath interaction is denoted by $-V(\hat{q})\sum_j c_j \hat{x}_j$, where $V(\hat{q})$ is a function for the system. Note that we included here the counter term $\sum_j c_j^2 V^2(\hat{q})/2m_j\omega_j^2$ presented in ref. 153 to maintain the translational symmetry for $U(\hat{q}) = 0$ required to describe a motion of a free Brownian particle. The reduced density matrix element for the above Hamiltonian with the heat bath is written as

$$\rho(q,q';t) = \int D[q(\tau)] \int D[q'(\tau)] \int \mathrm{d}q_i \int \mathrm{d}q_i' \, \rho(q_i,q_i') \rho_{\mathrm{CS}}(q,q',t;q_i,q_i') \times \exp\left\{ \frac{\mathrm{i}}{\hbar} S_A[q;t] \right\} F(q,q';t) \exp\left\{ -\frac{\mathrm{i}}{\hbar} S_A[q';t] \right\}, \tag{5.3}$$

where $S_A[q;t]$ is the action for $H_A(\hat{p},\hat{q})$,

$$S_A[q;t] \equiv \int_{t_i}^{t} \mathrm{d}\tau \left[\frac{1}{2} m \dot{q}^2(\tau) - U(q(\tau)) \right], \tag{5.4}$$

$\rho(q_i,q_i')$ is the initial state of the system at time t_i, $F(q,q';t)$ is the influence functional,[152] and $\rho_{\mathrm{CS}}(q,q',t;q_i,q_i')$ is the initial correlation function between the system and the bath.[155] The functional integrals for $q(\tau)$ and $q'(\tau)$ run from $q(t_i) = q_i$ to $q(t) = q$ and from $q'(t_i) = q_i'$ to $q'(t) = q'$, respectively. In our approach, we can set $\rho_{\mathrm{CS}}(q,q',t;q_i,q_i') = 1$ and regard $\rho(q_i,q_i')$ as the initial condition without scarifying generality; the effects of the initial correlation can be taken into account by a hierarchy of the initial condition, as will be shown in §5.4. The influence functional for the inverse temperature $\beta \equiv 1/k_{\mathrm{B}}T$ is given by[152–155]

$$F(q,q';t) = \exp\left\{ \left(-\frac{\mathrm{i}}{\hbar} \right)^2 \int_{t_i}^{t} \mathrm{d}\tau \, V^{\times}(q,q';\tau) \times \left[\frac{\partial}{\partial\tau} \int_{t_i}^{\tau} \mathrm{d}\tau' \, \mathrm{i}\bar{L}_1(\tau-\tau') V^{\circ}(q,q';\tau') + \int_{t_i}^{\tau} \mathrm{d}\tau' \, L_2(\tau-\tau') V^{\times}(q,q';\tau') \right] \right\}, \tag{5.5}$$

where $V^{\times}(q,q';\tau) \equiv V(q(\tau)) - V(q'(\tau))$ and $V^{\circ}(q,q';\tau) \equiv V(q(\tau)) + V\big(q'(\tau)\big)$. The kernels of the time integrals are expressed as

$$\bar{L}_1(t) = \int_0^{\infty} \mathrm{d}\omega \, \frac{J(\omega)}{\omega} \cos\omega t, \tag{5.6}$$

and

$$L_2(t) = \int_0^{\infty} \mathrm{d}\omega \, J(\omega) \cos\omega t \coth\left(\frac{\beta\hbar\omega}{2} \right), \tag{5.7}$$

with the distribution function

$$J(\omega) = \sum_j \frac{c_j^2 \hbar}{2m_j\omega_j} \delta(\omega - \omega_j). \tag{5.8}$$

If we consider the interaction coordinate of the bath modes as $\hat{X} \equiv \sum_j c_j \hat{x}_j$, system A is considered to be driven by the external force $\hat{X}(t)$ through the interaction $-V(\hat{q})\hat{X}$, where $\hat{X}(t)$ is the Heisenberg representation of $\hat{X}$ for the bath Hamiltonian $\hat{H}_{\mathrm{B}} = \sum_j (\hat{p}_j^2/2m_j + m_j\omega_j^2\hat{x}_j^2/2)$.[15] Since the bath is a harmonic that exhibits a Gaussian nature, the character of $\hat{X}(t)$ is specified by its two-time correlation functions, such as the symmetrized and canonical correlation functions respectively defined by

$$C(t) = \frac{1}{2} \langle \hat{X}(t)\hat{X}(0) + \hat{X}(0)\hat{X}(t) \rangle_{\mathrm{B}}, \tag{5.9}$$

and

$$\Psi(t) = \beta\langle\hat{X};\dot{\hat{X}}(t)\rangle_{\rm B}, \tag{5.10}$$

where $\langle\cdots\rangle_{\rm B}$ represents the thermal average of the bath degrees of freedom. The function $C(t)$ is analogous to the classical correlation function of $X(t)$. It is related to $\Psi(t)$ through the fluctuation–dissipation theorem $C[\omega] = \hbar\omega\coth(\beta\hbar\omega/2)/2\Psi[\omega]$. Since $\bar{L}_1(t) = -\hbar\Psi(t)/2$ and $L_2(t) = C(t)$, $L_2(t)$ corresponds to the correlation function of the noise, whereas $\bar{L}_1(t)$ corresponds to dissipation. Both effects are induced by the bath.

By carrying out the path integrals, the reduced density matrix elements were calculated analytically for a harmonic oscillator,[155] a free particle,[156] and a two-dimensional rotator.[59,60] Variational calculations including optimized perturbative calculations were also examined for a polaron[157] and a Morse oscillator[158] to evaluate the reduced density matrix. The equations of motion for eq. (5.3) were also derived by considering the time derivative of eq. (5.3).[153,154] In what follows in the next subsection, we shall obtain the equations of motion in a similar hierarchy form as eqs. (2.41)–(2.43) and eq. (2.62) by choosing a proper spectral distribution and a temperature.

5.2 *Quantum Fokker–Planck equation for nearly Markovian noise bath*

The function $L_2(t)$ arises from the correlation function of the bath coordinates and corresponds to the noise correlation function.[15] To have equations of motion in a similar hierarchy form as the stochastic Liouville equation, we need to choose $L_2(t)$ in exponential (Markovian) form. Hence, we assume[15–19,151,159–167]

$$J(\omega) = \frac{\hbar\eta}{\pi}\frac{\gamma^2\omega}{\gamma^2+\omega^2}, \tag{5.11}$$

to have

$$\bar{L}_1(t) = \frac{\hbar\eta\gamma}{2}{\rm e}^{-\gamma|t|}, \tag{5.12}$$

and

$$L_2(t) = c_0{\rm e}^{-\gamma|t|} + \sum_{k=1}^{\infty} c_k{\rm e}^{-\nu_k|t|}, \tag{5.13}$$

where $\nu_k \equiv 2k\pi/\beta\hbar$ are the Matsubara frequencies and

$$c_0 = \frac{\hbar\eta\gamma^2}{2}\left[\frac{2}{\beta\hbar\gamma} + \sum_{k=1}^{\infty}\frac{4\beta\hbar\gamma}{(\beta\hbar\gamma)^2-(2k\pi)^2}\right], \tag{5.14}$$

and

$$c_k = -\frac{\hbar\eta\gamma^2}{2}\frac{8k\pi}{(\beta\hbar\gamma)^2-(2k\pi)^2}. \tag{5.15}$$

The profiles of $L_2(t)$ for different γ and $\beta\hbar$ values are illustrated in Fig. 7. If we further assume the high temperature case $\beta\hbar\gamma \ll 1$, we obtain the desired feature as $L_2(t) \approx \eta\gamma\exp[-\gamma|t|]/\beta$. Since $L_2(t)$ has the same exponential form as the noise correlation function eq. (2.10), we may derive the equation of motion for eq. (5.3) in hierarchy form as eqs. (2.41)–(2.43). To illustrate the derivation, we rewrite the influence functional as

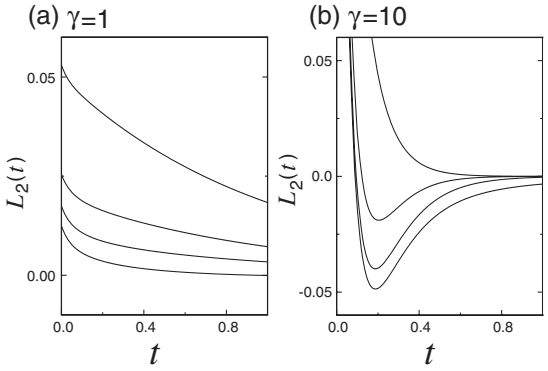

Fig. 7. The kernel $L_2(t)$ defined by eq. (5.13) is depicted as a function of the non-dimensional time t for (a) $\gamma = 1$ and (b) $\gamma = 10$. In each of the figures, from top to bottom, the inverse temperatures are $\beta\hbar = 0.2, 0.5, 1.0$, and 10. The constant $\hbar\eta\gamma^2/2$ is set to unity. This function becomes negative at low temperature $\beta\hbar\gamma \gg 1$ in the region of small t's for the case of (b). This is characteristic of a quantum noise. In the classical limit with $\hbar$ tending to be zero, $L_2(t)$ always becomes positive.

$$F(q,q';t) = \exp\left\{-\int_{t_i}^{t}{\rm d}\tau\,\Phi(q(\tau),q'(\tau)) \times\left[\int_{t_i}^{\tau}{\rm d}\tau'\,{\rm e}^{-\gamma(\tau-\tau')}\Theta(q,q';\tau') + G(q_i,q_i';\tau)\right]\right\}, \tag{5.16}$$

where

$$\Phi(q(\tau),q'(\tau)) \equiv \frac{\rm i}{\hbar}\big[V\big(q(\tau)\big) - V\big(q'(\tau)\big)\big], \tag{5.17}$$

$$\Theta(q,q';\tau) \equiv \frac{\gamma\eta}{2}\left\{\frac{\partial V\big(q(\tau)\big)}{\partial\tau} + \frac{\partial V\big(q'(\tau)\big)}{\partial\tau} - \frac{2{\rm i}}{\beta\hbar}\big[V\big(q(\tau)\big) - V\big(q'(\tau)\big)\big]\right\}, \tag{5.18}$$

and

$$G(q_i,q_i';\tau) \equiv \frac{\eta\gamma}{2}{\rm e}^{-\gamma(\tau-t_i)}\big[V\big(q_i\big) + V\big(q_i'\big)\big]. \tag{5.19}$$

We follow a procedure similar to the derivation of eqs. (2.14)–(2.17) to determine the equations of motion. The density matrix element with a time increment ϵ is expressed as

$$\begin{aligned}\rho(q,q';t+\epsilon) &= \frac{1}{C^2}\int{\rm d}y\int{\rm d}y'\int D'[q(\tau)]\int D'[q'(\tau)]\int{\rm d}q_i\int{\rm d}q_i'\exp\left[\frac{{\rm i}my^2}{2\hbar\epsilon} - \frac{{\rm i}\epsilon}{\hbar}U\big(q-y\big)\right]\exp\left[-\frac{{\rm i}my'^2}{2\hbar\epsilon} + \frac{{\rm i}\epsilon}{\hbar}U\big(q'-y'\big)\right]\\ &\times\exp\left\{-\epsilon\Phi(q-y,q'-y')\left[\int_{t_i}^{t}{\rm d}\tau'\,{\rm e}^{-\gamma(t-\tau')}\Theta(q,q';\tau') + G(q_i,q_i';t)\right]\right\}\\ &\times\exp\left\{\frac{\rm i}{\hbar}S_A[q;t]\right\}F(q,q';t)\exp\left\{-\frac{\rm i}{\hbar}S_A[q';t]\right\}\rho(q_i,q_i'),\end{aligned} \tag{5.20}$$

where C is the normalization constant for the integral y or y', and the functional integrals $\int D'[q(\tau)]$ and $\int D'[q'(\tau)]$ now run from $q(t_i) = q_i$ to $q(t) = q - y$ and from $q'(t_i) = q'_i$ to $q'(t) = q' - y'$, respectively. Since $\hbar\varepsilon$ is very small, the integrations of $\exp[\mathrm{i}my^2/2\hbar\epsilon]$ on y and $\exp[-\mathrm{i}my'^2/2\hbar\epsilon]$ on y' can contribute to the very small regions of y and y'. Hence, we can expand the remaining integrant using y and y'. Then, by further expanding ϵ and by taking the limit $\epsilon \to 0$ for $[\rho(q, q'; t+\epsilon) - \rho(q, q'; t)]/\epsilon$, we can calculate the time derivative of the density matrix element as[15,18,162,164]

$$\begin{aligned}\frac{\partial}{\partial t}\rho(q,q';t) = &-\frac{\mathrm{i}}{\hbar}\hat{L}(q,q')\rho(q,q';t)\\ &-\Phi(q,q')\int D[q(\tau)]\int D[q'(\tau)]\int \mathrm{d}q_i\int \mathrm{d}q'_i\left[\int_{t_i}^{t}\mathrm{d}\tau'\,\mathrm{e}^{-\gamma(t-\tau')}\Theta\big(q,q';\tau'\big)+G(q_i,q'_i;t)\right]\\ &\times\exp\left\{\frac{\mathrm{i}}{\hbar}S_A[q;t]\right\}F(q,q';t)\exp\left\{-\frac{\mathrm{i}}{\hbar}S_A[q';t]\right\}\rho(q_i,q'_i),\end{aligned} \tag{5.21}$$

where

$$\hat{L}(q,q') \equiv -\frac{\hbar^2}{2m}\left(\frac{\partial^2}{\partial q^2}-\frac{\partial^2}{\partial q'^2}\right)+U(q)-U(q') \tag{5.22}$$

is the quantal Liouvillian. To avoid the explicit treatment of inherent memory effects during the time evolution of the reduced density matrix and to make the treatment tractable, we introduce auxiliary functions for any nonnegative integer n defined by

$$\begin{aligned}\rho_n(q,q';t) \equiv &\int D[q(\tau)]\int D[q'(\tau)]\int \mathrm{d}q_i\int \mathrm{d}q'_i\left[\int_{t_i}^{t}\mathrm{d}\tau'\,\mathrm{e}^{-\gamma(t-\tau')}\Theta(q,q';\tau')+G(q_i,q'_i;t)\right]^n\\ &\times\exp\left\{\frac{\mathrm{i}}{\hbar}S_A[q;t]\right\}F(q,q';t)\exp\left\{-\frac{\mathrm{i}}{\hbar}S_A[q';t]\right\}\rho(q_i,q'_i).\end{aligned} \tag{5.23}$$

Then the element with $n = 0$ corresponds to the exact distribution function $\rho(q, q'; t) = \rho_0(q, q'; t)$. Using the above auxiliary function, we can rewrite eq. (5.21) as

$$\frac{\partial}{\partial t}\rho_0(q,q';t) = -\frac{\mathrm{i}}{\hbar}\hat{L}(q,q')\rho_0(q,q';t)-\Phi(q,q')\rho_1(q,q';t). \tag{5.24}$$

To evaluate $\rho_1(q, q'; t)$, we reduce the equation of motion for eq. (5.23) with $n = 1$. Repeating the same procedure for $\rho_n(q, q'; t)$, we can construct the hierarchy of equations as

$$\frac{\partial}{\partial t}\rho_n(q,q';t) = -\left[\frac{\mathrm{i}}{\hbar}\hat{L}(q,q')+n\gamma\right]\rho_n(q,q';t)-\Phi(q,q')\rho_{n+1}(q,q';t)+n\Theta(q,q')\rho_{n-1}(q,q';t), \tag{5.25}$$

where $\Theta(q, q')$ is now expressed as

$$\Theta(q,q') \equiv \frac{\gamma\eta}{2}\left\{-\frac{\mathrm{i}\hbar}{m}\left[V'\big(q\big)\frac{\partial}{\partial q}-V'\big(q'\big)\frac{\partial}{\partial q'}\right]-\frac{\mathrm{i}\hbar}{2m}\big[V''\big(q\big)-V''\big(q'\big)\big]-\frac{2\mathrm{i}}{\beta\hbar}\big[V\big(q\big)-V\big(q'\big)\big]\right\}, \tag{5.26}$$

where $V'(q) \equiv \partial V(q)/\partial q$ and $V''(q) \equiv \partial^2 V(q)/\partial q^2$. As shown by eq. (2.62), for large $(N+1)\gamma \gg \eta/\beta$ and ω_A, where ω_A is a characteristic frequency of the system, the hierarchy of equations can be terminated using

$$\frac{\partial}{\partial t}\rho_N(q,q';t) = -\left[\frac{\mathrm{i}}{\hbar}\hat{L}(q,q')+N\gamma\right]\rho_N(q,q';t)-\frac{1}{\gamma}\Phi(q,q')\Theta(q,q')\rho_N(q,q';t)+N\Theta(q,q')\rho_{N-1}(q,q';t). \tag{5.27}$$

Here, to obtain the above equation, we used the relation

$$\rho_{N+1}(q,q';t) = \frac{1}{\gamma}\Theta(q,q')\rho_N(q,q';t). \tag{5.28}$$

The equations of motion eqs. (5.24), (5.25), and (5.27) are the coordinate state representation of the quantum Fokker–Planck equation for a nearly Markovian bath.[18,162,164] The depth of the hierarchy N is chosen according to the time scale of the correlation time $1/\gamma$ and the strength of the system–bath interactions. A physical interpretation of these hierarchy elements will be given in §5.4 in the context of the correlated initial condition.

5.3 Wigner distribution function and classical limit

The density operator representation of the equations of motion eqs. (5.24), (5.25), and (5.27) is obtained by replacing $\hat{L}(q,q')\rho(q,q') \to \hat{H}_A^{\times}\hat{\rho}$, $[V(q)-V(q')]\rho(q,q') \to V^{\times}(\hat{q})\hat{\rho}$, and $-\mathrm{i}\hbar[V'(q)\partial/\partial q - V'(q')\partial/\partial q']\rho(q,q')/m \to [V'(\hat{q})\hat{p}\hat{\rho}+\hat{\rho}\hat{p}V'(\hat{q})]$, respectively. We then introduce the Wigner distribution function, which is the quantum analog of the classical distribution function in phase space. For the density matrix element $\rho_n(q, q')$, this is defined as[168]

$$W_n(p,q) \equiv \frac{1}{2\pi\hbar}\int_{-\infty}^{\infty}\mathrm{d}x\,\mathrm{e}^{\mathrm{i}px/\hbar}\rho_n\left(q-\frac{x}{2},q+\frac{x}{2}\right). \tag{5.29}$$

The Wigner distribution function is a real function in contrast to the complex density matrix. Following the transformations[169]

$$\begin{aligned}A(\hat{p},\hat{q})\hat{\rho} &\to A\left(p+\frac{\hbar}{2\mathrm{i}}\frac{\partial}{\partial q},q-\frac{\hbar}{2\mathrm{i}}\frac{\partial}{\partial p}\right)W(p,q),\\ \hat{\rho}A(\hat{p},\hat{q}) &\to A\left(p-\frac{\hbar}{2\mathrm{i}}\frac{\partial}{\partial q},q+\frac{\hbar}{2\mathrm{i}}\frac{\partial}{\partial p}\right)W(p,q),\end{aligned} \tag{5.30}$$

we can easily express the equations of motions in the Wigner representation.

To write the equations in explicit form, we assume that the system–bath interaction consists of the linear–linear (LL) interaction qX[18,19] and the square–linear (SL) interaction q^2X,[105,161,162] where $X \equiv \sum_j c_j x_j$. We then employ[164,165]

$$V(q) = V_1 q + \frac{1}{2} V_2 q^2. \tag{5.31}$$

As mentioned in §5.1, the system–bath interaction can be regarded as the time-dependent external force applied to the system and we may include the interaction into the effective potential as $U'(q,t) \equiv U(q) - V(q)X(t)$. If we consider the harmonic potential $U(q) = m\omega_0^2 q^2/2$, we have $U'(q,t) = m\omega_0^2[q - \bar{V}_1 X(t)]^2/2 - m\omega_0^2 \bar{V}_1^2 X^2(t)/2$ for the LL interaction, whereas $U'(q,t) = m\omega^2(t)q^2/2$ for the SL interaction, where $\bar{V}_1 \equiv V_1/m\omega_0^2$ and $\omega^2(t) \equiv \omega_0^2 - V_2 X(t)/m$. Thus, for a random noise $X(t)$, LL coupling swings the position of the potential, whereas SL coupling shakes the potential surface as illustrated in Fig. 8. Since the SL interaction causes the frequency modulation of the potential, the fast modulation limit of SL interaction corresponds to the case of homogeneous distribution as depicted in Fig. 9(a), whereas the slow modulation corresponds to the case of inhomogeneous distribution as depicted in Fig. 9(b), like the case of a two-level system shown in Figs. 1(a) and 1(b), respectively. Notice that, in the white noise limit with a rotating wave approximation (RWA), LL coupling is responsible for longitudinal (T_1) and transversal (T_2) vibrational relaxations in a two-level system, whereas SL coupling is for $T_2^{\dagger}$.[151,162,164]

The operators defined by eqs. (5.17) and (5.26) are respectively expressed in Wigner form as[164,165]

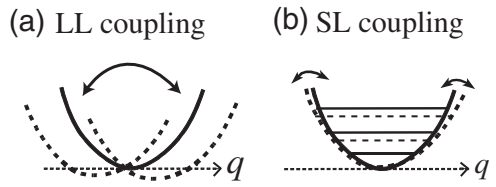

Fig. 8. Schematic illustration of effects of (a) the linear–linear (LL) and (b) the square–linear (SL) system–bath couplings on harmonic potential system. The bold lines represent the unperturbed potential, while the dashed lines represent the perturbed one. LL coupling swings the position of the potential, whereas SL coupling shakes the potential surface.

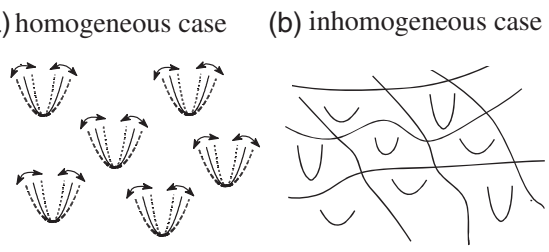

Fig. 9. Schematic views of homogeneous (fast-modulation limit) and inhomogeneous (slow-modulation limit) distributions of potential system perturbed by SL system–bath interaction. The situations are analogous to those in the cases shown in Fig. 1.

$$\hat{\Phi}_{\rm W} \equiv -\big(V_1 + V_2 q\big)\frac{\partial}{\partial p}, \tag{5.32}$$

and

$$\hat{\Theta}_{\rm W} \equiv \zeta\gamma\bigg[(V_1 + V_2 q)\bigg(p + \frac{m}{\beta}\frac{\partial}{\partial p}\bigg) + \frac{V_2\hbar^2}{4}\frac{\partial^2}{\partial p \partial q}\bigg], \tag{5.33}$$

where we set

$$\zeta \equiv \frac{\eta}{m}. \tag{5.34}$$

For a general form of the potential $U(q)$ or the coupling $V(q)$, the integrating form of the commutator, which is defined for any function $\hat{A}(q)$ by

$$\frac{\rm i}{\hbar}[\hat{A}(q), \hat{\rho}(t)] \to \frac{1}{\hbar}\int_{-\infty}^{\infty}\frac{{\rm d}p'}{2\pi\hbar} A_{\rm W}(p - p', q) W(p', q; t), \tag{5.35}$$

with

$$A_{\rm W}(p,q) = 2\int_0^{\infty} {\rm d}x \sin\bigg(\frac{px}{\hbar}\bigg)\bigg[A\bigg(q + \frac{x}{2}\bigg) - A\bigg(q - \frac{x}{2}\bigg)\bigg], \tag{5.36}$$

is convenient to carry out numerical calculations. The quantal Liouvillian is then rewritten as[170]

$$\begin{aligned} -\hat{L}_A(p,q)W(p,q;t) \equiv& -\frac{p}{m}\frac{\partial}{\partial q}W(p,q;t) \\ &- \frac{1}{\hbar}\int_{-\infty}^{\infty}\frac{{\rm d}p'}{2\pi\hbar} U_{\rm W}(p - p', q) W(p', q; t), \end{aligned} \tag{5.37}$$

and $U_{\rm W}(p,q)$ is defined by eq. (5.36) for the function $U(q)$. Thus, we can rewrite the hierarchy of equations in the form[18,19,161–165]

$$\begin{aligned} \frac{\partial}{\partial t}W_n(p,q;t) =& -\big(\hat{L}_A(p,q) + n\gamma\big)W_n(p,q;t) \\ &- \hat{\Phi}_{\rm W} W_{n+1}(p,q;t) \\ &+ n\hat{\Theta}_{\rm W} W_{n-1}(p,q;t), \end{aligned} \tag{5.38}$$

for $n \geqslant 0$ and

$$\begin{aligned} \frac{\partial}{\partial t}W_N(p,q;t) =& -\big(\hat{L}_A(p,q) + N\gamma\big)W_N(p,q;t) \\ &+ \hat{\Gamma}_{\rm W} W_N(p,q;t) \\ &+ N\hat{\Theta}_{\rm W} W_{N-1}(p,q;t), \end{aligned} \tag{5.39}$$

for $(N+1)\gamma \gg m\zeta/\beta$, ω_A, where

$$\begin{aligned} \hat{\Gamma}_{\rm W} \equiv& \zeta\big(V_1 + V_2 q\big)^2 \frac{\partial}{\partial p}\bigg(p + \frac{m}{\beta}\frac{\partial}{\partial p}\bigg) \\ &+ \frac{\hbar^2\zeta V_2(V_1 + V_2 q)}{4}\frac{\partial^3}{\partial p^2 \partial q}. \end{aligned} \tag{5.40}$$

We set $n\Theta_{\rm W} W_{n-1}(p,q;t) = 0$ for $n = 0$. The above equation is a generalization of the quantum Fokker–Planck (F–P) equation for a nearly Markovian noise bath with a non-linear system–bath interaction. Note that it is possible to keep the density matrix in the coordinate representation and solve the hierarchy of the equations of motion for $\rho_n(q,q';t)$, eqs. (5.25) and (5.27). In such a case, the equations are simple since the Liouvillian is a local operator in the coordinate space. Nevertheless, the Wigner representation has at least three advantages: First, it allows us to compare

the quantum density matrix directly with its classical counterpart. Second, using phase space distribution functions, we can further impose the necessary boundary conditions easily (e.g., periodic or open boundary conditions), where particles can move in and out of the system.[170] These features are very difficult to include in the coordinate representation. Third, it allows better usage of computer memory, since the Wigner function $W_n(p,q)$ is a real function and is localized more or less centered at $p=0$ due to the form of $\hat{\Gamma}_{\rm W}$, whereas the density matrix element $\rho_n(q,q')$ is a complex and nonlocalized function.

In the linear–linear coupling $V(q)=V_1 q$, the present equations of motion further reduce to[18,19]

$$\frac{\partial}{\partial t}W_n(p,q;t) = -\big(\hat{L}_A(p,q)+n\gamma\big)W_n(p,q;t) + V_1\frac{\partial}{\partial p}W_{n+1}(p,q;t) + n\gamma\zeta V_1\left(p+\frac{m}{\beta}\frac{\partial}{\partial p}\right)W_{n-1}(p,q;t), \quad (5.41)$$

and

$$\frac{\partial}{\partial t}W_N(p,q;t) = -\big(\hat{L}_A(p,q)+N\gamma\big)W_N(p,q;t) + \hat{\Gamma}_{\rm OU}W_N(p,q;t) + N\gamma\zeta V_1\left(p+\frac{m}{\beta}\frac{\partial}{\partial p}\right)W_{N-1}(p,q;t), \quad (5.42)$$

where

$$\hat{\Gamma}_{\rm OU}\equiv\zeta V_1^2\frac{\partial}{\partial p}\left(p+\frac{m}{\beta}\frac{\partial}{\partial p}\right), \quad (5.43)$$

is the Ornstein–Ülenbeck operator.[171] In the white noise limit, where the correlation time of the noise is very short, $\gamma\gg\omega_A$, we may set the depth of hierarchy N to zero and reduce it to the quantum F–P equation for the Gaussian-white noise bath[153,154]

$$\frac{\partial}{\partial t}W_0(p,q;t) = -\hat{L}_A(p,q)W_0(p,q;t)+\hat{\Gamma}_{\rm OU}W_0(p,q;t). \quad (5.44)$$

Besides the classical limit $\hbar\to 0$, however, this equation can be applied to a high-temperature system only, since we have assumed $\beta\hbar\gamma\ll 1$.

The classical limit of all the equations of motion derived in this subsection can be obtained by taking the limit $\hbar\to 0$. This leads to the replacement of the Liouvillian by

$$-\hat{L}_{\rm cl}(p,q)W(p,q;t)\equiv-\left(\frac{p}{m}\frac{\partial}{\partial q}-\frac{\partial U(q)}{\partial q}\frac{\partial}{\partial p}\right)W(p,q;t). \quad (5.45)$$

Since $\beta\hbar\gamma=0$ is always satisfied, the validity of the equation is not limited to a high-temperature regime in the classical case. The classical limit of eq. (5.44) was first developed by Kramers[172] to study the influence of dissipation on chemical reaction rates.[173]

In this subsection, we present a quantum Fokker–Planck equation for the nearly Markovian bath. The Wigner representation can be employed in various Gaussian wavepackets approximation.[174–176] Other types of quantum F–P equation for non-Gaussian media have been explored and applied to nonlinear optical spectroscopy.[177,178]

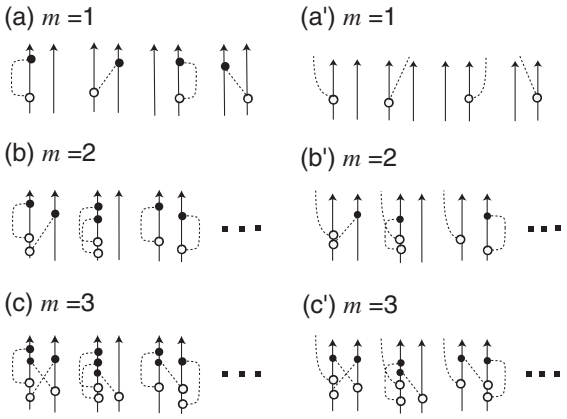

Fig. 10. Double-sided Feynman diagram of density matrix with the three lowest system–bath interactions given in eq. (5.46). (a)–(c) show the elements of $\rho_0(q,q';t)$ for $m=1$, 2, and 3, whereas (a′)–(c′) show those of $\rho_1(q,q';t)$, respectively. In each diagram, the left and right solid lines represent the time evolution of the system, whereas the dashed lines represent the bath excitations. The white and black circles correspond to the system–bath interaction involved in $\Theta(q,q';\tau')$ and $\Phi(q,q';\tau)$.

5.4 *Hierarchy elements and correlated initial condition*

In §5.2, we introduce the hierarchy elements $\rho_n(q,q';t)$ and $W_n(p,q;t)$ to bypass the explicit treatment of inherent memory effects. Here, we explore their physical meaning in some detail. As can be seen from the expansion form of eq. (5.16)

$$F(q,q';t)=\sum_{m=0}^{\infty}\frac{1}{m!}\left\{-\int_{t_i}^{t}{\rm d}\tau\,\Phi(q,q';\tau)\times\left[\int_{t_i}^{\tau}{\rm d}\tau'\,{\rm e}^{-\gamma(\tau-\tau')}\Theta(q,q';\tau')+G(q_i,q_i';\tau)\right]\right\}^m, \quad (5.46)$$

the influence functional contains any (2^m)th order of system–bath interactions. In the above equation, $V(q(\tau))$ and $V(q'(\tau))$ in $\Phi(q,q';\tau)$ create system excitation at τ, whereas $V(q(\tau'))$ and $V(q'(\tau'))$ in $\Theta(q,q';\tau')$ demolish this system excitation at τ; both are induced by system–bath interactions. The elements of $\rho_0(q,q';t)$ for $m=1$, 2, and 3 in eq. (5.46) are depicted in Figs. 10(a)–10(c), respectively. In eq. (5.24), the term $\Phi(q,q')\rho_1(q,q';t)$ arises from the time derivative of the influence functional. Since $\rho_1(q,q';t)$ is defined by excluding $\Phi(q,q')$, the orders of system–bath interactions in $\rho_1(q,q';t)$ are one order lower than those in $\rho_0(q,q';t)$, as illustrated in Figs. 10(a′)–10(c′). Similarly, $\rho_n(q,q';t)$ involves n-order-lower interactions than $\rho_0(q,q';t)$. Thus, one can think of eq. (5.25) [or eq. (5.38)] as a type of rate law among the density matrix with three different bath-excited states, $\rho_n(q,q';t)$ and $\rho_{n\pm1}(q,q';t)$; the time evolution of $\rho_n(q,q';t)$ is determined by its time evolution operator $[{\rm i}\hat{L}(q,q')/\hbar+n\gamma]$ and the incoming and outgoing contributions of $\rho_{n-1}(q,q';t)$ and $\rho_{n+1}(q,q';t)$ connected through $\Theta(q,q')$ and $\Phi(q,q')$, respectively.[17] Therefore, the present approach conceptually differs from conventional perturbative expansion approaches,[3] where the 0th member does not include any system–bath interactions and then higher members take into account higher-order system–bath interactions. In the present approach, $\rho_0(q,q';t)$ (or $W_0(p,q;t)$) includes all orders of system–bath interactions, and it is the exact solution of the Hamiltonian eq. (5.1).

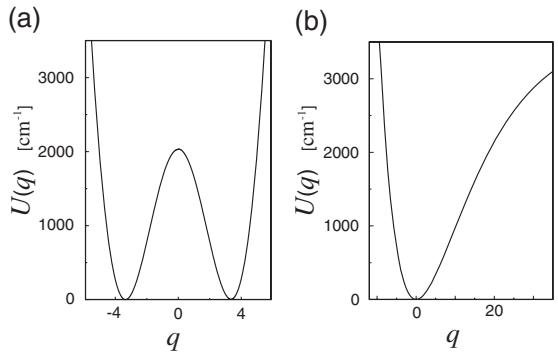

Fig. 11. (a) Double-well potential and (b) Morse potential defined by eqs. (5.48) and (5.52), respectively.

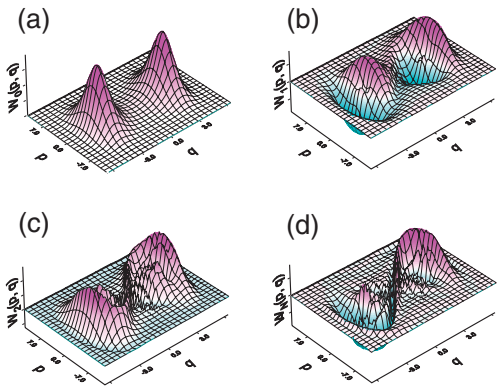

Fig. 12. Hierarchy elements of equilibrium Wigner distribution at $T = 800\,\mathrm{K}$ for the double-well potential system depicted in Fig. 11(a). The equilibrium elements $W_n(p,q)$ are obtained by numerically integrating the equations of motion (5.38) and (5.39) with $N = 3$ until the steady state is reached. The element (a) $W_0(p,q;t)$ corresponds to real distribution functions, whereas (b) $W_1(p,q;t)$, (c) $W_2(p,q;t)$, and (d) $W_3(p,q;t)$ correspond to auxiliary functions. Due to the quantum tunneling effect, there is some population around the barrier top even at low temperatures where the thermal energy of the system is much lower than the barrier height energy. Note that the dissipation terms, which are missing in the stochastic theory, are essential to having an equilibrium distribution at finite temperatures.

Either numerically or analytically, to solve the equations of motion, we have to choose the initial condition. For the F–P case, one may set a temporarily initial state to the equilibrium state of the system itself as

$$W_0(p,q;t_i) = \frac{1}{Z}\mathrm{e}^{-\beta H_A(p,q)}, \tag{5.47}$$

and $W_n(p,q;t_i) = 0$ for $n \geq 1$, where $Z = \mathrm{tr}\{\exp[-\beta H_A(p,q)]\}$. Although this is not the equilibrium state of the total system, since it neglects the quantum coherence (correlation) between the system and the bath that arises from system–bath interactions, such a correlation can be taken into account by nonzero hierarchy elements, i.e., $W_n(p,q;t) \neq 0$.[17] To set these elements, we integrate the equations of motion from time $t = t_i < 0$ to $t = 0$. If we choose $|t_i|$ to be sufficiently large compared with the characteristic times of the system, such as $|t_i| \gg 1/\gamma$ and $\beta/m\zeta$, the Wigner distribution function comes to the true equilibrium state described by the full set of hierarchy $W_n(p,q;t=0)$: We can use this set of hierarchy as the true initial condition. Such correlated initial condition has to be used to evaluate the correlation functions such as eqs. (3.8), (3.12), and (3.13).

In Fig. 12, we depict the hierarchy elements of the equilibrium distribution calculated using eqs. (5.38) and (5.39) for the double-well potential system illustrated in Fig. 11(a). Here, we consider the potential,

$$U(q) = E_c\left(\frac{1}{2}q^2 + A\mathrm{e}^{-\alpha q^2}\right) - E_0, \tag{5.48}$$

and the parameters are chosen to express the inversion motion of NH_3 as $E_c = 974\,\mathrm{cm}^{-1}$, $A = 17.1$, $\alpha = 0.052$, and $E_0 = 15050\,\mathrm{cm}^{-1}$ for the dimensionless coordinate q.[179] The kinetic term is then expressed as $\omega_0 p\mathrm{d}/\mathrm{d}q$, where the characteristic frequency is given by $\omega_0 = 80\,\mathrm{cm}^{-1}$. The bath parameters are chosen to be $\zeta V_1^2 = 10\,\mathrm{cm}^{-1}$, $\gamma = 100\,\mathrm{cm}^{-1}$, and $N = 3$. The temperature is set to be $T = 800\,\mathrm{K}$. Due to the quantum effects, there is a distribution around the top of barrier even at low temperatures. To set the correlated initial condition, we must use all hierarchy elements $W_n(p,q;t)$ as the initial state. Examples of calculating chemical reaction rates are presented in refs. 18, 19, and 166.

5.5 *Fokker–Planck equation approach to multi-dimensional vibrational spectroscopy*

As mentioned in §4.5, there are essential drawbacks in applying the stochastic theory to vibrational spectroscopy. A serious one is the lack of a dissipation term, which relates with the fluctuation through the fluctuation–dissipation theorem, that keeps the system in the thermal equilibrium state at finite temperatures.[3] Without the dissipation term, either we employ the coordinate representation or the energy state representation, the system heats up toward infinite temperatures by stochastic fluctuation, which makes the definition of vibrational motion meaningless. These drawbacks may cause a problem particularly for the case of two-dimensional (2D) vibrational spectroscopy, due to the sensitivity of the 2D profile to system dynamics. Since the vibrational motion of molecules is in principle defined by the coordinates and since the temperature effects can be included through the dissipation term, the F–P equation presented in this section is suitable for clarifying the role of thermal fluctuation in vibrational spectroscopy. From this approach, the effects of anharmonicity as well as LL and SL interactions were studied for the fifth- and seventh-order 2D Raman, and third-order 2D infrared (IR) processes, respectively.[25,151,161–166] Here, we briefly explain a way to calculate the multibody correlation function and show the wavepacket dynamics involved in the third-order 2D IR response function. Then, we present 2D signals for harmonic and Morse potential systems.

Following the same procedure illustrated in eq. (3.23) and eqs. (4.32)–(4.37), we can rewrite the fifth-order Raman and third-order IR response functions, i.e., eqs. (4.46) and (4.47), as[25]

$$R^{(5)}_{\mathrm{Raman}}(t_2,t_1) = -\frac{1}{\hbar^2}\mathrm{tr}\{\hat{\alpha}\hat{G}(t_2)[\hat{\alpha}^{\times}\hat{G}(t_1)(\hat{\alpha}^{\times}\hat{\rho}^{\mathrm{eq}})]\}, \tag{5.49}$$

and

$$R^{(3)}_{\mathrm{IR}}(t_3,t_2,t_1) = -\frac{\mathrm{i}}{\hbar^3}\mathrm{tr}\{\hat{\mu}\hat{G}(t_3)\{\hat{\mu}^{\times}\hat{G}(t_2)[\hat{\mu}^{\times}\hat{G}(t_1)(\hat{\mu}^{\times}\hat{\rho}^{\mathrm{eq}})]\}\}, \tag{5.50}$$

where $\hat{\alpha}$ and $\hat{\mu}$ are the polarization and dipole operators, respectively, and

$$\hat{G}(t)\hat{A} \equiv \exp\left(-\frac{\mathrm{i}}{\hbar}\hat{H}t\right)\hat{A}\exp\left(\frac{\mathrm{i}}{\hbar}\hat{H}t\right) \equiv \exp\left(-\frac{\mathrm{i}}{\hbar}\hat{H}^{\times}t\right)\hat{A} \tag{5.51}$$

is the Green's function of the system–bath Hamiltonian without the external force $\hat{H}$ for any operator $\hat{A}$. The above expressions allow us to employ the equations of motion to calculate the response functions and give us an intuitive picture of higher-order optical processes. Here, we illustrate this point for the third-order IR response. The right-hand side of eq. (5.50) can be read from the right to left as follows: The total system is initially in the equilibrium state $\hat{\rho}^{\mathrm{eq}}$. The initial state is then modified by the first laser pulses via the dipole operator as $\mathrm{i}(\hat{\mu}^{\times}\hat{\rho}^{\mathrm{eq}})/\hbar$ at $t = 0$ and is propagated for time t_1 by $\hat{G}(t_1)$. In the third-order IR measurements, the system is excited by the second and third dipole interactions expressed as $\mathrm{i}\hat{\mu}^{\times}/\hbar$, respectively, separated by the time propagator $\hat{G}(t_2)$. After these excitations, the system is further propagated for the time period t_3 by $\hat{G}(t_3)$ and, finally, the expectation value of the dipole moment at $t = t_1 + t_2 + t_3$ is obtained by calculating the trace of $\hat{\mu}$.

Here, we express the time propagator by Green's function for the total system, but, in practice, we can trace over the heat-bath part from eqs. (5.49) and (5.50), and can replace it with the propagator for the reduced equation of motion.[36,37] The sequence of modifying and propagating the density matrix can be translated conveniently in the Wigner representation, as illustrated in Fig. 13.[25] In this way, the hierarchy of the equations of motion, eqs. (5.41) and (5.42), was used to investigate the roles of LL+SL interactions on the fifth-order Raman and third-order IR signals for a harmonic system.[161–165]

It has turned out that multi-dimensional spectroscopies are extremely sensitive to the anharmonicity of the potential and system–bath coupling. For example, if the system is harmonic and the polarizability or the dipole moment is the linear function of molecular coordinate, the 2D signals $R^{(5)}_{\mathrm{Raman}}(t_2,\ t_1) \propto \langle[[\hat{q}(t_{12}), \hat{q}(t_1)], \hat{q}]\rangle$ and $R^{(3)}_{\mathrm{IR}}(t_3,\ t_2,\ t_1) \propto \langle[[[\hat{q}(t_{123}), \hat{q}(t_{12})], \hat{q}(t_1)], \hat{q}]\rangle$ for $t_{12} \equiv t_1 + t_2$ and $t_{123} \equiv t_1 + t_2 + t_3$ will vanish due to the Gaussian integrals involved in the thermal average for the Raman case and the destructive contribution of the coherence in optical Liouville paths for the IR case.[25,161] Thus, the nonlinear coordinate dependence of the polarizability or dipole,[24,128] the anharmonicity of potential,[25,130,133,140] and the nonlinear system–bath interaction[161–165] as well as anharmonic mode coupling[134–136,143] are essential to having the signal. Since the LL+SL coupling is a nonlinear interaction, 2D spectroscopies are ideal for exploring these effects: We focus on the roles of dephasing and relaxation induced by LL+SL coupling in optical transition. Note that multi-dimensional spectroscopy can detect dephasing and relaxation separately, since multiple pulses can create sequences of the population state $|n\rangle\langle n|$ and the coherent state $|n\rangle\langle n'|$ $(n \neq n')$ at different time periods, where $|n\rangle$ and $\langle n|$ are the vibrational energy states introduced in §4.5.

A detailed analysis of LL+SL interactions for a harmonic potential system has already been reported.[161–165] To demonstrate the calculation, here we consider the case of the Morse potential system defined by

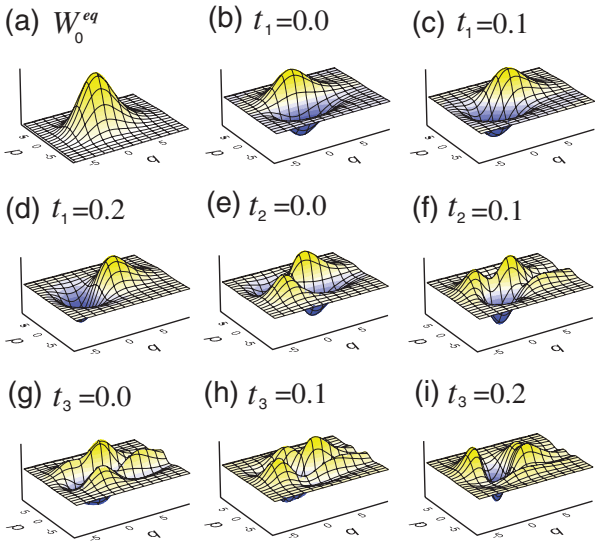

Fig. 13. The time evolution of the distribution function in the third-order IR response function, eq. (5.50), is calculated in the Wigner space using eqs. (5.38) and (5.39) for the potential depicted in Fig. 11(b). In Fig. 13(a), the system is initially in the equilibrium state $W^{\mathrm{eq}}(p,q)$. (b) At $t_1 = 0$ ps, the system is excited by the first dipole interaction as $\mu_1 \cdot \partial W^{\mathrm{eq}}(p,q)/\partial q$ for the dipole moment $\mu(q) = \mu_1 q$. The perturbed distribution function then evolves in time by $\hat{G}(t_1)$. This evolution is calculated from the equation of motion as (c) $t_1 = 0$ and (d) $t_1 = 0.2$. (e) At $t_1 = 0.2$, the system is excited by the second dipole interaction. This time is set to be $t_2 = 0$. (f) After the distribution function evolves in time, (g) at $t_2 = 0.1$, the system is again excited by the third dipole interaction. This time is set to be $t_3 = 0$. The distribution function then evolves in time as (h) $t_3 = 0.1$ and (i) $t_3 = 0.2$. Finally, the response function $R^{(3)}_{\mathrm{IR}}(t_3,\ t_2,\ t_1)$ defined by eq. (5.50) is calculated from the expectation value of the dipole moment, $\mathrm{tr}\{\mu_1 q \cdot W_0(p,q;t)\}$. The calculated results followed by this procedure are shown in Figs. 14 and 15.

$$U(q) = E_c(1 - \mathrm{e}^{-aq})^2, \tag{5.52}$$

where E_c and a are the dissociation energy and the curvature of the potential, respectively [see Fig. 11(b)]. We employ the dimensionless coordinate q and the momentum p. The polarizability and dipole moment are assumed to be $\alpha(q) = \alpha_1 q$ for 2D Raman and $\mu(q) = \mu_1 q$ for 2D IR, respectively. To carry out the calculation, we set $\alpha_1 = 1$ and $\mu_1 = 1$. The parameters of the potential are set to be $E_c = 3649\,\mathrm{cm}^{-1}$ and $a = 0.6361$ to have the fundamental frequency $\omega_0 = 38.7\ \mathrm{cm}^{-1}$ as in ref. 25. We chose the heat-bath parameters as (i) and (iv) $\bar{\zeta}_{\mathrm{LL}} \equiv V_1^2\zeta/(\hbar\omega_0) = 0.26$ and $\bar{\zeta}_{\mathrm{SL}} \equiv \hbar\zeta V_2^2/(4m\omega_0^2) = 0$, (ii) and (v) $\bar{\zeta}_{\mathrm{LL}} = 0.26$ and $\bar{\zeta}_{\mathrm{SL}} = 0.01$, and (iii) and (vi) $\bar{\zeta}_{\mathrm{LL}} = 0$ and $\bar{\zeta}_{\mathrm{SL}} = 0.1$, respectively. Note that here we chose the SL parameters to be positive for the positive LL parameter, but the sign of the SL parameter also affects the signals for the LL+SL case.[164,165] The fifth-order Raman signals and third-order IR signals are calculated for the two sets of inverse correlation times $\gamma = \omega_0$ and $\gamma = 0.1\omega_0$, at temperature $T = 300\,\mathrm{K}$. We then numerically integrate eqs. (5.38) and (5.39) for $N = 10-40$ following the procedure depicted in Fig. 13. To illustrate the anharmonic effects, we also plot the results for the harmonic potential with the fundamental frequency $\omega_0 = 38.7\,\mathrm{cm}^{-1}$ and $\alpha(q) = \alpha_1 q + \alpha_2 q^2$ with $\alpha_2 = 0.1$ for the Raman signals and $\mu(q) = \mu_1 q + \mu_2 q^2$ with $\mu_2 = 0.1$ for the IR signals, respectively.

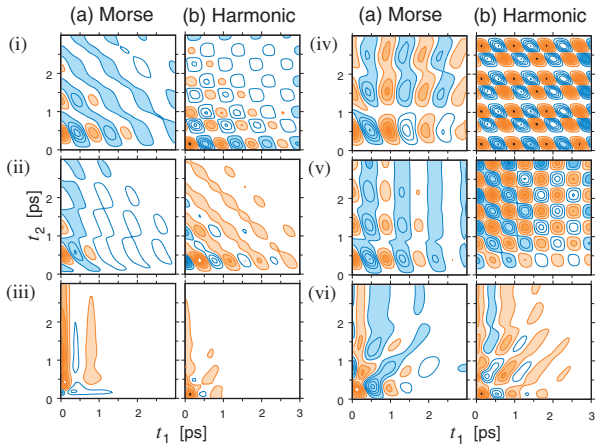

Fig. 14. Fifth-order 2D Raman signals $R^{(5)}_{\mathrm{Raman}}(t_2,\, t_1)$ in (i)–(iii) fast-modulation case $\gamma = \omega_0$ and (iv)–(vi) slow-modulation case $\gamma = 0.1\omega_0$ for (a) Morse potential and (b) harmonic potential. (i) and (iv) show the signals for LL coupling, whereas (ii) and (v), and (iii) and (vi) show the signals for LL+SL, and SL coupling, respectively. The contours in light orange and blue represent positive and negative values, respectively. The harmonic results are reproduced from refs. 161–165.

First, we discuss the fifth-order 2D signal $I^{(5)}_{\mathrm{Raman}}(t_1,\, t_2) = R^{(5)}_{\mathrm{Raman}}(t_2,\, t_1)$ in the fast modulation case for the (a) Morse oscillator system and (b) harmonic oscillator system. Figures 14(i-a) and 14(i-b) show results for the LL coupling case. These results are similar to those calculated using the conventional quantum F–P equation,[25,163] since eqs. (5.41) and (5.42) with the LL interaction reduces to eq. (5.44) in the fast-modulation limit. The contribution such as $\alpha_1^3\langle q(t_{12})q(t_1)q\rangle$ vanishes for the harmonic LL case due to the Gaussian integral in $\langle\cdots\rangle$. The dominant contributions are therefore $\alpha_1^2\alpha_2\langle q(t_{12})q^2(t_1)q\rangle$, $\alpha_1^2\alpha_2\langle q(t_{12})q(t_1)q^2\rangle$, etc. in the harmonic case, whereas $\alpha_1^3\langle q(t_{12})q(t_1)q\rangle$, $\alpha_1^3\langle q(t_1)q(t_{12})q\rangle$, etc. in the Morse case, because the thermal average in $\langle\cdots\rangle$ leads to a nonGaussian integral in the latter case due to the anharmonicity of potential. This is also true for the SL case shown in Fig. 14(iii-a) and 14(iii-b), where the leading order contribution is also $\alpha_1^2\alpha_2$ in (iii-b), whereas it is α_1^3 in (iii-a). The middle panels (ii-a) and (ii-b) in Fig. 14 are for the SL+LL coupling case. Since bath coupling always operates on the system as the product $V(q(\tau))V(q(\tau'))$ as shown in eq. (5.46), where $V(q) = V_1 q + V_2 q^2/2$, the LL+SL coupling gives rise to cubic interactions such as $\propto V_1 V_2 q(\tau)q^2(\tau')$ in the system. Thus, the dominant contribution to the signal in the LL+SL case becomes on the order of $\alpha_1^3\langle q(t_{12})q(t_1)q\rangle$ even in the harmonic case.

The signals in Figs. 14(i-a), 14(ii-a), and 14(ii-b) are similar and exhibit nodes along the $(t_1 + t_2)$ direction indicating the interference of the coherences in the first and second propagation times. This is because LL coupling mainly contributes to population relaxation so that the coherences decay slowly as long as SL coupling is weak. Since the signal in Fig. 14(i-b) arises from the correlation function on the order of $\alpha_1^2\alpha_2$, the profile is very different from the others. For pure SL coupling cases in Fig. 14(iii), due to the fast dephasing that arises from SL coupling, the oscillatory behaviors of the signals almost vanished and we only see a slowly decaying component along the t_2 axis for a small t_1. This is because, in 2D Raman experiments, a population state $|n\rangle\langle n|$ is involved in one of the Liouville path during the second propagation time t_2,[128,129] and this path will not decay in pure dephasing.[161,162]

Figures 14(iv)–14(vi) show results for a slow modulation case. Effective system–bath coupling strength changes as a function of γ as $\gamma^2/(\gamma^2 + \omega_0^2)$, as mentioned in ref. 19. The slowly decaying components along the t_2 axis in some of the figures indicate that the relaxation of population is slower than the dephasing. Echolike peaks along the $t_1 = t_2$ direction are also observed in Figs. 14(vi-a) and 14(vi-b). As depicted in Fig. 9, the slow modulation limit of the SL coupling case corresponds to that of the inhomogeneously distributed oscillators case. The echolike peaks result from the rephasing of the coherences in the first and second propagation times as in the case of spin echo measurement.[162] In the Morse case, since resonant frequencies between the vibrational energy levels are all different, dephasing and rephasing play a more significant role in such a case than in the harmonic case. Hence, if the system–bath coupling is the same, we observe more prominent echolike peaks in the Morse case than in the harmonic case as shown in Figs. 14(vi-a) and 14(vi-b). On the other hand, the absence of an echolike component in the LL case [Fig. 14(iv-b)] clearly indicates that rephasing paths for the response function on the order of $\alpha_1^2\alpha_2$ are not the primary contributor to the optical response.

We now present third-order 2D IR signals $I^{(3)}_{\mathrm{IR}}(t_1, t_2, t_3) = R^{(3)}_{\mathrm{IR}}(t_3, t_2, t_1)$, for the (a) Morse and (b) harmonic systems. The leading order contribution of signals for the harmonic case with LL coupling is $\mu_1^2\mu_2^2$,[24] indicating that two-quantum transitions induced by $\mu_2 q^2$ are involved in the optical process, whereas the contributions of Morse, LL+SL, and SL cases are μ_1^4 indicating only one-quantum transitions induced by $\mu_1 q$ play a role in these processes. Since $\mu_1 q = \mu_1 \sum_n (|n+1\rangle\langle n| + |n\rangle\langle n+1|)$, the main contribution of Liouville paths involved in the signal for μ_1^4 is well explained by Fig. 3. Figures 15(i) and 15(iv) are for the LL coupling, whereas Figs. 15(ii) and 15(v), and Figs. 15(iii) and 15(vi) are for the LL+SL coupling and SL coupling, respectively.

In the fast modulation case, the signals shown in

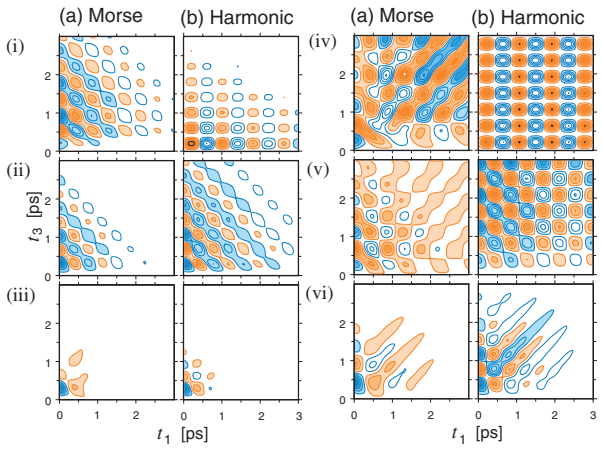

Fig. 15. Third-order 2D IR signals $R^{(3)}_{\mathrm{IR}}(t_3, t_2, t_1)$ with $t_2 = 0$, in (i)–(iii) fast modulation case $\gamma = \omega_0$ and (iv)–(vi) slow modulation case $\gamma = 0.1\omega_0$ for (a) Morse potential and (b) harmonic potential. In each panel, the parameters are chosen to be the same as those in Fig. 14. The harmonic results are reproduced from refs. 161–165.

Figs. 15(i-a) and 15(ii-a) are very different from those shown in Fig. 15(i-b), and rather resemble those shown in Fig. 15(ii-b). The contribution of the signals in Figs. 15(i-a), 15(ii-a), and 15(iii-b) are from the correlation functions with the order of μ_1^4, whereas the contribution of the signals Fig. 15(i-b) is from that of $\mu_1^2\mu_2^2$. Since multi-dimensional spectroscopy can monitor the coherence in optical transition, we can clearly distinguish the order of correlation functions from their profiles. Without the heat bath, the third-order IR signal for a harmonic oscillator is evaluated as $\mu_1^2\mu_2^2 \sin(\omega_0 t_1)\sin^2(\omega_0 t_3)$[24,162] and there is no coherence between the t_1 and t_3 directions. Qualitatively, the nonlinearity of the system–bath interaction plays a similar role as the anharmonicity of potential in the fast modulation case. The bottom panels in Fig. 15 are for the SL case. Since the fast-modulation limit in the SL case corresponds to that in the case of homogeneously distributed oscillators illustrated in Fig. 9, we cannot observe the echo signal in the $t_1 = t_3$ direction in both the Morse and harmonic cases.

In the slow modulation cases, Figs. 15(iv)–15(vi), we observe qualitative changes of the signals in the fast modulation case. Echolike peaks caused by the rephasing of the dipole element appear along $t_1 = t_3$ for the Morse case Figs. 15(iv-a), 15(v-a), and 15(vi-a), and the harmonic case Fig. 15(vi-b). We also observe many peaks parallel to $t_1 = t_3$ corresponding to the interference between the coherences in t_1 and t_3 periods. Such peaks also arise from the stochastic model due to the factor $\exp[i\omega_0(t_1 - t_3)]$ involved in the third-order response function. The absence of such echolike peaks in Fig. 15(iv-b) indicates that the primary contribution of the signal on the order of $\mu_1^2\mu_2^2$ does not involve rephasing paths. In the 15(vi-a) and 15(vi-b) panels, we also observe a slowly decaying component along the t_3 axis for t_1 less than the dephasing time $t_1 < 1$ ps. These components are predicted from the inhomogeneously distributed oscillator model.[162]

In ref. 151, we compared third-order IR signals calculated using the stochastic approach and the quantum F–P equation approach. It was shown that, while the conditions $\beta\hbar\omega_0 \gg 1$ and $\gamma \ll \omega_0$ are met, the signals from a stochastic three-level model agree very well with the signals from a high-frequency Morse potential model with LL+SL system–bath interactions. This is because under such conditions, the modulation is so slow that a relaxation does not play a major role. In the present study, the slow modulation case shown in Figs. 15(iv)–15(vi) corresponds to such situation and the calculated signals exhibit similar features to those from the stochastic model. In the fast modulation case [Figs. 15(i)–15(iii)], there are differences between the present results and stochastic ones.

5.6 *Quantum master equation for nearly Markovian noise bath*

To compare the present formula to the stochastic Liouville equation, we also consider the Hamiltonian expressed in the energy eigenstate representation as[180]

$$\hat{H} = \hat{H}_A(\hat{a}^+, \hat{a}^-) + \hat{V}(\hat{a}^+, \hat{a}^-)\sum c_j\hat{x}_j + \sum\left(\frac{\hat{p}_j^2}{2m_j} + \frac{1}{2}m_j\omega_j^2\hat{x}_j^2\right), \tag{5.53}$$

where $\hat{H}_A(\hat{a}^+, \hat{a}^-)$ is the Hamiltonian of system A and $\hat{V}(\hat{a}^+, \hat{a}^-)$ is the system part of the interaction both introduced in eq. (2.32). Note that if $\hat{a}^+$ and $\hat{a}^-$ respectively represent the creation and annihilation operators of spin states, the above Hamiltonian is called the spin-Boson Hamiltonian,[181] which has been studied from various approaches.[182–184] We assume a high-temperature bath with the distribution eq. (5.11). Then, eq. (5.13) is approximated as $L_2(t) \approx \eta\gamma \exp[-\gamma|t|]/\beta$. First let us consider the factorized initial condition

$$\hat{\rho}_{\rm tot}(t_i) = \hat{\rho}_A(t_i)\exp\left[-\beta\sum\left(\frac{\hat{p}_j^2}{2m_j} + \frac{1}{2}m_j\omega_j^2\hat{x}_j^2\right)\right], \tag{5.54}$$

where $\rho(t_i)$ is the initial density matrix of A. As shown in §2.3, the reduced density matrix element is expressed in the coherent state representation of path integrals. In this case, we have[15,17]

$$\rho(\phi^\dagger, \phi'; t) = \int D[\phi^\dagger(\tau)\phi(\tau)]\int D[\phi'^\dagger(\tau)\phi'(\tau)]\rho'_A(\phi_i^\dagger, \phi'_i) \times \exp\left\{\frac{\rm i}{\hbar}S_A[\phi^\dagger, \phi; t]\right\}F(\{\phi\}; t)\exp\left\{-\frac{\rm i}{\hbar}S_A^\dagger[\phi'^\dagger, \phi'; t]\right\}, \tag{5.55}$$

where $\{\phi, \phi'\}$ and their conjugate $\{\phi^\dagger, \phi'^\dagger\}$ denote complex variables for Boson and Grassman variables for Fermion for the operators $\hat{a}^-$ and $\hat{a}^+$, respectively, and $S_A[\phi^\dagger, \phi; t]$ is the action for the Hamiltonian $\hat{H}_A(\hat{a}^+, \hat{a}^-)$. The influence functional is expressed as

$$F(\{\phi\}; t) = \exp\left[\left(-\frac{\rm i}{\hbar}\right)^2\int_{t_i}^{t}{\rm d}\tau\int_{t_i}^{\tau}{\rm d}\tau'\,{\rm e}^{-\gamma(\tau-\tau')} \times V^\times(\{\phi\}; \tau)\Theta_0(\{\phi\}; \tau')\right]. \tag{5.56}$$

Here, we write $(\{\phi\}) \equiv (\phi^\dagger, \phi, \phi'^\dagger, \phi')$ and

$$V^\times(\{\phi\}; \tau) \equiv V\big(\phi^\dagger(\tau), \phi(\tau)\big) - V\big(\phi'(\tau), \phi'^\dagger(\tau)\big),$$
$$V^\circ(\{\phi\}; \tau) \equiv V\big(\phi^\dagger(\tau), \phi(\tau)\big) + V\big(\phi'(\tau), \phi'^\dagger(\tau)\big), \tag{5.57}$$

and

$$\Theta_0(\{\phi\}; \tau) \equiv c_0 V^\times(\{\phi\}; \tau) - \frac{{\rm i}\hbar\eta\gamma^2}{2}V^\circ(\{\phi\}; \tau) \tag{5.58}$$

with $c_0 = \eta\gamma/\beta$, where $V(\phi^\dagger, \phi)$ is the coherent representation of the operator $\hat{V}(\hat{a}^+, \hat{a}^-)$.

If we introduce the element

$$\rho_n(\phi^\dagger, \phi'; t) \equiv \int D[\phi^\dagger(\tau)\phi(\tau)]\int D[\phi'^\dagger(\tau)\phi'(\tau)] \times \rho'_A(\phi_i^\dagger, \phi'_i)\left[-\frac{\rm i}{\hbar}\int_{t_i}^{t}{\rm d}\tau'\,{\rm e}^{-\gamma(t-\tau')}\Theta_0(\{\phi\}; \tau')\right]^n \times \exp\left\{\frac{\rm i}{\hbar}S_A[\phi^\dagger, \phi; t]\right\}F(\{\phi\}; t) \times \exp\left\{-\frac{\rm i}{\hbar}S_A^\dagger[\phi'^\dagger, \phi'; t]\right\}, \tag{5.59}$$

we can construct the equations of motion for the density operator $\hat{\rho}_n(t) = N^{-2}\iint {\rm d}\phi^\dagger\,{\rm d}\phi\iint {\rm d}\phi'^\dagger\,{\rm d}\phi'|\phi\rangle\rho_n(\phi^\dagger, \phi'; t)\langle\phi'|$ as[17]

$$\frac{\partial}{\partial t}\hat{\rho}_n(t) = -\left(\frac{\rm i}{\hbar}\hat{H}_A^\times + n\gamma\right)\hat{\rho}_n(t) - \frac{\rm i}{\hbar}\hat{V}^\times\hat{\rho}_{n+1}(t) - \frac{{\rm i}n}{\hbar}\hat{\Theta}_0\hat{\rho}_{n-1}(t), \tag{5.60}$$

where we set $in\hat{\Theta}_0\hat{\rho}_{n-1}(t)/\hbar = 0$ for $n = 0$. For $(N+1)\gamma \gg \eta/\beta$ and ω_0, where ω_0 is the characteristic frequency of the system, the terminator is given by

$$\frac{\partial}{\partial t}\hat{\rho}_N(t) = -\left(\frac{\mathrm{i}}{\hbar}\hat{H}_A^{\times} + N\gamma\right)\hat{\rho}_N(t) - \frac{1}{\gamma\hbar^2}\hat{V}^{\times}\hat{\Theta}_0\hat{\rho}_N(t) - \frac{\mathrm{i}N}{\hbar}\hat{\Theta}_0\hat{\rho}_{N-1}(t). \tag{5.61}$$

Here,

$$\hat{\Theta}_0 \equiv \frac{\eta\gamma}{\beta}\left(\hat{V}^{\times} - \mathrm{i}\frac{\beta\hbar\gamma}{2}\hat{V}^{\circ}\right), \tag{5.62}$$

and we denote $\hat{A}^{\circ}\hat{\rho} \equiv \hat{A}\hat{\rho} + \hat{\rho}\hat{A}$ for any operator $\hat{A}$. If we introduce the dimensionless parameter $\Delta^2 = \eta\gamma/\beta$ and rescale $\hat{V} \to \hat{V}/\Delta$ and $\hat{\rho}_n(t) \to \Delta^{-n}\hat{\rho}_n(t)$, we have[15)]

$$\frac{\partial}{\partial t}\hat{\rho}_n(t) = -\left(\frac{\mathrm{i}}{\hbar}\hat{H}_A^{\times} + n\gamma\right)\hat{\rho}_n(t) - \frac{\mathrm{i}}{\hbar}\hat{V}^{\times}\hat{\rho}_{n+1}(t) - \frac{\mathrm{i}n}{\hbar}\left(\hat{V}^{\times} - \mathrm{i}\frac{\beta\hbar\gamma}{2}\hat{V}^{\circ}\right)\hat{\rho}_{n-1}(t). \tag{5.63}$$

The terminator can also be rewritten accordingly. Compared with the stochastic Liouville equation, the above equation has the temperature correction term $-\mathrm{i}\beta\hbar\gamma\hat{V}^{\circ}/2$. This term can be regarded as the reaction of the bath to the system and leads the system to the thermal equilibrium state. If the bath temperature is infinity, this term can be neglected. In the F–P equation with the LL interaction eq. (5.41), this term corresponds to p in $(p + m/\beta \cdot \partial/\partial p)$.

The hierarchy of equations in the energy state representation with the temperature correction term has been used to analyze resonant optical spectroscopy[15,16)] and electron transfer processes.[185)] To illustrate the temperature effects, we study the relaxation of a spin randomly modulated by a local random field under a weak external field. We calculate a free induction decay signal defined by the spin expectation value $\langle S_z(t)\rangle$ with the initial configuration $S_z(0) = 1$. As explained in §4.1, if the external field is zero, the situation corresponds to the zero field NMR or μSR measurements. To compare the former result obtained from eq. (4.3) by Kubo and Toyabe[41)] and others,[13,43,45,49)] we employ eq. (5.63) and its terminator instead of eqs. (5.60) and (5.61). The procedure for calculating the signals is similar to that in the case discussed in §4.1 except for the existence of the temperature correction term. We set the amplitude of the three-dimensional random field by $\Delta_x = \Delta_y = \Delta_z = \Delta = 1$. Then, we calculate the signals for three sets of the inverse correlation of noise $\gamma = 0.01$, 0.1, and 1.0, where $\gamma_x = \gamma_y = \gamma_z = \gamma$. In Fig. 16, we plot $\langle S_z(t)\rangle$ with and without the temperature correction term set by $\beta\hbar\gamma/2 = 0.2$ and $\beta\hbar\gamma/2 = 0$, respectively. The dashed lines correspond to the case discussed by Kubo and Toyabe and, when γ tends to zero, the line approaches the profile of the Kubo–Toyabe function that approaches 1/3 at a long time. As the figure shows, the population increases if we add the temperature correction terms. Since the stochastic limit corresponds $\beta \to 0$ in eq. (5.63), the term seems to suppress the population when the temperature becomes higher. This happens, however, because we renormalize the coupling constant as $\Delta^2 = \eta\gamma/\beta$. If we fix η instead of Δ, the temperature dependence becomes opposite as we usually expect.

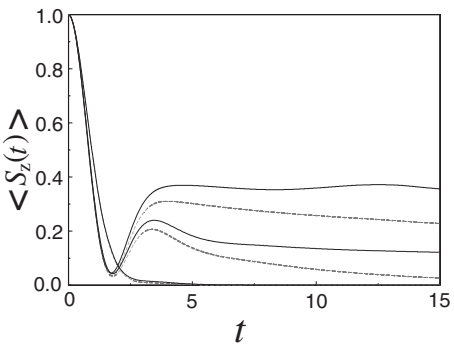

Fig. 16. The expectation value of a spin in the z direction $\langle S_z(t)\rangle$ is plotted at different γ values. The solid lines are calculated from eq. (5.63) with $\beta\hbar\gamma/2 = 0.2$; the dashed lines with $\beta\hbar\gamma/2 = 0$ correspond to the case of the stochastic Liouville equation [i.e., the case from eqs. (2.41)–(2.43)] with eq. (2.62). In each set of lines, from top to bottom, the modulation rates are $\gamma = 0.01$, 0.1, and 1, respectively.

5.7 *Positivity condition, low-temperature correction terms and nonMarkovian noise*

In a reduced equation of motion approaches, such as the quantum master equation approach[3)] and Redfield equation approach,[186)] the time evolution operators have to satisfy the positivity condition that, if all the diagonalized elements of the reduced density matrix $\hat{\rho}_{jj}(0)$ are positive, then the all elements of $\hat{\rho}_{jj}(t)$ are also positive for all $t > 0$.[187–189)] It has been shown that for the linear–linear system–bath interaction, the quantum master equation and Redfield equation do not satisfy the indispensable positivity condition.[190,191)] Careful discussions have been made on this issue.[192,193)] Typically, one modifies an interaction in the rotating wave approximation (RWA) form to preserve positivity,[48,194,195)] although this may differ the dynamics of original Hamiltonian. To derive the hierarchy of equations, we employed the Ohmic distribution with the Lorentzian cutoff, $J(\omega) = \hbar\eta\gamma^2\omega/\pi(\gamma^2 + \omega^2)$, and the high temperature assumption $\beta\hbar\gamma \ll 1$. As long as we keep the condition $\beta\hbar\gamma \ll 1$, our formalism does not violate the positivity condition without RWA (see also §6.3). Although the high-temperature condition retains its validity in many systems, there are still cases where the condition does not apply. In principle, it is possible to lift this condition and generalize it for the lower-temperature regime by extending the hierarchy of equations to include temperature correction terms.[17,196)] These formulations are, however, somewhat cumbersome for systems with large degrees of freedom, since the elements at every hierarchy are related to each other in a rather complex manner and their number rapidly increases as temperature decreases, besides the case of a weak system–bath interaction where one can bypass to construct the hierarchy.[197)] Following ref. 167, here, we present a simpler formulation to deal with low-temperature correction terms, although it requires more intensive calculations than the quantum Fokker–Planck or master equation for a nearly Markovian noise bath.

When the Hamiltonian eq. (5.53) with the distribution eq. (5.11) is considered, the function $L_2(t)$ is then given by eq. (5.13). If we choose K so as to satisfy $\nu_K = 2\pi K/(\beta\hbar) \gg \omega_0$, where ω_0 is the characteristic frequency of the system, the factor $\mathrm{e}^{-\nu_k|t|}$ in eq. (5.13) can be replaced by

Dirac's delta function as

$$\nu_k \mathrm{e}^{-\nu_k|t|} \simeq \delta(t) \quad (k \geqslant K+1). \tag{5.64}$$

Therefore, $L_2(t)$ is expressed as

$$L_2(t) = c_0\,\mathrm{e}^{-\gamma|t|} + \sum_{k=1}^{K} c_k\,\mathrm{e}^{-\nu_k|t|} + \delta(t)\sum_{k=K+1}^{\infty}\frac{c_k}{\nu_k}. \tag{5.65}$$

We then generalize the hierarchy elements eq. (5.59) as[17,167]

$$\begin{aligned}\rho_{n,j_1,\ldots,j_K}(\phi^\dagger,\phi';t) \equiv{}& \int D[\phi^\dagger(\tau)\phi(\tau)]\int D[\phi'^\dagger(\tau)\phi'(\tau)]\rho'_A(\phi_i^\dagger,\phi'_i)\left\{-\frac{\mathrm{i}}{\hbar}\int_{t_i}^{t}\mathrm{d}\tau'\,\mathrm{e}^{-\gamma(t-\tau')}\Theta_0(\{\phi\};\tau')\right\}^n\\ &\times\prod_{k=1}^{K}\left\{-\frac{\mathrm{i}}{\hbar}\int_{t_i}^{t}\mathrm{d}\tau'\,\mathrm{e}^{-\nu_k(t-\tau')}\Theta_k(\{\phi\};\tau')\right\}^{j_k}\\ &\times\exp\left\{\frac{\mathrm{i}}{\hbar}S_A[\phi^\dagger,\phi;t]\right\}F(\{\phi\};t)\exp\left\{-\frac{\mathrm{i}}{\hbar}S_A^\dagger[\phi'^\dagger,\phi';t]\right\},\end{aligned} \tag{5.66}$$

for the nonnegative integers $n, j_1, \ldots, j_K$. Here, $\Theta_0(\{\phi\};\tau)$ is given by eq. (5.58) with eq. (5.14), and we introduce

$$\Theta_n(\{\phi\};\tau) \equiv c_n V^\times(\{\phi\};\tau). \tag{5.67}$$

For the operator $\hat{\rho}_{n,j_1,\ldots,j_K}(t)$ we can construct the hierarchy of equations as

$$\begin{aligned}\frac{\partial}{\partial t}\hat{\rho}_{n,j_1,\ldots,j_K}(t) ={}& -\left[\frac{\mathrm{i}}{\hbar}\hat{H}_A^\times + n\gamma + \sum_{k=1}^{K}\left(j_k\nu_k - \frac{1}{\nu_k\hbar^2}\hat{V}^\times\hat{\Theta}_k\right) + \hat{\Gamma}_0\right]\hat{\rho}_{n,j_1,\ldots,j_K}(t)\\ &-\frac{\mathrm{i}}{\hbar}\hat{V}^\times\left[\hat{\rho}_{(n+1),j_1,\ldots,j_K}(t) + \sum_{k=1}^{K}\hat{\rho}_{n,j_1,\ldots,(j_k+1),\ldots,j_K}(t)\right]\\ &-\frac{\mathrm{i}n}{\hbar}\hat{\Theta}_0\hat{\rho}_{(n-1),j_1,\ldots,j_K}(t) - \sum_{k=1}^{K}\frac{\mathrm{i}j_k}{\hbar}\hat{\Theta}_k\hat{\rho}_{n,\ldots,(j_k-1),\ldots,j_K}(t),\end{aligned} \tag{5.68}$$

where

$$\hat{\Gamma}_0 \equiv \frac{\eta}{\beta\hbar^2}\left(1-\frac{\beta}{\gamma\eta}c_0\right)\hat{V}^\times\hat{V}^\times. \tag{5.69}$$

If $n\gamma + \sum_{k=1}^{K} j_k\nu_k$ is sufficiently large compared with the characteristic frequency of the system, then we have

$$\begin{aligned}&\frac{\partial}{\partial t}\hat{\rho}_{n,j_1,\ldots,j_K}(t)\\ &\quad\simeq -\left(\frac{\mathrm{i}}{\hbar}\hat{H}_A^\times - \sum_{k=1}^{K}\frac{1}{\nu_k\hbar^2}\hat{V}^\times\hat{\Theta}_k + \hat{\Gamma}_0\right)\hat{\rho}_{n,j_1,\ldots,j_K}(t),\end{aligned} \tag{5.70}$$

which works as the terminator for the hierarchy eq. (5.68). It is important to emphasize that the present formulation does not rely on Markov approximation, a high-temperature assumption, perturbative approximation, and rotating wave approximation (RWA). The conventional quantum master equations or Bloch equation without RWA cannot be applied in low-temperature systems, where quantum effects play a major role. Generalized quantum master equations can handle a colored-noise bath, but can treat only weak system–bath couplings. The present nonperturbative approach allows us to treat the strong system–bath interaction. Best of all, our formulation fits numerical calculations as demonstrated in refs. 167 and 151. By performing the Wigner transformation, we can easily obtain the quantum Fokker–Planck equation for a low-temperature system.

We have extended the hierarchy to include the low-temperature correction terms. It is also possible to study nonOhmic (nonMarkovian) distribution functions by extending the hierarchy. For example, a displaced harmonic oscillators system coupled to a white-noise bath can be studied by the spin-Boson Hamiltonian with the nonOhmic spectral distribution function[198]

$$J(\omega) = \frac{\hbar\eta}{\pi}\frac{4\gamma^2\omega_0^2\omega}{(\omega^2-\omega_0^2)^2+4\gamma^2\omega^2}, \tag{5.71}$$

where ω_0 is the oscillator frequency and γ is the coupling strength between the displaced harmonic oscillators system and the bath. The parameter η is a function of the displacement of the oscillators. Since the spectral density has two poles, $-\gamma \pm \mathrm{i}\delta$, where $\delta = \sqrt{\omega_0^2-\gamma^2}$, both $L_1(t)$ and $L_2(t)$ are expressed as linear functions of $\mathrm{e}^{(-\gamma+\mathrm{i}\delta)t}$ and $\mathrm{e}^{(-\gamma-\mathrm{i}\delta)t}$ for a high-temperature case. Then, the hierarchy for spin-Boson system is constructed as[37]

$$\begin{aligned}\frac{\partial}{\partial t}\hat{\rho}_{nm}(t) ={}& -\left[\frac{\mathrm{i}}{\hbar}\hat{H}_A^\times + (n+m)\gamma - \mathrm{i}(n-m)\delta\right]\hat{\rho}_{nm}(t)\\ &-\frac{\mathrm{i}}{\hbar}\hat{V}^\times\left[\hat{\rho}_{(n+1)m}(t) + \hat{\rho}_{n(m+1)}(t)\right]\\ &-\frac{\mathrm{i}n}{\hbar}\hat{\Theta}_-\hat{\rho}_{(n-1)m}(t) - \frac{\mathrm{i}m}{\hbar}\hat{\Theta}_+\hat{\rho}_{n(m-1)}(t)\end{aligned} \tag{5.72}$$

and

$$\hat{\Theta}_\pm \equiv \frac{\eta\gamma}{\beta}\left(\frac{\delta\pm\mathrm{i}\gamma}{\delta}\hat{V}^\times \pm \frac{\beta\hbar\omega_0^2}{2\delta}\hat{V}^\circ\right). \tag{5.73}$$

Equation (5.72) can be used to describe the dynamics of the electronic excitation of a molecule coupled with the heat bath through a molecular vibrational mode with a frequency ω_0. We could reduce the molecular degrees of freedom because the oscillators modes are harmonic. If the modes are not harmonic, one has to consider molecular coordinates explicitly as will be discussed in the next subsection.

5.8 Multi-state quantum Fokker–Planck equation

Thus far, we have separately discussed two types of dynamics employing distinct approaches; one is a vibrational coordinate system discussed from the quantum F–P

equation approach and another is a discrete energy-level system discussed from the quantum master equation approach. In many physical processes, however, vibrational motions and electronic excitation states are coupled and play important roles at the same time. Examples involve the electronically resonant laser excitations and nonadiabatic transitions briefly mentioned in §4.4.[79,185,199,200] Equations in phase space have been formulated to treat such problems.[201–206]

Here, we present the multi-state quantum Fokker–Planck equation, which can be applied to both optical and nonadiabatic transition problems taking into account the noise correlation and temperature effects. We consider the Hamiltonian expressed as

$$\hat{H}_A(t) = \frac{\hat{p}^2}{2m} + \sum_{jk} |j\rangle U_{jk}(\hat{q};t)\langle k|. \tag{5.74}$$

Here, $\hat{q}$ is the nuclear coordinate strongly coupled to the electronic state and $\hat{p}$ is its conjugate momentum. The diagonal element $U_{jj}(\hat{q};t)$ is the potential surface of the jth electronic state, and the off-diagonal element $U_{jk}(\hat{q};t)$ with $j \neq k$ represents the diabatic coupling between the jth and kth states.

The density matrix element for eq. (5.74) is then expanded in the electronic basis set as[202]

$$\hat{\boldsymbol{\rho}}(q,q';t) = \sum_{j,k} |j\rangle \rho_{jk}(q,q';t)\langle k|, \tag{5.75}$$

where $\rho_{jk}(q,q';t)$ is the jk element of the density matrix element expressed in the coordinate space. Alternatively, we can switch the notation to the Wigner representation

$$W_{jk}(p,q;t) \equiv \frac{1}{2\pi\hbar}\int_{-\infty}^{\infty} \mathrm{d}x\, \mathrm{e}^{\mathrm{i}px/\hbar}\rho_{jk}\left(q-\frac{x}{2}, q+\frac{x}{2};t\right). \tag{5.76}$$

We denote the Wigner functions for different electronic states in matrix form as $\mathbf{W}(p,q;t) \equiv \{W_{jk}(p,q;t)\}$. Likewise, the transition operator is written in Wigner representation form as

$$X_{ij}(p,q;t) = \mathrm{i}\int_{-\infty}^{\infty} \mathrm{d}x\, \mathrm{e}^{\mathrm{i}px/\hbar}U_{ij}\left(q-\frac{x}{2};t\right), \tag{5.77}$$

and

$$X_{ij}^{\dagger}(p,q;t) = -\mathrm{i}\int_{-\infty}^{\infty} \mathrm{d}x\, \mathrm{e}^{\mathrm{i}px/\hbar}U_{ij}\left(q+\frac{x}{2};t\right). \tag{5.78}$$

The quantum Liouvillian can also be expressed in matrix form as[202]

$$-\left\{\hat{\mathbf{L}}_A(p,q;t)\mathbf{W}(p,q;t)\right\}_{jk} = -\frac{p}{m}\frac{\partial}{\partial q}W_{jk}(p,q;t) + \frac{1}{\hbar}\int\frac{\mathrm{d}p'}{2\pi\hbar}\sum_m\left[X_{jm}(p-p',q;t)W_{mk}(p',q;t) + X_{mk}^{\dagger}(p-p',q;t)W_{jm}(p',q;t)\right]. \tag{5.79}$$

Thus, for the coordinate system coupled to the electronic states, the hierarchy of equations of motion (5.38) can be cast in matrix form as[159]

$$\frac{\partial}{\partial t}\mathbf{W}_n(p,q;t) = -\left(\hat{\mathbf{L}}_A(p,q;t) + n\gamma\right)\mathbf{W}_n(p,q;t) - \hat{\Phi}_{\mathrm{W}}\mathbf{W}_{n+1}(p,q;t) + n\hat{\Theta}_{\mathrm{W}}\mathbf{W}_{n-1}(p,q;t), \tag{5.80}$$

where the scalar operator $n\gamma$ and the operators $\hat{\Phi}_{\mathrm{W}}$ and $\hat{\Theta}_{\mathrm{W}}$ operate for all the elements $W_{jk}(p,q;t)$. The terminator eq. (5.39) can also be expressed in matrix form accordingly. Note that the present equations hold even if $U_{jk}(q)$ is time-dependent, as is the case of optical spectroscopy.

The wavepacket dynamics of nonadiabatic transition and optical responses for a system of displaced oscillators has been studied by numerically integrating the multi-state quantum F–P equation.[202] Here, we review the results for the system of displaced Morse oscillators coupled to a nearly Markovian noise bath.[159,160] As in §5.5, we employ the dimensionless coordinate q and momentum p. As illustrated in Fig. 17, we consider a system of the three levels $|g\rangle$, $|e\rangle$, and $|e'\rangle$ with their potentials respectively defined by

$$\begin{aligned} U_{gg}(q) &= E_c\left(1-\mathrm{e}^{-a(q-d_1)}\right)^2, \\ U_{ee}(q) &= E_c\left(1-\mathrm{e}^{-a(q-d_2)}\right)^2 + \hbar\omega_{ge}, \\ U_{e'e'}(q) &= E_c\mathrm{e}^{-2a'(q-d_2)} + \hbar\omega_{ge}. \end{aligned} \tag{5.81}$$

Here, a and E_c are defined in eq. (5.52) and are set to be $E_c = 3649\,\mathrm{cm}^{-1}$ and $a = 0.636$ to have the fundamental frequency $\omega_0 = 38.7\,\mathrm{cm}^{-1}$. The constants d_1 and d_2 represent the displacement of the potentials and are set to $d_1 = 40.6$ and $d_2 = 43.6$. The profile of the anti-bonding state is specified by a'; here, we choose $a' = 0.636$. The diabatic coupling between $|e\rangle$ and $|e'\rangle$ is expressed as

$$U_{ee'}(q) = A\mathrm{e}^{-\alpha(q-d_3)^2}, \tag{5.82}$$

where we set $A = 300\,\mathrm{cm}^{-1}$, $\alpha = 1$, and $d_3 = 51.7$. The transition between the state g and e is assumed to be induced by laser interactions. Although we can use any profile and intensity of laser in our approach, we employ an impulsive laser pulse that creates a wavepacket in $|e\rangle$ with the shape of

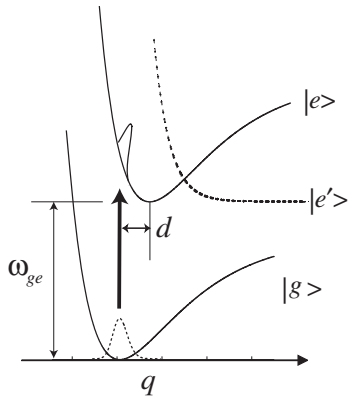

Fig. 17. Potential surfaces of displaced Morse oscillators system with anti-bonding (predissociation) state. The resonant frequency between $|g\rangle$ and $|e\rangle$ or $|e'\rangle$ is expressed by ω_{ge}. We assume that laser excitation creates a wavepacket with the same shape as that observed in the ground equilibrium state.

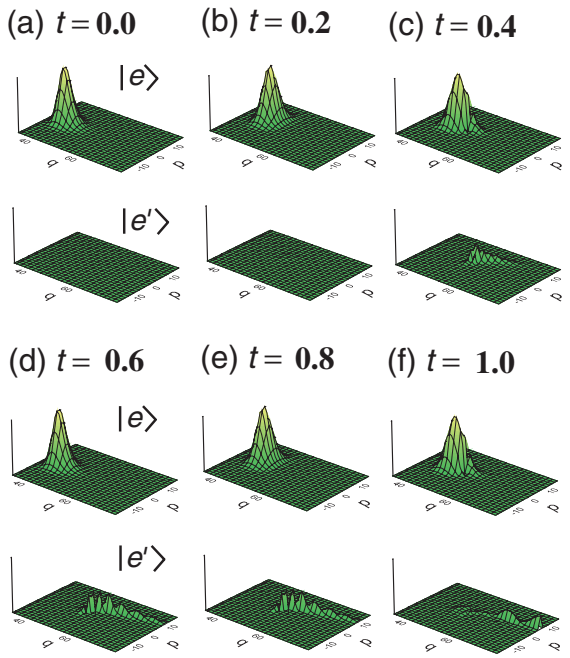

Fig. 18. Time evolution of $W_{ee}(p,q;t)$ and $W_{e'e'}(p,q;t)$ for weak damping case. In each panel, the upper one is for $|e\rangle$ (bonding state), whereas the lower one is for $|e'\rangle$ (anti-bonding state). At time (a) $t = 0$ ps, the wavepacket with the shape the same as that in the ground equilibrium state is created by the pump pulse. Then, the wavepacket rotates clockwise in phase space and reached a curve crossing point at time (b) $t = 0.2$ and passes the point (about $q = 50$) at (c) $t = 0.4$. The e' state population suddenly increases when the e state wavepacket passes the crossing point. Although the wavepacket in $|e\rangle$ exhibits oscillatory motion, the transferred wavepacket in $|e'\rangle$ moves to the positive direction and then goes out from the edge of the potential at (d) $t = 0.6$ and (e) 0.8. In the second period of such motion in the e state, the wavepacket transfers to $|e'\rangle$ again when it reaches the crossing point at (f) $t = 1.0$. Because of the dissipation, the wavepacket in $|e\rangle$ gradually loses its kinetic energy and approaches the steady state centered at the bottom of the e state potential. The above results are reproduced from the theory developed in ref. 159.

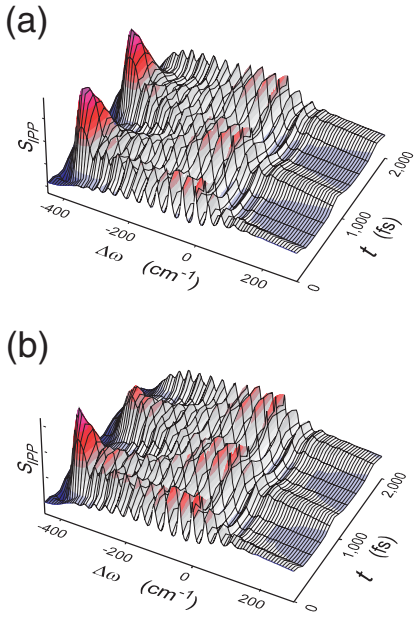

Fig. 19. Impulsive pump-probe spectra between $|g\rangle$ and $|e\rangle$. The probe spectra are plotted as a function of the pulse duration between the pump and the probe denoted by t. (a) shows results in the case without anti-bonding state, whereas (b) those in the case with the anti-bonding state. The peak at $-380\,\mathrm{cm}^{-1}$ and $t = 1.4$ ps in (b) is noticeably smaller than that in (a) owing to predissociation. The above results are reproduced from the theory developed in ref. 159.

the ground equilibrium state following the Frank–Condon principle. By numerically integrating the multi-state quantum F–P equation for the Gaussian–Markovian noise with the LL interaction, we calculated the wavepackets dynamics and linear and nonlinear signals. (See detail in refs. 159 and 160.) Here, we show the results for the weak coupling case $\zeta V_1^2 = 0.16\,\mathrm{cm}^{-1}$ and $\gamma = 4.8\,\mathrm{cm}^{-1}$ when the temperature is set to be $T = 300$ K, which satisfies the condition $\beta\hbar\gamma = 0.023 \ll 1$.

In Fig. 18, we present the time-evolution of $W_{ee}(p,q;t)$ and $W_{e'e'}(p,q;t)$. The pump–probe signals defined by eqs. (4.34)–(4.37) are then calculated from the procedure explained in refs. 159. Figure 19 shows the signals for displaced Morse oscillators system (a) without and (b) with diabatic coupling. Without diabatic coupling, the system is essentially a two-level system. If the displacement is small, the excited wavepacket moves around the bottom of the excited potential and exhibits a harmonic motion.[79,200] Since the displacement is not small in this case, the excited wavepacket has a large kinetic energy and the anharmonicity plays a role of dispersion. In Figs. 19(a) and 19(b), the height of each peak changes periodically at a period of about 800 fs corresponding to that observed in the coherent motion of the wavepacket in $|e\rangle$ created by the pump pulse. The small peaks in the figures correspond to vibronic bands. The envelope of those small peaks reflects the shape of the excited wavepacket which also shows oscillatory motion. Since the resonant frequency between $|g\rangle$ and $|e\rangle$ ($\delta\omega = U_{ee}(q) - U_{gg}(q) - \omega_{eg}$) is not a linear function of q, the shape of the envelope as a function of $\delta\omega$ is quite different from the original shape of the wavepacket. For instance, $\delta\omega$ is a rapidly decreasing function of q in the range of $q < 50$, but it gradually increases for $q > 50$ after reaching its minimum ($\delta\omega = -380\,\mathrm{cm}^{-1}$ for $d = 3$) at $q = 50$.

Thus, if the wavepacket is in the area of $q < 50$, the envelope reflecting the wavepacket motion is broadened and moves quickly, but if the wavepacket is at $q > 50$, the envelope becomes sharp and moves slowly compared with its actual shape and speed. Figure 19(b) shows the signal with diabatic transition. Compared with the peak at -380 cm^{-1} and $t = 1.4$ ps in Fig. 19(a), the peak at the same position in Fig. 19(b) is noticeably small. This is because the population in $|e\rangle$ decreased after passing the crossing point owing to predissociation.

6. Fokker–Planck Equation and Master Equation with Langevin Force

6.1 Generalized Langevin equation

The stochastic Liouville equation (2.37) explicitly contains the random variable, and the time evolution of density matrix elements is stochastic in nature. On the other hand, the hierarchy of equations, eqs. (2.41)–(2.43), derived from the stochastic Liouville equation is ensemble-averaged and the trajectory of the density matrix element is uniquely determined by the equations of motion. The relation between

the stochastic Liouville equation and the hierarchy of equations is somewhat similar to the relation between the classical Langevin equation,[14]

$$m\ddot{q} + m\zeta\dot{q} + \frac{\mathrm{d}U(q)}{\mathrm{d}q} + R(t) = 0, \tag{6.1}$$

with

$$\langle R(t)\rangle = 0, \quad \langle R(t)R(0)\rangle = \frac{m\zeta}{\beta}\delta(t), \tag{6.2}$$

and the classical Fokker–Planck equation, eq. (5.44) with eqs. (5.43) and (5.45). The differences between the two descriptions are that the classical Langevin equation describes the trajectory of a particle, whereas the stochastic Liouville equation describes the trajectory of the density matrix element. The Langevin force, i.e., the noise in eq. (6.1), is determined by the associated equation eq. (6.2), whereas the stochastic Liouville equation involves the time evolution operator of noise (Markov operator) in the equation of motion. Furthermore, the Langevin equation has a damping term, the second term on the left-hand side of eq. (6.1), which guarantees the system to be in the thermal equilibrium state at the inverse temperature β. Since the hierarchy of eqs. (5.41) and (5.60) with their terminators derived in §5 assures the thermal equilibrium state and such equations have a similar form to the stochastic Liouville equation (2.43), we may expect to reduce a Langevin-like stochastic equation from the Hamiltonian eq. (5.1) or eq. (5.53) with the spectral distribution eq. (5.11) that involves the damping term in addition to the random variable.

For this purpose, let us consider the auxiliary variable $\bar{\Omega}(t)$ for the density matrix elements eqs. (5.3) and (5.5). Then we rewrite the reduced density matrix elements as[207,208]

$$\begin{aligned}\rho(q,q';t) = \int \mathrm{d}\bar{\Omega}_f \int \mathrm{d}\bar{\Omega}_i \int_{\bar{\Omega}(t_i)=\bar{\Omega}_i}^{\bar{\Omega}(t)=\bar{\Omega}_f} D[\bar{\Omega}(\tau)] \int D[q(\tau)] \int D[q'(\tau)] \int \mathrm{d}q_i \int \mathrm{d}q_i' \\ \times \rho(q_i,q_i')\rho_{\mathrm{CS}}(q,q',t;q_i,q_i')P[\bar{\Omega}(\tau)]P_{\mathrm{eq}}(\bar{\Omega}_i) \\ \times \exp\left\{\frac{\mathrm{i}}{\hbar}S_A[q;t]\right\}F(q,q',\bar{\Omega}(\tau);t)\exp\left\{-\frac{\mathrm{i}}{\hbar}S_A[q';t]\right\},\end{aligned} \tag{6.3}$$

where $P_{\mathrm{eq}}(\bar{\Omega}_i)$ is given by eq. (2.21) and the influence functional eq. (5.5) is now expressed as

$$F(q,q',\bar{\Omega}(\tau);t) = \exp\left[\left(-\frac{\mathrm{i}}{\hbar}\right)^2 \int_{t_i}^{t} \mathrm{d}\tau\, V^{\times}(q,q';\tau)\frac{\partial}{\partial\tau}\int_{t_i}^{\tau}\mathrm{d}\tau'\,\mathrm{i}\bar{L}_1(\tau-\tau')V^{\circ}(q,q';\tau') - \frac{\mathrm{i}}{\hbar}\int_{t_i}^{t}\mathrm{d}\tau\,V^{\times}(q,q';\tau)\bar{\Omega}(\tau)\right], \tag{6.4}$$

with $\bar{\Omega}(\tau)$ given by

$$\bar{\Omega}(\tau) \equiv -\frac{\mathrm{i}}{\hbar}\int_{t_i}^{\tau}\mathrm{d}\tau'\,L_2(\tau-\tau')\big[V\big(q(\tau')\big) - V\big(q'(\tau')\big)\big], \tag{6.5}$$

and $P[\bar{\Omega}(\tau)]$ is the Gaussian functional defined by

$$P[\bar{\Omega}(\tau)] \equiv C^{-1}\exp\left[-\frac{1}{2}\int_{t_i}^{t}\mathrm{d}\tau\int_{t_i}^{t}\mathrm{d}\tau'\,L_2^{-1}(\tau-\tau')\bar{\Omega}(\tau)\bar{\Omega}(\tau')\right], \tag{6.6}$$

where C is the normalization constant. We introduced $L_2^{-1}(\tau)$ to satisfy

$$\int \mathrm{d}t\,L_2^{-1}(\tau-t)L_2(t-\tau') = \delta(\tau-\tau'), \tag{6.7}$$

and therefore

$$L_2^{-1}(t) = \frac{1}{\pi^2}\int_0^{\infty}\mathrm{d}\omega\,\frac{1}{J(\omega)}\tanh\left(\frac{\beta\hbar\omega}{2}\right)\cos\omega t. \tag{6.8}$$

The function $\bar{\Omega}(\tau)$ was originally the function of $q(t)$ and $q'(t)$, but by introducing the probability functional $P[\bar{\Omega}(\tau)]$, we can regard $\bar{\Omega}(\tau)$ as being independent of $q(t)$ and $q'(t)$: The transformation is similar to the Hubbard–Stratonovich transformation.[209,210] The first two moments for the above probability functional are given by

$$\big\langle\bar{\Omega}(\tau)\big\rangle = 0, \quad \big\langle\bar{\Omega}(\tau)\bar{\Omega}(\tau')\big\rangle = L_2(\tau-\tau'), \tag{6.9}$$

where, for any functional $A(\bar{\Omega}(\tau))$ $(t \geq \tau \geq t_i)$,

$$\big\langle A(\bar{\Omega}(\tau))\big\rangle \equiv \int \mathrm{d}\bar{\Omega}_f \int \mathrm{d}\bar{\Omega}_i \int_{\bar{\Omega}(t_i)=\bar{\Omega}_i}^{\bar{\Omega}(t)=\bar{\Omega}_f} D[\bar{\Omega}(\tau')]A(\bar{\Omega}(\tau))P[\bar{\Omega}(\tau')]P_{\mathrm{eq}}(\bar{\Omega}_i). \tag{6.10}$$

We first show that the function $\bar{\Omega}(\tau)$ plays the same role as the Langevin force in eq. (6.1). Consider a system in the coordinate representation defined by eq. (5.2) and the interaction $V(q) = V_1 q$. We respectively introduce the center and relative coordinate $r(t) \equiv (q(t)+q'(t))/2$ and $x(t) \equiv q(t) - q'(t)$. The initial correlation $\rho_{\mathrm{CS}}(q,q',t;q_i,q_i') \to \rho_{\mathrm{CS}}(x,r,t;x_i,r_i')$ is now a functional of $r(t)$ and $x(t)$. Here, we assume the form $\exp\{\mathrm{i}m\int_{t_i}^{t}\mathrm{d}\tau'\,x(\tau')[C_1(\tau')r(t_i) - \mathrm{i}C_2(\tau')x(t_i)]/\hbar\}$, where $C_1(\tau)$ and $C_2(\tau)$ are some functions for the system and bath parameters. Their explicit forms were given for the harmonic Brownian system.[155] Thus, we rewrite the density matrix element for the given function $R(\tau) \equiv \bar{\Omega}(\tau)V_1$ as

$$\rho(x,r,R(\tau);t)=\int D[x(\tau)]\int D[r(\tau)]\int \mathrm{d}x_i\int \mathrm{d}r_i\,\rho(x_i,r_i)\exp\left[\frac{\mathrm{i}}{\hbar}\Sigma(x,r,R(\tau),t)\right], \tag{6.11}$$

where the influence phase is given by

$$\begin{aligned}\Sigma(x,r,R(\tau),t)=\int_{t_i}^{t}\mathrm{d}\tau\Bigg[&m\dot{x}(\tau)\dot{r}(\tau)-U\left(r(\tau)+\frac{x(\tau)}{2}\right)+U\left(r(\tau)-\frac{x(\tau)}{2}\right)\\&-2mx(\tau)\frac{\partial}{\partial\tau}\int_{t_i}^{\tau}\mathrm{d}\tau'\,\zeta(\tau-\tau')r(\tau')-(R(\tau)+F_{\mathrm{CI}}(\tau))x(\tau)\Bigg].\end{aligned} \tag{6.12}$$

Here, we define viscosity as

$$\zeta(t)\equiv\frac{V_1^2}{m\hbar}\bar{L}_1(t), \tag{6.13}$$

and the effect of the initial correlation between the system and the bath as

$$F_{\mathrm{CI}}(\tau)=-m[C_1(\tau)r(t_i)-\mathrm{i}C_2(\tau)x(t_i)]. \tag{6.14}$$

We integrate by part in the first term of eq. (6.12). Then we expand the potential by x and replace that derivative from $\mathrm{d}/\mathrm{d}x$ to $\mathrm{d}/\mathrm{d}r$. Since the classical path of $r(t)$ is the minimal path of the phase for any $x(t)$ that satisfies $\delta\Sigma(x,r,R,t)/\,\delta x(\tau)=0$, we have

$$m\ddot{r}(t)+2m\frac{\partial}{\partial t}\int_{t_i}^{t}\mathrm{d}\tau\,\zeta(t-\tau)r(\tau)+\frac{1}{2}\frac{\mathrm{d}}{\mathrm{d}r(t)}\left[U\left(r(t)+\frac{x(t)}{2}\right)+U\left(r(t)-\frac{x(t)}{2}\right)\right]+F_{\mathrm{CI}}(t)+R(t)=0. \tag{6.15}$$

In the classical limit, we may set $x(t)\to 0$ and approximate it as

$$m\ddot{r}(t)+2m\frac{\partial}{\partial t}\int_{t_i}^{t}\mathrm{d}\tau\,\zeta(t-\tau)r(\tau)+\frac{\mathrm{d}U(r(t))}{\mathrm{d}r(t)}+F_{\mathrm{CI}}(t)+R(t)=0, \tag{6.16}$$

where $R(t)$ is determined to satisfy eq. (6.9) with $L_2(t)\to\tilde{L}_2(t)\equiv V_1^2L_2(t)$. Since $R(t)$ plays the same role as a random force in the classical Langevin equation, we shall call it Langevin force.[207,208] For a white noise case, we have

$$\zeta(t)=\zeta\delta(t),\quad \tilde{L}_2(t)=\frac{m\zeta}{\beta}\delta(t), \tag{6.17}$$

and eq. (6.16) reduces to the Langevin equation (6.1).

6.2 Fokker–Planck equation with Langevin force

We now derive a Langevin-like equation of motion for a density matrix element for a given random function, $\bar{\Omega}(\tau)$. We denote $\rho(q,q',\bar{\Omega}(\tau);t)\to\rho(q,q';\bar{\Omega};t)$. For an Ohmic spectral distribution with a Lorentzian cutoff, eq. (5.11), $\bar{L}_1(t)$ and $L_2(t)$ are calculated in terms of exponential functions as eqs. (5.12) and (5.13), respectively. The density matrix element is then expressed as

$$\rho(q,q';\bar{\Omega};t)=\int D[q(\tau)]\int D[q'(\tau)]\int \mathrm{d}q_i\int \mathrm{d}q_i'\,\rho(q_i,q_i')\exp\left\{\frac{\mathrm{i}}{\hbar}S_A[q;t]\right\}F(q,q',\bar{\Omega}(\tau);t)\exp\left\{-\frac{\mathrm{i}}{\hbar}S_A[q';t]\right\}, \tag{6.18}$$

where we set $\rho_{\mathrm{CS}}(q,q',t;q_i,q_i')=1$ as discussed in §5.1. The influence functional is written as

$$F(q,q',\bar{\Omega}(\tau);t)=\exp\left\{-\int_{t_i}^{t}\mathrm{d}\tau\,\Phi(q(\tau),q'(\tau))\left[\int_{t_i}^{\tau}\mathrm{d}\tau'\,\mathrm{e}^{-\gamma(\tau-\tau')}\Theta'(q,q';\tau')+\bar{\Omega}(\tau)+G(q_i,q_i';\tau)\right]\right\}. \tag{6.19}$$

Here, $\Phi(q,q')$ and $G(q_i,q_i';\tau)$ are given by eqs. (5.17) and (5.19), respectively, and

$$\Theta'(q,q';\tau)\equiv\frac{\eta\gamma}{2}\left[V'\big(q(\tau)\big)\dot{q}(\tau)+V'\big(q'(\tau)\big)\dot{q}'(\tau)\right], \tag{6.20}$$

where $V'(q)\equiv\partial V(q)/\partial q$ for any function $V(q)$. The time differentiation of $\rho(q,q';\bar{\Omega};t)$ is evaluated by a similar procedure described in §5.2. In the present case, the auxiliary function eq. (5.23) is replaced by

$$\begin{aligned}\rho_n(q,q';\bar{\Omega};t)\equiv&\int D[q(\tau)]\int D[q'(\tau)]\int \mathrm{d}q_i\int \mathrm{d}q_i'\,\rho(q_i,q_i')\left[\int_{t_i}^{t}\mathrm{d}\tau'\,\mathrm{e}^{-\gamma(t-\tau')}\Theta'(q,q';\tau')+G(q_i,q_i';t)\right]^n\\&\times\exp\left\{\frac{\mathrm{i}}{\hbar}S_A[q;t]\right\}F(q,q',\bar{\Omega}(\tau);t)\exp\left\{-\frac{\mathrm{i}}{\hbar}S_A[q';t]\right\}.\end{aligned} \tag{6.21}$$

We express $\rho_n(q,q';\bar{\Omega};t)$ in the Wigner representation as $W_n(p,q;\bar{\Omega};t)$. Then, for $V=V_1q+V_2q^2/2$, the equations of motion for the nth member of hierarchy are evaluated as

$$\frac{\partial}{\partial t}W_n(p,q;\bar{\Omega};t)=-\big\{\hat{L}_A(p,q)+n\gamma+\bar{\Omega}(t)\hat{\Phi}_{\mathrm{W}}\big\}W_n(p,q;\bar{\Omega};t)-\hat{\Phi}_{\mathrm{W}}W_{n+1}(p,q;\bar{\Omega};t)+n\hat{\Theta}'_{\mathrm{W}}W_{n-1}(p,q;\bar{\Omega};t), \tag{6.22}$$

where

$$\hat{\Theta}'_{\rm W} \equiv \zeta\gamma\left\{ V_1 p + V_2\left(qp + \frac{\hbar^2}{4}\frac{\partial^2}{\partial p\partial q}\right)\right\}, \tag{6.23}$$

and we set $nW_{n-1}(p,q;\bar{\Omega};t) = 0$ for $n = 0$, and $\hat{\Phi}_{\rm W}$ and $\hat{L}_A(p,q)$ are defined by eqs. (5.32) and (5.37), respectively. The terminator is given by

$$\begin{aligned}\frac{\partial}{\partial t} W_N(p,q;\bar{\Omega};t) = &-\left\{\hat{L}_A(p,q) + N\gamma + \bar{\Omega}(t)\hat{\Phi}_{\rm W}\right\} W_N(p,q;\bar{\Omega};t)\\ &+ \hat{\Gamma}'_{\rm W} W_N(p,q;\bar{\Omega};t) + N\hat{\Theta}'_{\rm W} W_{N-1}(p,q;\bar{\Omega};t),\end{aligned} \tag{6.24}$$

where

$$\hat{\Gamma}'_{\rm W} \equiv \zeta(V_1 + V_2 q)^2 \frac{\partial}{\partial p} p + \frac{\hbar^2\zeta V_2(V_1 + V_2 q)}{4}\frac{\partial^3}{\partial p^2\partial q}. \tag{6.25}$$

Equations (6.22) and (6.24) are quantum Fokker–Planck equations with the Langevin force; they can be used to study the quantum dynamics of a system even at low temperatures. The distribution function $W_0(p,q;t)$ is obtained from $W_0(p,q;\bar{\Omega};t)$ by averaging over $\bar{\Omega}(\tau)$ as

$$W_0(p,q;t) = \left\langle W_0(p,q;\bar{\Omega};t)\right\rangle, \tag{6.26}$$

where $\langle\cdots\rangle$ is defined by eq. (6.10). In practice, by generating $\bar{\Omega}(\tau)$ in such a way that it satisfies eq. (6.9) and by solving the equations of motion for $W_n(p,q;\bar{\Omega};t)$, we can evaluate $W_0(p,q;t)$ by summing over $W_0(p,q;\bar{\Omega};t)$ for different sets of $\bar{\Omega}(\tau)$ values without calculating $P[\bar{\Omega}(\tau)]$.

In the fast modulation limit $\gamma \gg \omega_A$, we can set $N = 0$ and eq. (6.24) is reduced to

$$\begin{aligned}\frac{\partial}{\partial t} W_0(p,q;\bar{\Omega};t) = &-\left\{\hat{L}_A(p,q) + \bar{\Omega}(t)\hat{\Phi}_{\rm W}\right\} W_0(p,q;\bar{\Omega};t)\\ &+ \hat{\Gamma}'_{\rm W} W_0(p,q;\bar{\Omega};t),\end{aligned} \tag{6.27}$$

which agrees with the result obtained by Stockburger *et al.* for $V_2 = 0$.[211–213] In the high-temperature white-noise limit $\gamma \gg \omega_A$ and $\beta\hbar\gamma \ll 1$, eq. (6.6) is reduced to

$$P[\bar{\Omega}(\tau)] = C^{-1}\exp\left[-\frac{\beta}{2\zeta}\int_{t_i}^{t} {\rm d}\tau\,\bar{\Omega}^2(\tau)\right]. \tag{6.28}$$

Then, from eq. (6.26), we have the quantum Fokker–Planck equation for the white-noise bath, eq. (5.44). Alternatively, one can also express the equations of motion to generalize eqs. (5.38) and (5.39). If we rewrite $L_2(t)$ in eq. (5.13) as

$$L_2(t) = m\gamma\zeta c'_0 {\rm e}^{-\gamma|t|} + L'_2(t), \tag{6.29}$$

where we set $c'_0 = c_0/m\gamma\zeta$ and $L'_2(t) \equiv L_2(t) - m\gamma\zeta c'_0{\rm e}^{-\gamma|t|}$, then

$$\begin{aligned}&\frac{\partial}{\partial t} W_n(p,q;\bar{\Omega}';t)\\ &\quad= -\left\{\hat{L}_A(p,q) + n\gamma + \bar{\Omega}'(t)\hat{\Phi}_{\rm W}\right\} W_n(p,q;\bar{\Omega}';t)\\ &\qquad- \hat{\Phi}_{\rm W} W_{n+1}(p,q;\bar{\Omega}';t) + n\hat{\Theta}'_{\rm W} W_{n-1}(p,q;\bar{\Omega}';t),\end{aligned} \tag{6.30}$$

where

$$\hat{\Theta}'_{\rm W} \equiv \zeta\gamma\left\{(V_1 + V_2 q)\left(p + c'_0\frac{\partial}{\partial p}\right) + \frac{V_2\hbar^2}{4}\frac{\partial^2}{\partial p\partial q}\right\}. \tag{6.31}$$

The terminator can also be defined in a similar manner. Here, $\bar{\Omega}'(t)$ satisfies

$$\left\langle\bar{\Omega}'(t)\right\rangle = 0, \quad \left\langle\bar{\Omega}'(t)\bar{\Omega}'(t')\right\rangle = L'_2(t-t'). \tag{6.32}$$

The term $\bar{\Omega}'(t)$ works as the low-temperature correction factor for the Fokker–Planck equation.

Contrary to the equations of motion presented in §5.3, both eqs. (6.22) and (6.30) with their terminators are not limited by temperature for any γ. The implementation of a random force defined by eq. (6.9) or (6.32) in the computer program is not easy, since $L'_2(t)$ which is numerically defined by $\int_0^T {\rm d}\tau\,\bar{\Omega}'(\tau+t)\bar{\Omega}'(\tau)/T$ often becomes negative for a certain range of t's as depicted in Fig. 7. An example of the numerical calculation for a spin system will be presented in §6.4.

6.3 *Energy state representation of Fokker–Planck equation with Langevin force*

In §6.2, we consider the Fokker–Planck equation in coordinate space. It is instructive to write the same equation using the single-mode harmonic (Boson) creation and annihilation operators $\hat{a}^-$ and $\hat{a}^+$. For later convenience, we introduce $\hat{a}_x \equiv \hat{a}^- + \hat{a}^+$, and $\hat{a}_y \equiv {\rm i}(\hat{a}^- - \hat{a}^+)$. The Hamiltonian of the system is assumed to be given by

$$\hat{H}_A(t) = \frac{1}{2}\hbar\omega_0(\hat{a}^+\hat{a}^- + \hat{a}^-\hat{a}^+) + \hat{F}(t). \tag{6.33}$$

Here, $\hat{F}(t)$ is a function of $\hat{q} \equiv \bar{q}\hat{a}_x$ and is an external interaction. For a laser interaction, this is expressed as $\hat{F}(t) = \mu\bar{q}E(t)(\hat{a}^+ + \hat{a}^-)$, where $\bar{q} \equiv \sqrt{\hbar/2m\omega_0}$ for the harmonic system with a frequency ω_0 and a mass m. In the linear system–bath interaction case $\hat{V} = \bar{V}_1\hat{a}_x$ with $\bar{V}_1 = V_1\bar{q}$, we have

$$\dot{\hat{V}}(t) \to \dot{\hat{a}}_x(t) = -\omega_0\hat{a}_y(t), \tag{6.34}$$

where $\hat{V}(t)$ and $\hat{a}_j(t)$ are the Heisenberg operators of $\hat{V}$ and $\hat{a}_j$ for $\hat{H}_A(t)$. Then the equation of motion (6.22) is rewritten as

$$\begin{aligned}\frac{\partial}{\partial t}\hat{\rho}_n(\bar{\Omega};t) = &-\left(\frac{\rm i}{\hbar}\hat{H}_A^{\times}(t) + n\gamma + \frac{\rm i}{\hbar}\bar{V}_1\bar{\Omega}(t)\hat{a}_x^{\times}\right)\hat{\rho}_n(\bar{\Omega};t)\\ &- \frac{\rm i}{\hbar}\bar{V}_1\hat{a}_x^{\times}\hat{\rho}_{n+1}(\bar{\Omega};t) - \frac{n\omega_0\eta\bar{V}_1}{2}\hat{a}_y^{\circ}\hat{\rho}_{n-1}(\bar{\Omega};t),\end{aligned} \tag{6.35}$$

where $\hat{A}^{\circ}\hat{\rho} \equiv \hat{A}\hat{\rho} + \hat{\rho}\hat{A}$ for any operator $\hat{A}$. The terminator for $N(\gamma+1) \gg \omega_0$ is expressed as the basis of the above equations with $n = N$ by substituting $\hat{\rho}_{N+1}(\bar{\Omega};t) = -\omega_0\eta\bar{V}_1 a_y^{\circ}\hat{\rho}_N(\bar{\Omega};t)/2$. In the white noise limit $N \to 0$, since $\hat{\rho}(t) = \langle\hat{\rho}_0(\bar{\Omega};t)\rangle$ with $\langle\cdots\rangle$ defined by eq. (6.10), the result reduces to

$$\frac{\partial}{\partial t}\hat{\rho} = -\frac{\mathrm{i}}{\hbar}\hat{H}_A^{\times}(t)\hat{\rho} + \frac{\omega_0\eta\bar{V}_1^2}{2\hbar}\big[(\bar{n}+1)\big(2\hat{a}^-\hat{\rho}\hat{a}^+ - \hat{a}^+\hat{a}^-\hat{\rho} - \hat{\rho}\hat{a}^+\hat{a}^-\big) + \bar{n}\big(2\hat{a}^+\hat{\rho}\hat{a}^- - \hat{a}^-\hat{a}^+\hat{\rho} - \hat{\rho}\hat{a}^-\hat{a}^+\big) + (\bar{n})\big(\hat{a}^+\hat{\rho}\hat{a}^+ + \hat{a}^-\hat{\rho}\hat{a}^- - (\hat{a}^+)^2\hat{\rho} - \hat{\rho}(\hat{a}^-)^2\big) + (\bar{n}+1)\big(\hat{a}^+\hat{\rho}\hat{a}^+ + \hat{a}^-\hat{\rho}\hat{a}^- - (\hat{a}^-)^2\hat{\rho} - \hat{\rho}(\hat{a}^+)^2\big)\big], \tag{6.36}$$

where we denote

$$\frac{2}{\beta\hbar\omega_0} \approx \frac{\mathrm{e}^{\beta\hbar\omega_0}+1}{\mathrm{e}^{\beta\hbar\omega_0}-1} = 2\bar{n}+1. \tag{6.37}$$

A similar equation is used in quantum optics.[180] Note that eq. (6.36) can only be applied to a high-temperature system. As discussed in §5.7, the quantum master equation does not satisfy the positivity condition for the system–bath interaction $\hat{V}\hat{x}_j = \bar{V}_1(\hat{a}^- + \hat{a}^+)(\hat{b}_j^- + \hat{b}_j^+)$. This difficulty may be avoided by introducing the rotating wave approximation (RWA) form which is equivalent to approximately $\hat{V}$ as $\hat{V}\hat{x}_j \to \bar{V}_1(\hat{a}^-\hat{b}_j^+ + \hat{a}^+\hat{b}_j^-)$. The neglect of the off-resonant terms $\bar{V}_1(\hat{a}^+\hat{b}_j^+ + \hat{a}^-\hat{b}_j^-)$, however, may fail to describe the true dynamics of original Hamiltonian.

Since we have the relations $\hat{a}^- + \hat{a}^+ = \hat{q}\sqrt{2m\omega_0/\hbar}$ and $\mathrm{i}(\hat{a}^- - \hat{a}^+) = \hat{p}\sqrt{2/m\omega_0\hbar}$, the Fokker–Planck equation is expressed as[153,154,214,215]

$$\frac{\partial}{\partial t}\hat{\rho}(t) = -\frac{\mathrm{i}}{\hbar}\hat{H}_A^{\times}(t)\hat{\rho}(t) + \frac{\eta V_1^2}{2m}\left\{-\frac{\mathrm{i}}{\hbar}\big[\hat{q},\{\hat{p},\hat{\rho}(t)\}\big] + \frac{2m}{\beta}\left(\frac{\mathrm{i}}{\hbar}\right)^2\big[\hat{q},\big[\hat{q},\hat{\rho}(t)\big]\big]\right\}. \tag{6.38}$$

The above equation reduces to eq. (5.44) by Wigner transformation.

6.4 *Bloch equation with Langevin force and numerical simulation*

In this subsection, we numerically solve the equations of motion given in eq. (6.35). We consider the two-level spin system defined by $|1\rangle$ and $|0\rangle$. The system Hamiltonian is expressed as

$$\hat{H}_A = \frac{1}{2}\hbar\omega_0\hat{\sigma}_z + \mu E\hat{\sigma}_x, \tag{6.39}$$

where $\hat{\sigma}_i$ for $i = x, y$, and z are the Pauli matrices. We choose $\hat{V} = \bar{V}_1\hat{\sigma}_x$. We treat the system without using the rotating wave approximation (RWA). To simplify the procedure, we consider the white noise limit $\gamma \gg \omega_0$. The equation of motion is then reduced to

$$\frac{\partial}{\partial t}\hat{\rho}_0(\bar{\Omega};t) = -\frac{\mathrm{i}}{\hbar}\hat{H}_A^{\times}\hat{\rho}_0(\bar{\Omega};t) + \frac{\mathrm{i}\omega_0\eta\bar{V}_1^2}{2\hbar}\hat{\sigma}_x^{\times}\hat{\sigma}_y^{\circ}\hat{\rho}_0(\bar{\Omega};t) - \frac{\mathrm{i}\bar{V}_1}{\hbar}\bar{\Omega}(t)\hat{\sigma}_x^{\times}\hat{\rho}_0(\bar{\Omega};t). \tag{6.40}$$

As was explained in §6.1, $\bar{\Omega}(t)$ plays the same role as a random force in the classical Langevin equation. We study the time evolution of the above equation by numerically integrating the equations of motion for various sets of noise $\bar{\Omega}(t)$ and then average over $\bar{\Omega}(t)$ to evaluate $\hat{\rho}(t) = \langle\hat{\rho}_0(\bar{\Omega};t)\rangle$. The Langevin force satisfies the correlation $\langle\bar{\Omega}(t)\bar{\Omega}(0)\rangle = L_2(t)$, in which $L_2(t)$ is given by eq. (5.13).

As the form of $L_2(t)$ indicates, the present equation as well as eqs. (6.35) can be applied for a system at very low temperatures. The key to the present approach is the Gaussian nature of the noise, i.e., processes are completely determined by $\langle\bar{\Omega}(\tau')\bar{\Omega}(\tau)\rangle$. In practice, however, it is not easy to employ this algorithm for numerical calculation, since $L_2(t)$ often becomes negative for a certain range of t's as depicted in Fig. 7, whereas $\langle\bar{\Omega}(\tau')\bar{\Omega}(\tau)\rangle$ is usually a positive definite function. To incorporate a negative part of the correlation function, here we assume that the system–bath interaction is weak and rewrite the equations of motion by introducing the hierarchy member for the Matsubara frequencies ν_k denoted by $\hat{\rho}_0^k(\bar{\Omega};t)$ as

$$\frac{\partial}{\partial t}\hat{\rho}_0(\bar{\Omega};t) = -\frac{\mathrm{i}}{\hbar}\hat{H}_A^{\times}\hat{\rho}_0(\bar{\Omega};t) + \frac{\mathrm{i}\omega_0\eta\bar{V}_1^2}{2\hbar}\hat{\sigma}_x^{\times}\hat{\sigma}_y^{\circ}\hat{\rho}_0(\bar{\Omega};t) - \mathrm{i}\sum_{k=0}^{\infty}|\Delta_k|\bar{\Omega}_k(t)\hat{\sigma}_x^{\times}\hat{\rho}_0^k(\bar{\Omega};t), \tag{6.41}$$

and

$$\frac{\partial}{\partial t}\hat{\rho}_0^k(\bar{\Omega};t) = -\frac{\mathrm{i}}{\hbar}\hat{H}_A^{\times}\hat{\rho}_0^k(\bar{\Omega};t) + \frac{\mathrm{i}\omega_0\eta\bar{V}_1^2}{2\hbar}\hat{\sigma}_x^{\times}\hat{\sigma}_y^{\circ}\hat{\rho}_0^k(\bar{\Omega};t) - \nu_k\hat{\rho}_0^k(\bar{\Omega};t) - \mathrm{i}\sum_{k=0}^{\infty}\Delta_k\bar{\Omega}_k(t)\hat{\sigma}_x^{\times}\hat{\rho}_0(\bar{\Omega};t) \tag{6.42}$$

where $\bar{\Omega}_k(t)$ is the Gaussian noise with its correlation given as

$$\big\langle\bar{\Omega}_k(\tau)\bar{\Omega}_l(0)\big\rangle = \delta_{kl}\mathrm{e}^{-\nu_k|\tau|}, \tag{6.43}$$

in which $\Delta_k = c_k\bar{V}_1/\hbar|c_k|$ with the definition eqs. (5.14) and (5.15). Since c_k quickly converges to zero as k increases even at low temperatures, the above equations can be handled easily. Note that we add the term proportional to $-\nu_k\hat{\rho}_0^k(\bar{\Omega};t)$ in eq. (6.42). This term does not play any role on a time scale shorter than the correlation time of the noise; however, it stabilizes the equation of motion by neglecting the effects of noise longer than the correlation time.

To carry out numerical calculations, we set $\hbar\omega_0 = 1$ and $E = 0$ in the Hamiltonian eq. (6.39) and choose the noise parameters $\eta\bar{V}_1^2/\hbar = 0.001$ and $\nu_0 \equiv \gamma = 20$. We employ a discrete time step Δt to use the Runge–Kutta method integrating the equation of motion. All the parameters are the dimensionless. The random force $\bar{\Omega}_k(t)$ is generated to satisfy the correlation $\langle\bar{\Omega}_k(\tau)\bar{\Omega}_k(0)\rangle = \exp[-\nu_k\tau]$ and updated with the time step $\Delta\tau$. This time step must be larger than Δt to stabilize the Runge–Kutta routine, but not too large compared with the characteristic time scale of the system (i.e. $\Delta\tau < 1/\omega_0$) because otherwise the system will not show random motion. Here, we choose $\Delta t = 0.001$ and $\Delta\tau = 0.025$. We denote the element of $\hat{\rho}_0(\bar{\Omega};t)$ for the excited state $|1\rangle\langle 1|$, the ground state $|0\rangle\langle 0|$, and their coherence $|1\rangle\langle 0|$ at time t by $\rho_{11}(t)$, $\rho_{00}(t)$, and $\rho_{10}(t)$, respectively.

Figures 20 and 21 illustrate how $\rho_{11}(t)$ and the imaginary part of $\rho_{10}(t)$ attain the equilibrium values for a sequence of random forces. We set the initial state $\rho_{11}(0) = 0$, $\rho_{10}(0) = 0$, and $\rho_{00}(0) = 1$. Figure 20 shows the time evolution of $\rho_{11}(t)$ for various temperatures (from top to bottom, $\beta\hbar = 0.1$, 0.5, and 2.0). After about $t = 2000$ ($\approx 1/\beta\hbar$), $\rho_{11}(t)$ reaches the equilibrium state and fluctuates around the

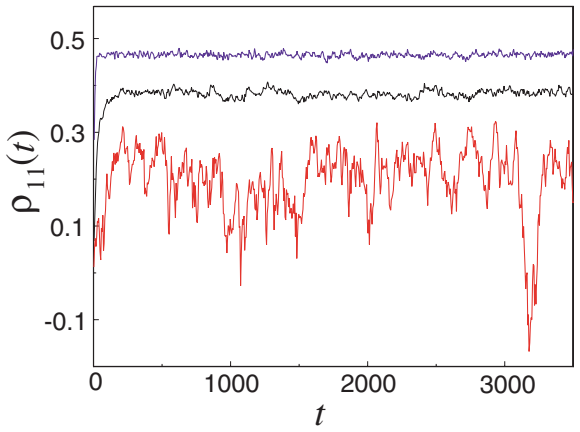

Fig. 20. The trajectories of the excited state population $[\rho_{11}(t)]$ for a sequence of random forces are depicted for different temperatures (from top to bottom, $\beta\hbar = 0.1, 0.5$, and 2.0).

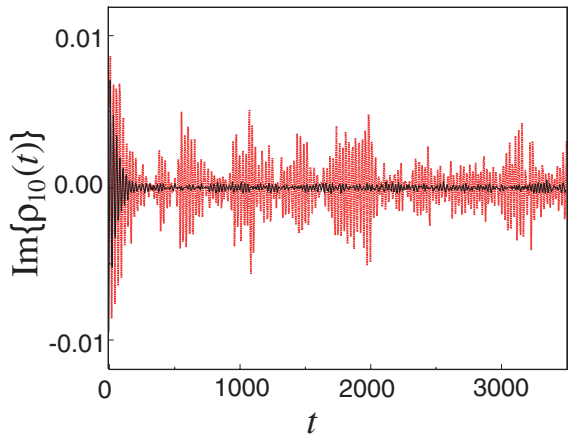

Fig. 21. The trajectories of the imaginary part of coherent state $[\rho_{10}(t)]$ for a sequence of random forces are depicted for $\beta\hbar = 0.5$ (solid line) and $\beta\hbar = 2.0$ (dotted line).

equilibrium values $[\rho_{11}^{\mathrm{eq}} \approx \tanh(\beta\hbar\omega_0/2)$ for small $\hbar\Delta]$. At high temperatures, the fluctuation of the population is small. Since $\bar{\Omega}(t)$ acts as the Langevin force for a classical potential system, one may regard the trajectories of $\rho_{00}(t)$ at high temperatures ($\beta\hbar\omega_0 \ll 1$) as a random walk. The amplitude of fluctuations increases as temperature decreases due to the contribution of noise elements with an amplitude c_k ($k > 0$). The enhancement of the fluctuations is of quantum origin, since all c_k and ν_k for ($k > 0$) involve $\hbar$. The initial time evolution from $t = 0$ to $t \approx 100$ $(1/\beta\hbar)$ may be regarded as the time evolution of the system for a specific noise sequence. Notice that the physical process, which involves the real trajectory, is obtained by averaging over all possible trajectories, i.e., $\hat{\rho}(t) = \langle\hat{\rho}_0(\bar{\Omega};\, t)\rangle$; each trajectory for some noises at very low temperatures is not necessary to be a positive definite as can be seen in the case of $\beta\hbar = 2.0$. This flexibility makes it possible to obtain the equilibrium distribution at low temperatures. Figure 21 shows the imaginary part of the coherence $\rho_{10}(t)$ for $\beta\hbar = 0.1$ (solid line) and $\beta\hbar = 2.0$ (dotted line), respectively. The amplitude becomes large when the quantum transition between the excited and ground states becomes large. For a high-temperature case, $\rho_{10}(t)$ plays a role only at the initial stage; it decays quickly to zero with small fluctuations.

Since the damping term and random force presented in this section play the same role as those in the Langevin equation, the trajectory of a density matrix element obtained for a sequence of a random noise is thus regarded as a quantum random walk. From the definition of expectation values, a physical trajectory is obtained after averaging over random walk trajectories. The formalism presented in this section incorporated with a Monte Carlo (MC) simulation follows the dissipative dynamics defined by the Hamiltonian. Thus, one can use this approach to calculate dynamical variables such as a time-correlation function of population while taking advantage of the MC approach, e.g., a coarse-grained characterization and parallelization of the routine. Note that the other MC approaches such as Galuber's approach[216] based on the Metropolis algorithm[217,218] are not related to real dynamics, since they filter dynamics to gain the thermal equilibrium state, and thus cannot be used to evaluate time-dependent variables such as the time-correlation functions of physical variables. The present approach is also fully quantum-mechanical, whereas many other MC approaches are classical.

Here, we introduced the Hubbard–Stratonovich-type transformation to the fluctuation part. There has been also an attempt to use such transformation not only for the dissipation but also for the fluctuation.[219,220] The reduced equation of motion derived from such methodology handles two random variables, and covers a wider parameter range than the equation of motion with a single random variable. The random trajectories of density matrix elements with two-random variables are, however, no longer related to any real processes.

7. Stochastic Liouville Equation and Temperature Correction Term

The equations of motion presented in eq. (6.22) with eq. (6.24) contain the stochastic variable $\bar{\Omega}(t)$; however, the character of the noise is not determined by the equations themselves, but by the associated equations, i.e., eq. (6.9). In this section, we show that the time evolution operator of the noise can be included in the equation of motion in the nearly Markovian noise case. The temperature correction term can also be expressed as a function of noise and can be included in the equations of motion. Consider the case in which the correlation functions are given by eqs. (5.12) and (5.13). For a high-temperature bath, eq. (5.13) is expressed as

$$L_2(t) = \gamma\Delta^2 \mathrm{e}^{-\gamma|t|}, \tag{7.1}$$

where $\Delta^2 = \eta/\beta$. We introduce nondimensional stochastic variable and functions as follows: $\Omega(\tau) \equiv \bar{\Omega}(\tau)/\sqrt{\gamma}\Delta$, $\bar{L}_2(t) \equiv L_2(t)/\gamma\Delta^2$, and $\bar{L}_2^{-1}(t) \equiv \Delta^2 L_2^{-1}(t)/\gamma$. Therefore,

$$\int \mathrm{d}t\, \bar{L}_2^{-1}(\tau - t)\bar{L}_2(t - \tau') = \frac{1}{\gamma^2}\,\delta(\tau - \tau'). \tag{7.2}$$

Since $L_1(t) = \beta\hbar\gamma\Delta\bar{L}_2(t)/2$, we can write the density matrix element given in §5.6 as

$$\rho(\phi^\dagger,\phi',\Omega;t)=\int d\Omega_i\int_{\Omega(t_i)=\Omega_i}^{\Omega(t)=\Omega}D[\Omega(\tau)]\int D[\phi^\dagger(\tau)\phi(\tau)]\int D[\phi'^\dagger(\tau)\phi'(\tau)]\exp\left\{\frac{i}{\hbar}S_A[\phi^\dagger,\phi;t]\right\}$$
$$\times\exp\left[\frac{i}{\hbar}\Xi(\{\phi\};\Omega(\tau);t)\right]\rho'_A(\phi_i^\dagger,\phi'_i)\exp\left\{-\frac{i}{\hbar}S_A^\dagger[\phi'^\dagger,\phi';t]\right\}P[\Omega(\tau)]P_{\rm eq}(\Omega_i),\tag{7.3}$$

where the phase of the influence functional is expressed as

$$\Xi(\{\phi\};\Omega(\tau);t)\equiv\frac{\beta\hbar\gamma\Delta}{2}\int_{t_i}^{t}d\tau\int_{t_i}^{\tau}d\tau'\,i\bar{L}_2(\tau-\tau')V^\times(\{\phi\};\tau)V^\circ(\{\phi\};\tau')-\Delta\int_{t_i}^{t}d\tau\,V^\times(\{\phi\};\tau)\Omega(\tau)\tag{7.4}$$

in which $V^\times(\{\phi\};\tau)$ and $V^\circ(\{\phi\};\tau)$ are defined by eq. (5.57). The probability density $P[\Omega(\tau)]$ is now redefined as

$$P[\Omega(\tau)]=C^{-1}\exp\left[-\frac{\gamma^2}{2}\int_{t_i}^{t}d\tau\int_{t_i}^{t}d\tau'\,\bar{L}_2^{-1}(\tau-\tau')\Omega(\tau)\Omega(\tau')\right].\tag{7.5}$$

The above expression is identical to eq. (2.8).

To derive the equation of motion for eq. (7.3), we rewrite eq. (7.4). From the definition of $\Omega(t)$, we have

$$V^\times(\{\phi\};\tau)=\ddot{\Omega}(\tau)-\gamma^2\Omega(\tau).\tag{7.6}$$

Since we have the boundary condition $\dot{\Omega}(t)+\gamma\Omega(t)=0$, the phase of the influence functional can be rewritten as

$$\Xi(\{\phi\};\Omega(\tau);t)=\frac{\beta\hbar\Delta}{2}\int_{t_i}^{t}d\tau\big[\dot{\Omega}(\tau)+\gamma\Omega(\tau)\big]V^\circ(\{\phi\};\tau)-\Delta\int_{t_i}^{t}d\tau\,V^\times(\{\phi\};\tau)\Omega(\tau).\tag{7.7}$$

As shown in §2.1, the distribution function for $\langle\Omega(\tau)\rangle=0$ and $\langle\Omega(\tau)\Omega(\tau')\rangle=\exp(-\gamma\,|\tau-\tau'|)$ follows

$$\frac{\partial}{\partial t}P(\Omega;t)=\gamma\frac{\partial}{\partial\Omega}\left(\Omega+\frac{\partial}{\partial\Omega}\right)P(\Omega;t).\tag{7.8}$$

If we regard $\Omega(t)$ as the stochastic variable Ω, then we can reduce the equation of motion as

$$\frac{\partial}{\partial t}\hat{\rho}(\Omega;t)=-\frac{i}{\hbar}\hat{H}_A^\times\hat{\rho}(\Omega;t)-\frac{i\Delta\beta\hbar\gamma}{2\hbar}\left(\Omega+\frac{\partial}{\partial\Omega}\right)\hat{V}^\circ\hat{\rho}(\Omega;t)-\frac{i\Delta}{\hbar}\Omega\hat{V}^\times\hat{\rho}(\Omega;t)+\gamma\frac{\partial}{\partial\Omega}\left(\Omega+\frac{\partial}{\partial\Omega}\right)\hat{\rho}(\Omega;t).\tag{7.9}$$

The above equation is the generalization of the stochastic Liouville equation.[15] The second term on the right-hand side is the temperature correction term. Note that if we include the counter term, the second term becomes $\dot{V}^\circ\hat{\rho}(\Omega;t)$ instead of $V^\circ\hat{\rho}(\Omega;t)$. For the Hamiltonian eq. (5.2) with $\hat{V}=V_1\hat{q}$, we have

$$\frac{\partial}{\partial t}W(p,q,\Omega;t)=-\hat{L}_A(p,q)W(p,q,\Omega;t)$$
$$+\Delta V_1\beta\gamma\left(\Omega+\frac{\partial}{\partial\Omega}\right)pW(p,q,\Omega;t)-\Delta V_1\Omega\frac{\partial}{\partial p}W(p,q,\Omega;t)$$
$$+\gamma\frac{\partial}{\partial\Omega}\left(\Omega+\frac{\partial}{\partial\Omega}\right)W(p,q,\Omega;t).\tag{7.10}$$

Following the same procedure as §2.4, the above equations can be cast into the hierarchy form as eqs. (5.41) and (5.63).

8. Conclusions

The stochastic theory has been used for over half a century to describe the classical and quantum dynamics of a system in a dissipative environment. Among various approaches, the stochastic Liouville equation approach has been widely used because it allows us to treat stochastic modulation in a nonperturbative manner including the effect of a noise correlation. The advantage of this approach lies in the structure of the equation of motion; a set of simultaneous differential equations for hierarchy elements can be solved either analytically using the resolvent utilizing in a tridiagonally continued fractional form or numerically by integrating the equations of motion utilizing a terminator. A variety of problems in NMR, μSR, neutron scattering, linear, and nonlinear optical measurements have been studied by the stochastic approach. Several novel phenomena such as motional narrowing, a slow relaxation of spin, and a broadened Raman process have been explained by the stochastic theory. Although it has many successful applications, the stochastic theory can be applied only to a system at infinite temperature. This gives a serious limitation to the system represented by a coordinate such as a double-well potential system, since one cannot define the equilibrium distribution.

We have shown that, on the basis of a system–bath Hamiltonian, we can derive the equations of motion that are valid at finite temperatures using similar hierarchy members to those of the stochastic Liouville equation, assuming an Ohmic spectral distribution with a Lorentzian cutoff. These equations now involve the temperature correction term that guarantees the steady-state solution of the equation of motion to be an equilibrium equation. By virtue of the hierarchy form, we could deal with the system–bath interaction nonperturbatively including the finite correlation effects of a noise. Within this framework, we have calculated several observables for systems expressed in coordinates and discrete energy levels. The extension of the

formula to a low-temperature system, and the relation of stochastic Liouville equation to the Langevin equation are also discussed by deriving the quantum Fokker–Planck equation and quantum master equation, both of which explicitly involve the random force in addition to the dissipation term. The dissipation term and random force are related to each other through the fluctuation–dissipation theorem and play the same role as the friction term in the Langevin equation. The trajectory of a density matrix element obtained for a sequence of the random noise is thus regarded as a quantum random walk. This formalism incorporated with Monte Carlo (MC) simulations follows the dissipative dynamics defined by the Hamiltonian and provides a framework for studies of quantum dynamics strongly coupled to a colored noise bath.

Although much progress has been achieved in the quest to understand dissipative dynamics by extending the stochastic theory, there are several important issues that remain to be unexplored. For example, even though we can investigate the effects of temperature through the temperature correction terms, the spectral distribution function for system–bath coupling is still limited to an Ohmic form with a Lorentzian cutoff.

Realistic spectral distributions, which may be obtained either from experiments[221,222] or molecular dynamics simulations,[223,224] have to be included in the theory to account for the dynamics of molecules in a complex environment such as protein. The extension to the fractal noise which is characterized by its correlation function $1/t^{\beta}$, where $0 < \beta < 1$, is also possible in a similar framework to the stochastic theory.[225] For a two-level system with the two-state jump fractal modulation case, we can evaluate correlation functions analytically.[226] Few attempts have been made to investigate realistic spectral distributions.[227,228]

The heat bath discussed in the present review is restricted to the harmonic oscillator system assumed as the Gaussian distribution for perturbation. Owing to the central limiting theorem, the applicability of this assumption is verified, yet for many systems, where the interactions between a system and the bath have a large heterogeneity, the Gaussian assumption breaks down. If we consider the quantum dynamics, anharmonic effects of bath oscillators become important, since the action path of the quantum harmonic oscillator system is similar to that of the classical one. This can be understood from the fact that the quantum Liouvillian defined by eq. (5.37) is identical to the classical one eq. (5.45), if the potential is harmonic.

One practical way to solve this problem is to introduce a subsystem between the main system and the bath to represent an anharmonic local environment. For example, suppose if we want to study the dynamics of impurity atoms in an Ising lattice for the environment,[111] we can define the system by three parts: the main system A, which represents the impurity, the subsystem A', which represents a local spin environment consisting of many but finite degrees of freedom, and the oscillator–bath system B, which is supposed to represent the phonon interactions that bring the system to the thermal equilibrium state. It is our belief that as we increase the size of A' so as to regard A' as the bath, we will find statistical behavior of the anharmonic bath. This approach allows us to investigate, for example, quantum dynamics in a frustrated environment. This is, however, computationally costly, since we have to deal with the density matrix of the $A + A'$ system. The advent of parallel computers equipped with tremendous memory makes it possible to solve such problems. If a high accuracy of calculations is not required, the Monte-Carlo type calculation explained in §6.4 may be a practical way of solving the problems.

Dealing with the subsystem A' also brings another important issue, the dimensionality of the system. We have employed a one-dimensional Fokker–Planck equation as in eqs. (5.38) and (5.39), but there are many problems in physics and chemistry, particularly biology, for example, the optimal choice of dynamical model is a system with more than two or three dimensions. For example, electron transfer phenomena are well described by more than one molecular coordinate and one solvation coordinate. Proton tunneling in Tropolon is also well described by multi-dimensional potential. If we use $N \times M$ mesh points to solve one-dimensional problems, we have to compute a system with $(N \times M)^n$ mesh points for n-dimensional problem. However, at present, the only case in which solving the equation of motion is practical is that of two-dimensional system due to the limit of the CPU power of current computers. To overcome this difficulty, another scheme like Langevin dynamics in a phase space described by §6.2 has to be extended. Such an approach might, for example, allow closer contact with nonlinear optical experiments that could measure the dynamics of many additional modes.

In conclusion, the present formalism provides a powerful means for the study of various physical and chemical processes including reaction processes at low temperatures in which the quantum effects play a major role. One can generalize the present approach to studying a variety of measurements involving NMR, neutron scattering, linear, and nonlinear spectroscopies, where the interplay between thermal activation and dissipation becomes important. Theories should now be able to characterize these effects and establish microscopic description of the dynamics be related to experiments. Further development of the formulation and algorithm must be a key to studying experimental systems.

Acknowledgments

I wish to express my gratitude to N. Ueki, A. Ishizaki, K. Ando, K. Miyazaki, N. Sakumichi, and J. Ono for helpful comments. The financial support from a Grant-in-Aid for Scientific Research A 15205005 from the Japan Society for the Promotion of Science and Morino Science Foundation is acknowledged.

1) P. W. Anderson: J. Phys. Soc. Jpn. **9** (1954) 316.
2) R. Kubo: J. Phys. Soc. Jpn. **9** (1954) 935.
3) R. Kubo, M. Toda and N. Hashitsume: *Statistical Physics* (Springer-Verlag, 1985) Vol. 2.
4) U. Weiss: *Quantum Dissipative Systems* (World Scientific, Singapore, 1999) 2nd ed.
5) R. Kubo: in *Fluctuation, Relaxation, and Resonance in Magnetic Systems*, ed. D. TerHaar (Oliver and Boyd, Edinburgh, 1962) p. 23.
6) R. Kubo: J. Math. Phys. **4** (1962) 174.
7) R. Kubo: J. Phys. Soc. Jpn. **26** (1969) Suppl., p. 1.
8) R. Kubo: Adv. Chem. Phys. **15** (1969) 101.

9) P. Talkner: Z. Phys. B **41** (1981) 365.
10) N. G. Van Kampen: *Stochastic Processes in Physics and Chemistry* (North-Holland, Amsterdam, 1981).
11) H. Grabert, U. Weiss and P. Talkner: Z. Phys. B **55** (1984) 87.
12) S. Dattagupta: *Relaxation Phenomena in Condensed Matter Physics* (Academic Press, Orlando, 1987).
13) Y. Aoyama and M. Tanaka: J. Phys. Soc. Jpn. **62** (1993) 2869.
14) W. T. Coffey, Y. P. Kalmykov and J. T. Waldron: *The Langevin Equation* (World Scientific, Singapore, 1996).
15) Y. Tanimura and R. Kubo: J. Phys. Soc. Jpn. **58** (1989) 101.
16) Y. Tanimura and R. Kubo: J. Phys. Soc. Jpn. **58** (1989) 1199.
17) Y. Tanimura: Phys. Rev. A **41** (1990) 6676.
18) Y. Tanimura and P. G. Wolynes: Phys. Rev. A **43** (1991) 4131.
19) Y. Tanimura and P. G. Wolynes: J. Chem. Phys. **96** (1992) 8485.
20) R. L. Stratonovich: *Topics in the Theory of Random Noise* (Gordon and Breach, New York, 1967) Vols. I and II.
21) F. W. Wiegel: Phys. Rep. **16** (1975) 57.
22) M. Chaichia and A. Demichev: *Path Integrals in Physics* (IOP Publishing, Bristol, 2001) Vol. I.
23) B. Sakita: *Quantum Theory of Many Variables Systems and Fields* (World Scientific, Singapore, 1985).
24) Y. Tanimura and S. Mukamel: J. Chem. Phys. **99** (1993) 9496.
25) Y. Tanimura: Chem. Phys. **233** (1998) 217.
26) R. Kubo: J. Phys. Soc. Jpn. **12** (1957) 570.
27) S. Saito and I. Ohmine: J. Chem. Phys. **106** (1997) 4889.
28) S. Saito and I. Ohmine: J. Chem. Phys. **108** (1998) 240.
29) J. Cao, J. Wu and S. Yang: J. Chem. Phys. **116** (2002) 3739.
30) J. Cao, J. Wu and S. Yang: J. Chem. Phys. **116** (2002) 3760.
31) Y. Nagata and Y. Tanimura: J. Chem. Phys. **124** (2006) 024508.
32) Y. Nagata, T. Hasegawa and Y. Tanimura: J. Chem. Phys. **124** (2006) 194504.
33) J. H. Eberly and K. Wódkiewics: J. Opt. Soc. Am. **67** (1977) 1252.
34) T. Chikama, K. Saikawa and R. Kubo: J. Phys. Soc. Jpn. **53** (1984) 991.
35) Y. Tanimura, T. Suzuki and R. Kubo: J. Phys. Soc. Jpn. **58** (1989) 1850.
36) Y. Tanimura and R. Kubo: J. Phys. Soc. Jpn. **58** (1989) 3001.
37) Y. Tanimura and S. Mukamel: J. Phys. Soc. Jpn. **63** (1994) 66.
38) L. Van Hove: Phys. Rev. **95** (1954) 249.
39) M. H. Levitt: *Spin Dynamics* (John Wiley & Sons, New York, 2001).
40) S. Dattagupta: Hyperfine Interactions **11** (1981) 77.
41) R. Kubo and T. Toyabe: in *Magnetic Resonance and Relaxation, Proc. 14th Colloque Ampére*, ed. R. Blinc (North-Holland, Amsterdam, 1967).
42) F. Bloch: Phys. Rev. **70** (1946) 460.
43) R. Kubo: Hyperfine Interactions **8** (1981) 731.
44) R. S. Hayano, Y. J. Uemura, J. Imazato, N. Nishida, T. Yamazaki and R. Kubo: Phys. Rev. B **20** (1979) 850.
45) R. Kubo, T. Endo, S. Kamohara, M. Shimizu, M. Fujii and H. Takano: J. Phys. Soc. Jpn. **56** (1987) 1172.
46) F. Shibata and I. Sato: Physica A **143** (1987) 468.
47) A. Y. Serebrennikov and M. I. Majitov: Chem. Phys. Lett. **157** (1989) 462.
48) C. Uchiyama and F. Shibata: Phys. Lett. A **267** (2000) 7.
49) Y. Aoyama and M. Tanaka: J. Phys. Soc. Jpn. **61** (1992) 722.
50) M. Suzuki and R. Kubo: Mol. Phys. **7** (1964) 201.
51) N. P. Benetis, D. J. Schneider and J. H. Freed: J. Magn. Reson. **85** (1989) 275.
52) A. Schleicher, K. Muller and G. Kothe: J. Chem. Phys. **92** (1990) 432.
53) D. Abergel and A. G. Palmer III: Concepts Magn. Reson., Part A **19** (2003) 134.
54) P. Debye: *Polar Molecules* (Reinhold, New York, 1929).
55) R. Kubo and N. Hashitsume: Prog. Theor. Phys. Suppl. No. 46 (1970) 210.
56) C. Uchiyama and F. Shibata: Physica A **153** (1988) 469.
57) C. Uchiyama and F. Shibata: Physica A **161** (1989) 23.
58) F. Shibata, C. Uchiyama and K. Maruyama: Physica A **161** (1989) 42.
59) Y. Suzuki and Y. Tanimura: J. Phys. Soc. Jpn. **71** (2002) 2414.
60) Y. Suzuki and Y. Tanimura: J. Chem. Phys. **119** (2003) 1650.
61) L. D. Favro: Phys. Rev. **119** (1960) 53.
62) E. N. Ivanov: Sov. Phys. JETP **18** (1964) 1041.
63) L. D. Favro: in *Fluctuation Phenomena in Solids*, ed. R. E. Burgess (Academic Press, New York, 1965) p. 79.
64) A. Kawabata: Prog. Theor. Phys. **48** (1972) 2237.
65) K. Miyazaki and K. Seki: J. Chem. Phys. **108** (1998) 7052.
66) M. Blume and J. A. Tjon: Phys. Rev. **165** (1968) 446.
67) M. Blume and J. A. Tjon: Phys. Rev. **165** (1968) 456.
68) M. Blume: Phys. Rev. **174** (1968) 351.
69) S. Dattagupta and M. Blume: Phys. Rev. B **10** (1974) 4540.
70) S. Dattagupta and M. Blume: Phys. Rev. B **10** (1974) 4551.
71) S. Dattagupta: Philos. Mag. **33** (1976) 59.
72) S. Dattagupta: Solid State Commun. **24** (1977) 19.
73) S. Mukamel: *Principles of Nonlinear Optical Spectroscopy* (Oxford University Press, New York, 1995).
74) E. Hanamura: J. Phys. Soc. Jpn. **52** (1983) 2258.
75) E. Hanamura: J. Phys. Soc. Jpn. **52** (1983) 3265.
76) H. Tsunetsugu, T. Taniguchi and E. Hanamura: Solid State Commun. **52** (1984) 663.
77) H. Tsunetsugu and E. Hanamura: Solid State Commun. **55** (1985) 397.
78) H. Tsunetsugu and E. Hanamura: J. Phys. Soc. Jpn. **55** (1986) 3636.
79) Y. Tanimura and S. Mukamel: Phys. Rev. E **47** (1993) 118.
80) T. Takagahara, E. Hanamura and R. Kubo: J. Phys. Soc. Jpn. **43** (1977) 802.
81) T. Takagahara, E. Hanamura and R. Kubo: J. Phys. Soc. Jpn. **43** (1977) 811.
82) T. Takagahara, E. Hanamura and R. Kubo: J. Phys. Soc. Jpn. **43** (1977) 1522.
83) T. Takagahara, E. Hanamura and R. Kubo: J. Phys. Soc. Jpn. **44** (1978) 728.
84) T. Takagahara, E. Hanamura and R. Kubo: J. Phys. Soc. Jpn. **44** (1978) 742.
85) H. Sumi: J. Chem. Phys. **67** (1977) 2943.
86) S. Mukamel: J. Chem. Phys. **82** (1985) 5398.
87) S. Mukamel and R. F. Loring: J. Opt. Soc. Am. B **3** (1986) 595.
88) Y.-J. Yan and S. Mukamel: J. Chem. Phys. **86** (1987) 6085.
89) M. Mikami and S. Saikan: J. Phys. Soc. Jpn. **63** (1994) 3581.
90) Y. Tanimura, H. Takano and R. Kubo: J. Phys. Soc. Jpn. **55** (1986) 4550.
91) K. Maruyama and F. Shibata: Physica A **149** (1988) 447.
92) K. Maruyama, F. Shibata and M. Aihara: Physica A **153** (1988) 441.
93) J. Watanabe, S. Kinoshita and T. Kushida: Chem. Phys. Lett. **126** (1986) 197.
94) S. Kinoshita, N. Nishi and T. Kushida: Chem. Phys. Lett. **134** (1987) 605.
95) R. F. Loring and S. Mukamel: Chem. Phys. Lett. **114** (1985) 426.
96) W. B. Bosma, Y. J. Yan and S. Mukamel: Phys. Rev. A **42** (1990) 6920.
97) J. R. Schemidt, N. Sundlass and J. L. Skinner: J. Chem. Phys. Lett. **378** (2003) 559.
98) H. Nakamura: *Nonadiabatic Transition: Concepts, Basic Theories and Applications* (World Scientific, Singapore, 2002).
99) K. Kayanuma: J. Phys. Soc. Jpn. **53** (1984) 108.
100) K. Kayanuma: J. Phys. Soc. Jpn. **53** (1984) 118.
101) K. Kayanuma: J. Phys. Soc. Jpn. **54** (1985) 2037.
102) W. G. Rothschild: J. Chem. Phys. **65** (1976) 455.
103) D. W. Oxtoby: Adv. Chem. Phys. **40** (1979) 1.
104) D. W. Oxyoby: Adv. Chem. Phys. **47** (1981) 487.
105) K. Okumura and Y. Tanimura: Phys. Rev. E **56** (1997) 2747.
106) W. G. Johnson and D. W. Oxtoby: J. Chem. Phys. **87** (1987) 781.
107) R. M. Stratt and M. Maroncelli: J. Phys. Chem. **100** (1996) 12981.
108) H. Torii: J. Phys. Chem. A **106** (2002) 3281.
109) H. Torii: J. Phys. Chem. A **108** (2004) 2103.
110) W. P. Ambrose, Th. Basche and W. E. Moerner: J. Chem. Phys. **95** (1991) 7150.
111) Y. Tanimura, H. Takano and J. Klafter: J. Chem. Phys. **108** (1998) 1851.
112) V. Chernyak, M. Schulz and S. Mukamel: J. Chem. Phys. **111** (1999) 7416.
113) E. Barkai, R. Silbey and G. Zumofen: J. Chem. Phys. **113** (2000) 5853.
114) Y. Jung, E. Barkai and R. J. Silbey: Adv. Chem. Phys. **123** (2002) 199.

115) J. L. Skinner and W. E. Moerner: J. Phys. Chem. **100** (1996) 13251.
116) P. D. Reilly and J. L. Skinner: J. Chem. Phys. **102** (1995) 1540.
117) P. Hamm, M. Lim and R. M. Hochstrasser: J. Phys. Chem. B **102** (1998) 6123.
118) L. J. Kaufman, J. Heo, L. D. Ziegler and G. R. Fleming: Phys. Rev. Lett. **88** (2002) 207402.
119) K. J. Kubarych, C. L. Milne, S. Lin, V. Astinov and J. D. Miller: J. Chem. Phys. **116** (2002) 2016.
120) S. Woutersen and P. Hamm: J. Phys. Chem. B **104** (2000) 11316.
121) S. Woutersen and P. Hamm: J. Chem. Phys. **115** (2001) 7737.
122) M. T. Zanni, S. Gnanakaran, J. Stenger and R. M. Hochstrasser: J. Phys. Chem. B **105** (2001) 6520.
123) I. V. Rubtsov and R. M. Hochstrasser: J. Phys. Chem. B **106** (2002) 9165.
124) M. Khalil, N. Demirdoven and A. Tokmakoff: J. Phys. Chem. A **107** (2003) 5258.
125) K. Ohta, H. Maekawa, S. Saito and K. Tominaga: J. Phys. Chem. A **107** (2003) 5643.
126) J. B. Asbury, T. Steinel, C. Stromberg, S. A. Corcelli, C. P. Lawrence, J. L. Skinner and M. D. Fayer: J. Phys. Chem. A **108** (2004) 1107.
127) S. Mukamel and W. Zhuang: Proc. Natl. Acad. Sci. U.S.A. **102** (2005) 13717.
128) T. Steffen and K. Duppen: Chem. Phys. **233** (1998) 267.
129) J. T. Fourkas: Adv. Chem. Phys. **117** (2001) 235.
130) K. Okumura and Y. Tanimura: J. Chem. Phys. **106** (1997) 1687.
131) K. Okumura and Y. Tanimura: J. Chem. Phys. **107** (1997) 2267.
132) K. Okumura and Y. Tanimura: Chem. Phys. Lett. **277** (1997) 159.
133) M. Cho, K. Okumura and Y. Tanimura: J. Chem. Phys. **108** (1998) 1326.
134) K. Okumura and Y. Tanimura: Chem. Phys. Lett. **278** (1997) 175.
135) K. Okumura, A. Tokmakoff and Y. Tanimura: J. Chem. Phys. **111** (1999) 492.
136) K. Okumura, D. M. Jonas and Y. Tanimura: Chem. Phys. **266** (2001) 237.
137) A. Ma and R. M. Stratt: Phys. Rev. Lett. **85** (2000) 1004.
138) T. I. C. Jansen, J. G. Snijders and K. Duppen: J. Chem. Phys. **114** (2001) 10910.
139) R. A. Denny and D. R. Reichman: J. Chem. Phys. **116** (2002) 1979.
140) S. Saito and I. Ohmine: Phys. Rev. Lett. **88** (2002) 207401.
141) R. F. Loring and S. Mukamel: J. Chem. Phys. **83** (1985) 2116.
142) D. V. Bout and M. Berg: J. Raman Spectrosc. **26** (1995) 503.
143) H.-D. Kim and Y. Tanimura: J. Chem. Phys. **123** (2005) 224310.
144) A. Tokmakoff and M. D. Fayer: J. Chem. Phys. **103** (1995) 2810.
145) K. F. Everitt and J. L. Skinner: Chem. Phys. **266** (2001) 197.
146) K. F. Everitt, E. Geva and J. L. Skinner: J. Chem. Phys. **114** (2001) 1326.
147) K. A. Merchant, W. G. Noid, D. E. Thompson, R. Akiyama, R. F. Loring and M. D. Fayer: J. Phys. Chem. B **107** (2003) 4.
148) T. I. C. Jansen, W. Zhuang and S. Mukamel: J. Chem. Phys. **121** (2004) 10577.
149) T. I. C. Jansen, T. Hayashi, W. Zhuang and S. Mukamel: J. Chem. Phys. **123** (2005) 114504.
150) H. Torii: J. Phys. Chem. A **110** (2006) 4822.
151) A. Ishizaki and Y. Tanimura: to be published in J. Chem. Phys. **125** (2006).
152) R. P. Feynman and F. L. Vernon, Jr.: Ann. Phys. (N.Y.) **24** (1963) 118.
153) A. O. Caldeira and A. J. Leggett: Physica A **121** (1983) 587.
154) L.-D. Chang and D. Waxman: J. Phys. C **18** (1985) 5873.
155) H. Grabert, P. Schramm and G.-L. Ingold: Phys. Rep. **168** (1988) 115.
156) V. Hakim and V. Ambegaokar: Phys. Rev. A **32** (1985) 423.
157) R. P. Feynman, R. W. Hellwarth, C. K. Iddings and P. M. Platzman: Phys. Rev. **127** (1962) 1004.
158) Y. Suzuki and Y. Tanimura: Phys. Rev. E **59** (1999) 1475.
159) Y. Tanimura and Y. Maruyama: J. Chem. Phys. **107** (1997) 1779.
160) Y. Maruyama and Y. Tanimura: Chem. Phys. Lett. **292** (1998) 28.
161) T. Steffen and Y. Tanimura: J. Phys. Soc. Jpn. **69** (2000) 3115.
162) Y. Tanimura and T. Steffen: J. Phys. Soc. Jpn. **69** (2000) 4095.
163) Y. Tanimura: in *Proc. Two-Dimensional Correlation Spectroscopy*, ed. Y. Ozaki (American Institute of Physics, New York, 2000) p. 144.
164) T. Kato and Y. Tanimura: J. Chem. Phys. **117** (2002) 6221.
165) T. Kato and Y. Tanimura: J. Chem. Phys. **120** (2004) 260.
166) A. Ishizaki and Y. Tanimura: J. Chem. Phys. **123** (2005) 14503.
167) A. Ishizaki and Y. Tanimura: J. Phys. Soc. Jpn. **74** (2005) 3131.
168) E. Wigner: Phys. Rev. **40** (1932) 749.
169) R. Kubo: J. Phys. Soc. Jpn. **19** (1964) 2127.
170) W. R. Frensley: Rev. Mod. Phys. **62** (1990) 745.
171) H. Riskin: *The Fokker–Planck Equation* (Springer-Verlag, Berlin, 1988) 2nd ed.
172) H. A. Kramers: Physica **7** (1940) 284.
173) P. Hanggi, P. Talkner and M. Borkovec: Rev. Mod. Phys. **62** (1990) 252.
174) P. A. Frantsuzov and V. A. Mandelshtam: J. Chem. Phys. **121** (2004) 9247.
175) E. Pollak and S. Miret-Artés: J. Phys. A **37** (2004) 9669.
176) M. Saltzer and E. Pollak: J. Chem. Theory Comput. **1** (2005) 439.
177) Y. J. Yan: Phys. Rev. A **58** (1998) 2721.
178) F. Shung, C. Yang and Y.-J. Yan: J. Chem. Phys. **114** (2001) 3868.
179) J. B. Coon, N. W. Naugle and R. D. Mckenzie: J. Mol. Spectrosc. **20** (1966) 107.
180) P. Meystre and M. Sargent III: *Elements of Quantum Optics* (Springer-Verlag, 1991) 2nd ed.
181) A. J. Leggett, S. Chakravarty, A. T. Dorsey, M. P. A. Fisher, A. Garg and Z. Zwerger: Rev. Mod. Phys. **59** (1987) 1.
182) R. Egger and C. H. Mak: Phys. Rev. B **50** (1994) 15210.
183) N. Makri: J. Math. Phys. **36** (1995) 2430.
184) J. Cao, L. W. Ungar and G. A. Voth: J. Chem. Phys **104** (1996) 4189.
185) P. Han, R. X. Xu, B. Li, J. Xu, P. Cui, Y. Mo and Y. J. Yan: J. Phys. Chem. B **110** (2006) 11438.
186) A. G. Redfield: Adv. Magn. Reson. **1** (1965) 1.
187) E. B. Davies: *Quantum Theory of Open Systems* (Academic Press, 1976).
188) V. Gorini, A. Frigerio, M. Verri, A. Kossakowski and E. C. G. Sudarshan: Rep. Math. Phys. **13** (1978) 149.
189) H. Spohn: Rev. Mod. Phys. **52** (1980) 569.
190) V. Gorini, A. Kossakowski and E. C. G. Sudarshan: J. Math. Phys. **17** (1976) 821.
191) R. Dümcke and H. Spohn: Z. Phys. B **34** (1979) 419.
192) P. Pechukas: Phys. Rev. Lett. **73** (1994) 1060.
193) K. F. F. Romero, P. Talkner and P. Hanggi: Phys. Rev. **69** (2004) 052109.
194) A. Frigerio, J. T. Lewis and J. V. Pulé: Adv. Appl. Math. **2** (1981) 456.
195) A. Frigerio, J. T. Lewis and J. V. Pulé: J. Approx. Theor. **45** (1985) 310.
196) R. X. Xu, P. Cui, X. Q. Li, Y. Mo and Y. J. Yan: J. Chem. Phys. **122** (2005) 041103.
197) C. Meier and D. J. Tannor: J. Chem. Phys. **111** (1999) 3365.
198) A. Garg, J. N. Onuchic and V. Ambegaokar: J. Chem. Phys. **83** (1985) 4491.
199) Y.-J. Yan, M. Sparpaglione and S. Mukamel: J. Phys. Chem. **92** (1988) 4842.
200) Y. Tanimura and K. Okumura: J. Chem. Phys. **106** (1997) 2078.
201) Y.-J. Yan and S. Mukamel: J. Chem. Phys. **89** (1988) 5735.
202) Y. Tanimura and S. Mukamel: J. Chem. Phys. **101** (1994) 3049.
203) V. Chernyak and S. Mukamel: J. Chem. Phys. **105** (1996) 4565.
204) R. Kapral and G. Ciccotti: J. Chem. Phys. **110** (1999) 8919.
205) R. Kapral and A. Sergi: J. Chem. Phys. **121** (2004) 7565.
206) K. Ando and M. Santer: J. Chem. Phys. **118** (2003) 10399.
207) N. Hashitsume, M. Mori and T. Takahashi: J. Phys. Soc. Jpn. **55** (1987) 1887.
208) N. Hashitsume, K. Naito and A. Washiwo: J. Phys. Soc. Jpn. **59** (1990) 464.
209) R. L. Stratonovich: Sov. Phys. Dokl. **2** (1958) 416.
210) J. Hubbard: Phys. Rev. Lett. **3** (1959) 77.
211) J. T. Stockburger and C. H. Mak: J. Chem. Phys. **110** (1999) 4983.
212) J. T. Stockburger and H. Grabert: Chem. Phys. **268** (2001) 249.
213) J. T. Stockburger and H. Grabert: Phys. Rev. Lett. **88** (2002) 170407.
214) J. Cao: J. Chem. Phys. **107** (1997) 3024.
215) R. X. Xu, Y. Mo, P. Cui, S.-H. Lin and Y. J. Yan: in *Progress in Theoretical Physics: Advanced Topics in Theoretical Chemical Physics*, ed. J. Maruani, R. Lefebre and E. Brandas (Kluwer, Dordrecht, 2003) Vol. 12, p. 7.
216) R. J. Glauber: J. Math. Phys. **4** (1963) 294.

217) N. Metropolis, A. W. Rosenbluth, M. N. Rosenbluth, A. H. Teller and E. Teller: J. Chem. Phys. **21** (1953) 1087.
218) K. Binder and D. W. Heermann: *Monte Carlo Simulation in Statistical Physics* (Springer, Berlin, 1997) 3rd ed.
219) J. Shao: J. Chem. Phys. **120** (2004) 5053.
220) Y. Yan, F. Yang, Y. Liu and J. Shao: Chem. Phys. Lett. **395** (2004) 216.
221) S. Palese, S. Mukamel, R. J. D. Miller and W. T. Lotshaw: J. Phys. Chem. **100** (1996) 10380.
222) A. Tokmakoff, M. J. Lang, D. S. Larsen, X. J. Jordanides and G. R. Fleming: Chem. Phys. **233** (1998) 231.
223) K. Moritsugu, O. Miyashita and A. Kidera: Phys. Rev. Lett. **85** (2000) 3970.
224) I. Ohmine and S. Saito: Acc. Chem. Res. **32** (1999) 741.
225) R. Metzler and J. Klafter: Phys. Rep. **339** (2000) 1.
226) G. Gangopadhyay and Y. Tanimura: Chem. Phys. Lett. **289** (1998) 97.
227) J. Shao and P. Hanggi: Phys. Rev. Lett. **81** (1998) 5710.
228) Y. J. Yan and R. X. Xu: Annu. Rev. Phys. Chem. **56** (2005) 187.

Yoshitaka Tanimura was born in Akashi, Hyogo Prefecture, Japan in 1960. He received his B.S. (1984), M.E. (1986) and Ph. D. (1989) degrees from Keio University. He spent two years at University of Illinois at Urbana-Champaign and two and half years at University of Rochester as a Postdoctoral Fellow. He was an associate professor (1994–2003) at Institute for Molecular Science (IMS) before joining Faculty of Science at Kyoto University as a professor. His research interests are in chemical physics and nonequilibrium statistical physics. He is broadly concerned with classical and quantum dissipative dynamics of molecules in liquid, solid, and biological environments, where a large diversity of molecular states is involved.